SHORT-ARC ORBIT IMPROVEMENT FOR GPS SATELLITES

D. PARROT

June 1989

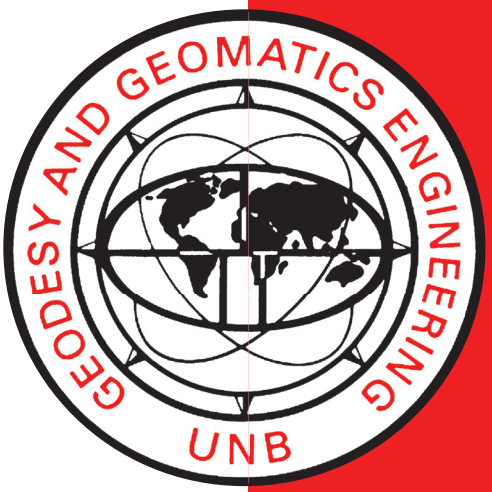

TECHNICAL REPORT
NO. 143

PREFACE

In order to make our extensive series of technical reports more readily available, we have scanned the old master copies and produced electronic versions in Portable Document Format. The quality of the images varies depending on the quality of the originals. The images, in this version of the report, have been converted to searchable text.

SHORT-ARC ORBIT IMPROVEMENT FOR GPS SATELLITES

Denis Parrot

Department of Geodesy and Geomatics Engineering
University of New Brunswick
P.O. Box 4400
Fredericton, N.B.
Canada
E3B 5A3

June 1989
Latest Reprinting March 1995

PREFACE

This technical report is a reproduction of an M.Sc.E. thesis submitted in partial fulfillment of the requirements of the degree of Master of Science in Engineering in the Department of Surveying Engineering, June 1989. Funding for the research undertaken was partially provided by the Natural Sciences and Engineering Research Council of Canada.

ABSTRACT

Over the past four years, different research groups involved in the application of the Global Positioning System (GPS) have investigated the possibility of solving for a combination of dynamical and orbital parameters, along with the station coordinates, in order to obtain geodetic solutions below the 1-ppm relative accuracy level over large networks.

It has been shown, using the GPS carrier phase, that this modelling can yield solutions at the 0.1-ppm level or below. These results have been obtained using orbital arcs modelling varying in length from 1 to 6 days.

The scope of this thesis is to develop and demonstrate that a similar procedure over orbital arcs of about 6 to 8 hours can yield results of the same level of accuracy over large networks. We implemented our algorithms in the University of New Brunswick GPS software DIPOP 2.0 to demonstrate some results.

First, a numerical integrator was developed in order to generate short-arc a priori trajectories (up to 8 hours) rigourously related to the initial satellite state vectors. A force model including the earth's gravitional potential up to degree and order 10, the luni-solar gravitational perturbation and a simple solar radiation pressure model have been implemented. Afterwards, Keplerian motion is used, in the final least-squares adjustment, to approximate the partial derivatives with respect to the initial conditions.

Our orbit modelling was tested with a subset of the TI 4100 data from the Spring 1985 High Precision Baseline Test (HPBT) campaign (including baselines up to 4000 km). Free-network as well as fiducial network solutions were compared. It will be shown that, over long baselines, that these global-network solutions as well as the daily-network solutions are at the 0.1-ppm relative accuracy levels. Over shorter baselines, the repeatability is at the 0.25-ppm level.

To further assess the quality of the improved orbit, a pure orbit solution was performed in order to produce a set of improved initial conditions. Short-arc orbits are then numerically integrated from these improved state vectors, which in turn are used to solve a long and a short baseline vector. The relative accuracy of these solutions is at the same level as the previously stated accuracies. These results really demonstrate that the Keplerian approximation used to compute the partial derivatives with respect the satellite initial state vectors is well justified when short-arc approach is used.

TABLE OF CONTENTS

LIST OF FIGURES

LIST OF TABLES

ACKNOWLEDGEMENTS

First of all, I would like to thank my employer PHOTOSUR GEOMAT Inc. for their financial support, and also for the use of their computer facilities which were always at my disposal during the writing of my thesis.

Secondly, I would like to thank the members of the Geodesy Group for their support and also for their advice which was of great help to me during my stay at the University of New Brunswick. I would especially like to thank Rock Santerre, Alfred Kleusberg, and See Hean Quek for their invaluable advice in parts of my research.

Thirdly, I would like to thank my supervisor Dr. R.B. Langley, who was always there for me and who showed such patience with me in the use/abuse of the English language. I also want to thank him for giving me the opportunity, early in my stay at UNB, to take part in a GPS project.

Finally, I owe much to my family and close friends for their constant support in some of my most difficult times while writing this thesis.

1. INTRODUCTION

Although the Global Positioning System (GPS) is not fully operational, it is currently used for geodetic applications by several private companies [Leeman et al., 1985; Cain, 1986; Collins and Leick 1985; McLellan and Schleppe, 1987; Klau, 1986, Lachapelle and Cannon, 1986] and by some government agencies [Merell, 1986a; Strange, 1985; McArthur et al., 1985; Moreau et al., 1985; Tessier, 1987; Jones et al., 1987; Willis et al., 1986]. Most of these applications have demonstrated clearly that phase observations with broadcast ephemeris can provide daily solutions at the 1-3 ppm relative accuracy level [Vanicek et al., 1985; Delikaraoglou, 1985; Remondi, 1984].

When phase observations are used to compute precise geodetic coordinates, the principal biases affecting the solution are: the correct phase ambiguity resolution, the ionospheric and tropospheric delay, the satellite and receiver clock misalignment, the multipath effect, and finally the satellite orbit errors. The observation pre-processing can be, to some extent, a factor affecting the solution, for example, the capability to correct cycle slips exactly, the optimization of the cut-off angle in order to use the tropospheric models properly. Over short-baseline vectors (< 20 km), the effect of the tropospheric delay, ionospheric delay and orbital errors are of the same order of magnitude (highly correlated) at both ends of the baseline. Thus, by differencing the observations from one satellite recorded at both stations (single-difference observable), these biases tend to cancel out; moreover, the satellite clock misalignment cancels out as well. The receiver clock error can be removed by differencing two single-difference observations to two different satellites, from a common epoch (double-difference observable). The multipath effect can be handled, to a certain extent, by removing all reflecting objects surrounding the GPS antenna. For high-precision observations, absorbing material can be used around the base of the antenna. When double-difference observables are used over short-baselines, the integer value of the ambiguities is usually recovered and fixed in a subsequent adjustment to yield a strengthened solution. Usually all solutions over

small-scale networks (< 20 km) are at centimetre-level accuracy.

Over longer baselines, the correlation of the biases at each site decreases and mathematical models are required to correct the observations properly; dual-frequency observations must be used to correct the bulk (first-order term) of the ionospheric delay at each site, whereas surface meteorological data are necessary to model the dry part of the tropospheric delay properly; the wet part component can be poorly approximated by a surface meteorological model or estimated more accurately using water-vapor radiometer (WVR) observations [Ware et al., 1985]. The remaining (unmodelled or mismodelled) biases are the second-order term of the ionospheric delay, which is, at the present time, of the order of few centimetres [Kleusberg, 1986] (to get worse as the sunspot maximum approaches); the mismodelled effect of the wet part of the troposphere (when surface meteorological values are used), which is at the centimetre level [Hogg et al., 1981], and finally the orbital errors, which can easily reach, for broadcast orbits, up to 25-50 metres.

Among these unmodelled biases over long baselines, the orbital error (with broadcast ephemerides) is certainly the most important one affecting the GPS phase solution. The systematic effect of the orbital errors is evident in the double-difference residuals plot from a long-baseline solution. Fig. 6.8 is an example of such a plot.

The orbital error has been investigated by Vanicek et al. [1985]. They demonstrated that the relative accuracy of a baseline vector obtained from double-difference GPS observations can be related to the satellite position error by a simple rule of thumb:

$$\frac{db}{b} = \frac{dr}{r} \tag{1.1}$$

where db is the baseline error, b is the baseline length, dr the orbital error and r is the receiver-satellite distance (~20 000 km). According to this relation, 25-metre errors in the satellite trajectory will give a relative baseline accuracy of the order of 1 ppm. On the other hand, two different results obtained on the same baseline, with orbit differences of up to 60 metres (JPL and MIT orbit), have produced compatible solutions at the 0.4 ppm level [Ware et al., 1986]. Moreover, with broadcast ephemerides, which are known to be at a 25-50 m accuracy level, Kleusberg and Wanninger [1987] recently obtained a network solution at a 0.3 ppm level. Although these latest results can be achieved by averaging the orbital errors over long observation periods, the relation (1.1) in fact

represents the maximum error introduced by a satellite trajectory and should be considered as a pessimistic approximation.

To study the possibility of estimating the orbital biases in a network solution, Thornton et al. [1983] used equation (1.1) in the inverse sense: if there is a tracking station network of high accuracy (better than 0.1 ppm), these stations, held fixed, can be used for precise orbit determination. They conducted a covariance analysis using POLARIS VLBI sites as fixed tracking stations (Westford, Richmond, Fort Davis) and concluded that an orbit accuracy of better than 3 metres is achievable with Doppler observations, and their results were even better with carrier phase observations.

Beutler et al. [1984a] introduced, in their double-difference analysis programs, PRMAC3 and PRMNET, a physical modelling of the orbit allowing the estimation of up to six corrective terms to the initial osculating elements for each satellite involved in the least-squares solution. At that time, with the data at hand (a small network), he did not really demonstrate the benefit of this procedure.

Beutler with his second generation Bernese software [Gurtner et al., 1985] and a part of the 1984 Alaska GPS data set, showed that over large networks (1000-km baselines), a solution with orbital parameters estimation can lead to a network accuracy of the order of a 0.25 ppm [Beutler et al., 1985].

The covariance analysis previously described has led to the fiducial network concept [Davidson et al. 1985]. In the fiducial network approach, simultaneous observations are performed by fixed receivers at stations whose positions are known with high accuracy (fiducial points) and by mobile receivers placed at sites of geodetic interest. Observations recorded in such sessions enable the simultaneous determination of accurate GPS satellite orbits and geodetic baselines. To demonstrate the possibility of this fiducial concept, the Jet Propulsion Laboratory (JPL), in conjunction with 17 other institutions, conducted a high-precision baseline test (HPBT) in the spring of 1985. Ten sites distributed throughout the United States were occupied by GPS receivers for ten days.

Nakiboglu et al. [1985] concluded, in a report produced for the Canadian Government, that GPS satellite orbits, over Canadian territory, can be computed at a 2.5-metre accuracy level with four tracking stations tied to VLBI sites. This analysis led the Canadian Geodetic Survey to undertake the Active Control System (ACS) project [Delikaraoglou et al., 1986]. One of the principal goals of this project is to establish a

set of Active Control Points (ACP) as a zero-order network. First, these ACPs will be used to compute precise orbits, and second, by making available the observations recorded at each site, the network will be an accessible reference geodetic network. This new concept of a reference system involving GPS technology has begun to be investigated by other governement agencies [Merrell, 1986b].

At the Fourth International Geodetic Symposium on Satellite Positioning held in 1986, some preliminary results on GPS orbit estimation were presented based on the analysis of the HPBT data set [Abbot et al., 1986; Beutler et al. 1986; Williams, 1986; Wu et al., 1986]. All conclusions showed that results of the order of a few parts in a 10^7 accuracy level in the station coordinates and baseline length are achievable.

Beutler et al. [1987a] presented an improved solution for the 1984 Alaska GPS campaign using the whole data set (5 receivers, 8 stations). A comparison of the GPS and VLBI solutions, established through a seven-parameter tranformation, showed an agreement of the order of 0.1 ppm for the station coordinates. The approach used by the Bernese group to solve the orbit problem is slightly different than the fiducial approach. It is a solution, known as free-network, where the station and satellite coordinates are allowed to vary simultaneously in an adjustment by way of imposing relatively strong a priori constraints on the orbits and letting the terrestrial network adjust freely [Delikaraoglou, 1987].

Some other results on GPS solutions including orbital parameters were presented at the IUGG meeting held in Vancouver in 1987 [King et al., 1987; Delikaraoglou, 1987]. It was concluded that agreement between results from different research groups (Berne, Jet Propulsion Laboratory, Massachusetts Institute of Technology, National Geodetic Survey) was below the 0.1 ppm level in baseline-length repeatability.

Most of the results presented have been obtained from a 2-day (or more) orbital arc length. Although some analysis have been done on the capabilities of a solution over short-arc orbits (6-8 hrs), very few results (other than simulation) have been presented in the literature. One of the main interest of the short-arc approach is the simplified force model that can be used to generate the satellite orbits as well as the possibility to used the Keplerian approximation to generate the partial derivatives with respect the initial state vectors.

The scope of this thesis is to develop and to implement a short-arc orbit

improvement model in DIPOP 2.0 [Santerre et al., 1987a], the UNB GPS relative positioning program, using the double-difference observable. It will be shown, using a subset of the previously described HPBT March 1985 data set, that a short-arc orbit improvement of ~ 6-8 hours can easily produce results of the order of 0.1 - 0.2 ppm relative accuracy level in a network mode (including few observation sessions) or even in a daily network solution.

As will be explained later, a rigourous orbit improvement procedure implies that all satellite positions must be functionally related epoch to epoch. Thus, the equations of motion, describing the satellite trajectory, must be integrated from a set of initial conditions. A short-arc orbit integrator has been developed allowing initial conditions to be computed from broadcast ephemerides.

The processing of the HPBT TI 4100 data set gave us a severe problem at the pre-processing stage, the data being extensively corrupted by cycle slips. This problem led us to develop a dual-frequency code-receiver pre-processor having the capability (to a certain extent) to detect and correct the cycle slips automatically.

The principal contributions of this thesis can thus be divided into three parts: the development of a procedure to detect, estimate and correct cycle slips in dual frequency double-difference data, the development of an orbit integrator, and finally the development of a technique to estimate the orbital parameters in DIPOP 2.0 software. The thesis has been organized in the following way:

- Chapter 2 describes the physical approaches used in orbit improvement to estimate the orbital parameters; the Keplerian orbit, the perturbed orbit as well as the GPS force model are discussed.
- Chapter 3 deals with the orbital integrator. The equations of motion, the inertial system, the force model, the integration technique and the orbit representation are described.
- Chapter 4 is dedicated to our pre-processor. The automatic procedure and algorithms used to detect and correct the cycle slips are explained.
- Chapter 5 is devoted to the GPS observation modelling used in our processing. The current DIPOP 2.0 overall adjustment procedure is described and our major modifications are presented.
- Chapter 6 gives the results of the analysis of 4 days of the HPBT March 1985 data set.

2. ORBIT IMPROVEMENT CONCEPT

2.1 Statement of the problem

As is well known in Newtonian mechanics, the motion of a body in an inertial system can be easily described if the forces acting on the body are known. The dynamics of the body are usually expressed by the equations of motion, which provide a relationship between the state vector of the body at any given time and its initial state.

The equations of motion describing a satellite's trajectory, in a geocentric inertial rectangular coordinate system, are of the form:

$$\mathbf{r}'' = -\frac{GM\,\mathbf{r}}{|\mathbf{r}|^3} + \mathbf{P}'' \qquad (2.1)$$

where:

- $\mathbf{r}''$ is the total acceleration vector of the satellite,
- GM is the geocentric gravitational constant,
- $\mathbf{r}$ is the satellite position vector,
- $\mathbf{P}''$ is the vector sum of all perturbing specific forces (force per unit of mass) acting on the satellite.

As in every differential equation, a unique solution of equation (2.1) is defined only when the initial state of the system is known, i.e. a set of integration constants or initial conditions must be provided. Equation (2.1) being a second-order differential equation in a vectorial form (3-d system), six initial conditions are required: the initial position (x,y,z) and velocity (x', y', z') of the satellite or its equivalent osculating

Keplerian elements at the initial epoch: the semi-major axis of the orbit a_o, the eccentricity e_o, the inclination of the orbital plane i_o, the argument of perigee ω_o, the ascending node Ω_o and the time of perigee passage T_o. The transformation of a set of Cartesian positions and velocities at a given epoch into osculating Keplerian elements can be found in Martin et al. [1980].

Integration of equation (2.1) produces a set of satellite positions and velocities as a function of the initial conditions. An orbit improvement process involves the estimation of corrections to these initial conditions in order to estimate the best orbit from satellite observations obtained at sites of known position or whose coordinates are to be estimated simultaneously with the initial condition corrections [King et al. 1985]. These corrective terms are usually referred to as orbital parameters or orbital biases. The corrected initial conditions can be used, afterwards, to re-evaluate (by integration) a new set of satellite positions and velocities to be used in a subsequent solution. In a more general sense, some dynamical parameters, which are coefficients in the perturbing forces expression (GM, geopotential coefficients, solar radiation pressure coefficients, air drag coefficients, etc.) can be estimated in the same way. The determination of the six initial values, required in the improvement process, is usually referred to as orbit determination [Escopal, 1976].

Some other methods can be used to minimize the orbit errors. For example an a priori orbit obtained from a broadcast ephemeris can be approximated by some polynomial functions (e.g. Chebychev polynomial) where the coefficients can be estimated in the least-squares solution using observational data. The program GEODOP developed to analyse the TRANSIT signal, used a procedure where the orbital arcs are simply shifted and rotated. Although this technique can give interesting results (especially over small areas), the resulting orbital arcs are not a specific solution of the equations of motion, and are thus, physically imprecise [Vanicek et al., 1985].

Because the physical modelling approach (using an appropriate force model) is more rigorous, it has been decided to follow this procedure to develop our orbit improvement procedure. In order to explain the principles of the physical modelling solution, the non-perturbed and the perturbed motion of a satellite are described in the following sections.

2.2 Keplerian orbit

A spacecraft orbiting in a central force field without perturbations follows an elliptic trajectory which is known as a Keplerian orbit. The satellite motion in a central force field is also known as a two-body problem. The interesting point about this problem is that an analytical solution is possible. The solution, for planetary problems, was obtained at the beginning of the 17th century by J. Kepler and is summarized in his three famous laws:

- within the domain of the solar system all planets describe elliptical paths with the sun at one focus,
- the radius vector from the sun to a planet sweeps equal areas in equal times,
- the squares of the periods of revolution of the planets about the sun are proportional to the cubes of their mean distances from the sun.

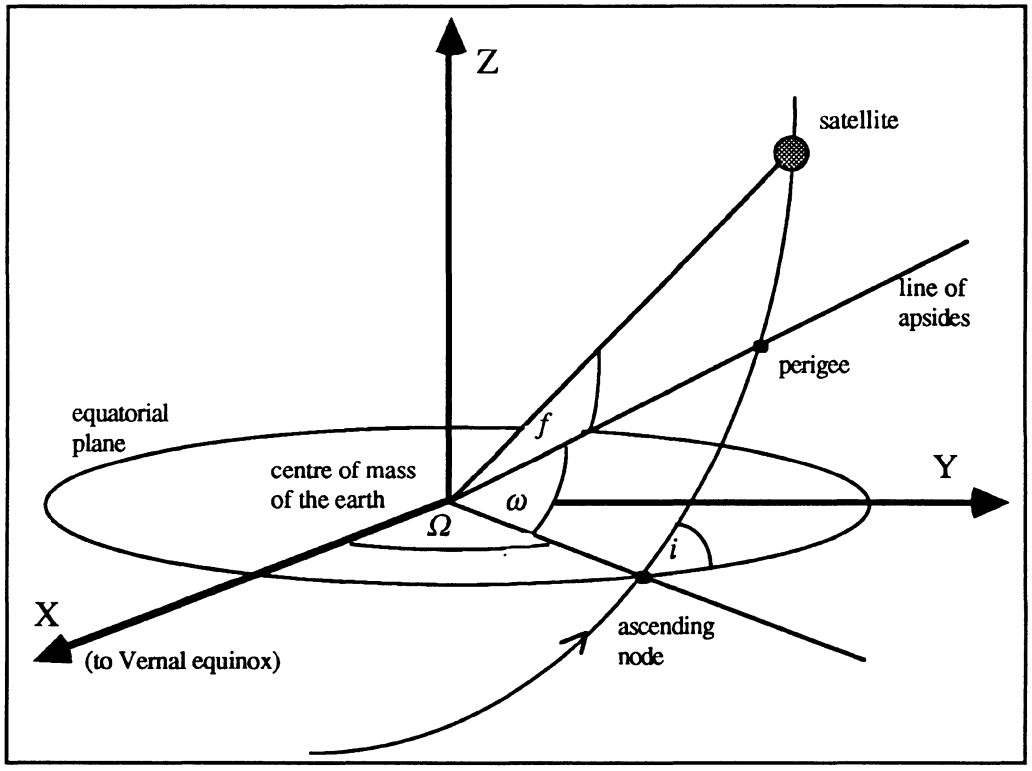

Keplerian orbit
FIGURE 2.1

These laws can be naturally extended to a satellite orbiting the earth. Although the mathematical expressions of these laws can be described in a Cartesian coordinate system, the usual way to represent an orbit is by means of the so-called Keplerian elements. Fig. 2.1 describes the geometry of the Keplerian orbit.

The shape and size of the elliptic path is given by the semi-major axis a and the eccentricity e; the orientation of the orbital plane with respect the inertial system is given by the inclination i and the right ascension of the ascending node Ω; and finally the position of the satellite on the ellipse is fixed by the argument of perigee ω and by the satellite anomaly or the time of perigee passage T. The perigee being the point of the satellite's closest approach to the earth, and the apogee being the point of farthest recession, both the perigee and the apogee lie at the ends of the semi-major axis of the orbital ellipse, called the line of apsides [Vanicek and Krakiwsky, 1986]. The satellite anomaly is the angular distance between the perigee and the satellite position on the ellipse. There are three kinds of anomaly, all of them related to each other.

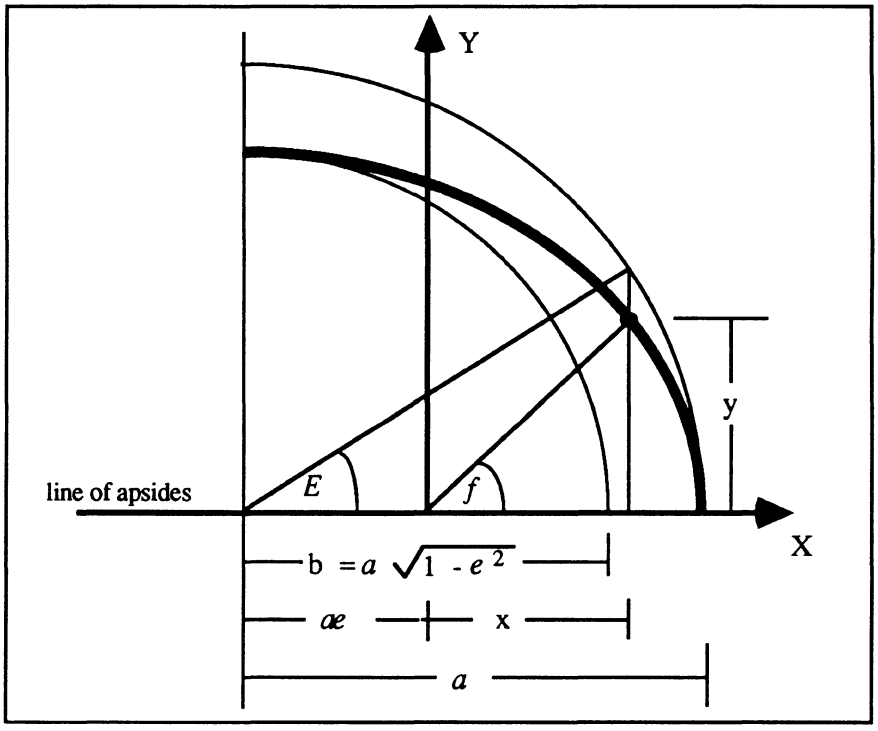

Orbital plane coordinates
FIGURE 2.2

The true anomaly f is the angle between the line of apsides and the line joining the focus to the satellite (see Fig. 2.2). The eccentric anomaly E is the angle between the line of apsides and the line joining the geometrical centre of the ellipse with the projection of the satellite position on the concentric circle of radius a. The mean anomaly M is the true anomaly corresponding to the motion of an imaginary satellite of uniform angular velocity.

The relationship between the true anomaly f and the eccentric anomaly E is easily deduced from Fig. 2.2 as:

$$\tan f = \frac{(1 - e^2)^{1/2} \sin E}{\cos E - e} \tag{2.2}$$

The relationship between the eccentric anomaly E and the mean anomaly M is given by Kepler's equation:

$$M = E - e \sin E \tag{2.3}$$

The mean motion n is a function of the geocentric gravitational constant GM and the semi-major axis a:

$$n = \sqrt{\frac{GM}{a^3}} \tag{2.4}$$

The mean anomaly M, the mean motion n, and the time of perigee passage T are related as follows:

$$n = \frac{M}{(t - T)} = \frac{M - M_o}{(t - T_o)} \tag{2.5}$$

T is defined as the time when $M = 0$, i.e. the epoch of the perigee passage, but T can be arbitrarily chosen as well at an epoch T_o where $M = M_o$.

The vis viva integral is also an interesting result deduced from the Keplerian orbit; it relates the specific kinetic energy K (kinetic energy per unit of mass) at a given epoch to the magnitude of the velocity $\mathbf{r}'$, the magnitude to the radius vector $\mathbf{r}$, and the semi-major axis a:

$$K = \frac{|\mathbf{r}'|^2}{2} = \frac{GM}{2}\left(\frac{2}{|\mathbf{r}|} - \frac{1}{a}\right) \tag{2.6}$$

Usually, the mean anomaly M is given (e.g. GPS broadcast message) and the eccentric anomaly E is required in order to compute the satellite Cartesian coordinates,

the coordinates being computed with the true anomaly f, which in turn is a function of E (eq. 2.2). This can be done by solving Kepler's equation (2.3) iteratively by a technique known as Newton's false root method [Krakiwsky and Wells, 1971]. Taking the total differential of equation 2.3,

$$\Delta M = (1 - e \cos E)\, \Delta E \tag{2.7}$$

Given M, we can start the iterative process by making $E_o = M$; using eq. 2.3 we have:

$$E \approx M + e \sin M \tag{2.8}$$

The iterative process is then performed using the following set of equations:

$$\begin{aligned} M_i &= E_i - e \sin E_i \\ \Delta M &= M - M_i \\ \Delta E &= \frac{\Delta M}{1 - e \cos E_i} \\ E_{i+1} &= E_i + \Delta E \end{aligned} \tag{2.9}$$

The process is repeated until convergence (i.e. ΔM is less than a certain small value). For small values of e, only two or three iterations are usually necessary.

For the computation of Cartesian satellite coordinates, let us assume for the time being that the coordinate system is an inertial frame defined as a right-handed system with a Z axis parallel to the CIO pole (average position of the rotation axis during the period 1900-1905) and an X axis directed towards the true vernal equinox (see Fig. 2.1). The procedure to obtain such a system is discussed in Section 3.3.

The first step is to compute a set of coordinates in the orbital plane, which is a rigth-handed system with an x axis being the line of apsides, the z axis perpendicular to the orbital plane. According to Fig. 2.2 and equation 2.2 we have:

$$\begin{bmatrix} x \\ y \\ z \end{bmatrix}_{orb} = r \begin{bmatrix} \cos f \\ \sin f \\ 0 \end{bmatrix} = \begin{bmatrix} a\,(\cos E - e) \\ a\,(1 - e^2)^{1/2} \sin E \\ 0 \end{bmatrix} \tag{2.10}$$

The inertial coordinates are obtained afterwards by three successive rotations to take into account the perigee angle, the inclination of the orbital plane and the right

ascension of the ascending node:

$$\begin{bmatrix} x \\ y \\ z \end{bmatrix}_{inertial} = R_3(-\Omega)\ R_1(-i)\ R_3(-\omega)\ \begin{bmatrix} x \\ y \\ z \end{bmatrix}_{orb} \tag{2.11}$$

The rotation matrices R_3 and R_1 are defined in Vanicek and Krakiwisky [1986].

In a central force field, five of the six Keplerian elements are constant; only the anomaly varies with time. From this point of view, a Keplerian orbit is known as a stationary orbit, since the elliptical path of the trajectory does not vary with time. When a satellite orbits the earth, its real trajectory departs from a Keplerian orbit since the force field acting on the satellite is not a perfect central force field.

There are perturbing forces, from different sources, acting on the spacecraft which cause the actual trajectory to depart from the ideal Keplerian orbit (elliptical motion). This real trajectory is still defined by Keplerian elements, but in this situation all of these are time-varying. At each epoch t, there is a specific set of Keplerian elements (osculating elements, $a(t)$, $e(t)$, $i(t)$, $\Omega(t)$, $\omega(t)$, $T(t)$) defining an ellipse which describes the instantaneous trajectory (osculating orbital ellipse); i.e, for a specific epoch t, the satellite rectangular coordinates can be computed with the previous formulas using these osculating elements. The inverse situation is the same: given a set of Cartesian coordinates and velocities, a set of osculating elements can be computed.

2.3 Perturbed orbit

The variation of Keplerian elements in time results in the regression of the nodes about the polar axis, constantly changing inclinations, the rotation of the line of apsides, and variations in the size and shape of the ellipse and the time of perigee passage. These perturbations can be classified by their period, and it is customary to divide them into secular, long-period, and short-period perturbations. In the case of secular perturbations the orbital element in question varies linearly (or very nearly so) with time. The long-period perturbations cause variations in the elements with relatively long periods. All other variations are short-period perturbations [Mueller, 1964].

These perturbations are usually expressed in the form of disturbing potential

functions R, which are to be added to the potential function describing a central field. The time derivatives of these elements, or linear perturbations, are given by the well-known Lagrangian equations [Mueller, 1964]:

$$\frac{d\Omega}{dt} = \frac{1}{n a^2 \sqrt{1-e^2}\ \sin i} \cdot \left(\frac{\partial R}{\partial i}\right)$$

$$\frac{di}{dt} = \frac{1}{n a^2 \sqrt{1-e^2}\ \sin i} \cdot \left(\frac{\partial R}{\partial \omega}\cos i - \frac{\partial R}{\partial \Omega}\right)$$

$$\frac{d\omega}{dt} = \frac{-\cos i}{n a^2 \sqrt{1-e^2}\ \sin i} \cdot \frac{\partial R}{\partial i} + \frac{\sqrt{1-e^2}}{n a^2 e} \cdot \frac{\partial R}{\partial e}$$

$$\frac{da}{dt} = \frac{2}{n a} \cdot \frac{\partial R}{\partial M}$$

$$\frac{de}{dt} = \frac{1-e^2}{n a^2 e} \cdot \frac{\partial R}{\partial M} - \frac{\sqrt{1-e^2}}{n a^2 e} \cdot \frac{\partial R}{\partial \omega}$$

$$\frac{dT}{dt} = \frac{1-e^2}{n^2 a^2 e} \cdot \frac{\partial R}{\partial e} + \frac{2}{n^2 a} \cdot \frac{\partial R}{\partial a} \qquad (2.12)$$

These perturbations are also known as first-order perturbations. For long- and short-period perturbations, a second-order correction can be obtained by solving equation set (2.12) a second time using the first-order results [Kaula, 1966].

The perturbing forces acting on earth satellites may be divided into two groups: gravitational and non-gravitational effects. By far the most important component of the gravitational effects is the one arising from the non-central part of the gravitational field, the elliptic term J_2 being the most important. The third-body effect is another source of gravitational disturbance. All surrounding celestial bodies possess their own attracting potentials, which "interfere" with the earth's attracting potential, the most important being those generated by the sun and the moon. Although of less importance, ocean and earth tides, which cause a variation of the mass distribution, introduce some perturbations which are also included in the gravitational effects.

Non-gravitational perturbations have less effect than gravitational perturbations

but should be taken into account to accurately model the satellite trajectory. One of the most important for low-orbiting satellites is air friction or drag. Since the atmospheric density decreases in altitude, the motion of a low-altitude satellite is more perturbed by collisions with air molecules than satellites orbiting at high-altitude. The magnitude of this force depends on the velocity (function of the altitude), the shape and size of the satellite as well as the atmospheric density.

The radiation from the sun in a whole spectrum of frequencies introduces another perturbation force, known as solar radiation pressure. This force is exerted by collisions of incoming photons, which are either absorbed or reflected and, in the process, they transfer some of their momentum to the spacecraft [Colombo, 1986]. The effect of this force depends largely on the mass of the satellite as well as its shape. Lighter and larger satellites are more affected than heavier and smaller ones. At higher altitudes this force is more important than air drag, even for small and heavy satellites. The direction of the biggest part of this force is usually given by the sun-satellite direction, but in certain cases, the solar radiation pressure can introduce a component in another direction due to different external factors, such as misalignment of the solar panel. This component is usually of less magnitude. The Y-bias effect on the GPS satellite is an example of such a perturbation [Fliegel et al., 1985].

The solar radiation also introduces an indirect effect: albedo pressure. This is simply the pressure of the portion of the direct radiation which is reflected from the surface of the earth. The disturbing acceleration introduced by this indirect effect is approximately two orders of magnitude smaller than the direct effect [Rizos and Stolz, 1985].

The list of non-gravitational forces can be extended to obtain more and more accurate modelling. These forces can range from the virtual effect introduced by the equations of motion written according to Newtonian mechanics, which neglects the relativistic effects [Martin et al., 1985], to the electromagnetic effects caused by the interaction between the electrical charge acquired by the satellite in the ionosphere and the magnetic field of the earth. However, for the level of accuracy sought for our orbital modelling (at the metre level), the perturbing forces described previously are the most important.

The disturbing acceleration vector sum, $\mathbf{P}''$, of equation (2.1) can thus be written in a more detailed form:

$$\mathbf{P}'' = \mathbf{p}''_g + \mathbf{p}''_d + \sum_{i=1}^{n} \mathbf{p}''_{ti} + \mathbf{p}''_{ot} + \mathbf{p}''_{et} + \mathbf{p}''_{rd} + \mathbf{p}''_{ri} + \sum_{i=1}^{m} \mathbf{p}''_{neg(i)} \qquad (2.13)$$

where:

$\mathbf{P}''$	is the vector sum of all perturbing accelerations acting on the close-orbiting satellite,
$\mathbf{p}''_g$	is the disturbing acceleration caused by the non-central part of the gravitational field,
$\mathbf{p}''_d$	is the disturbing acceleration caused by the air drag effect,
$\mathbf{p}''_{ti}$	is the disturbing acceleration introduced by the third-body effect from a celestial body i,
$\mathbf{p}''_{ot}$	is the disturbing acceleration introduced by ocean tides,
$\mathbf{p}''_{et}$	is the disturbing acceleration introduced by earth tides,
$\mathbf{p}''_{rd}$	is the disturbing acceleration caused by the direct effect of the solar radiation pressure,
$\mathbf{p}''_{ri}$	is the disturbing acceleration caused by the indirect effect of the solar radiation pressure (albedo effect),
$\mathbf{p}''_{neg(i)}$	is the sum of all neglected disturbing accelerations i.

If all the perturbing accelerations which are part of equation (2.13) were known, the satellite trajectory would by perfectly described. It is of course impossible to model all of these accelerations for the simple reason that not all of them are perfectly known and analytical expressions are impossible to obtain or are simply inaccurate.

The unmodelled perturbing accelerations will contaminate the satellite coordinates through the integration process as the integration interval or arc length increases; i.e. the absolute effect of an unmodelled acceleration is magnified in a long integration interval. Thus, for short-arc integration, only the principal disturbing accelerations have to be modelled in order to respect certain accuracy criteria, but to respect this same criteria over long orbital arcs, a better force field must be used.

The solved-for station coordinates from GPS observations being a function of the satellite coordinates, the compromise between the arc length and the force field is an important aspect of an orbit improvement process. The next section describes our adopted force field model for the GPS satellites.

2.4 GPS force model

The conventional way to analyze the effect of a perturbing force on the orbit trajectory (or Keplerian elements) is by means of the Lagragian equations. The potential of the disturbing force is introduced into the equation set (2.12) in order to evaluate the variation in Keplerian elements. This analytical procedure requires the disturbing potential in terms of Keplerian elements. This representation is rather complex to obtain and is not within the scope of this thesis.

Today, with computer facilities, the problem can be analyzed, to some extent, by a numerical approach. All possible forces are modelled and a reference trajectory is generated by integration; afterwards, the force field is modified by subtracting a specific force, and a new trajectory is generated according to this modified force field. The two trajectories can thus be compared to analyze the effect of the subtracted disturbing forces. Such analyses, for GPS satellites, have been performed by different investigators [Nakiboglu et al., 1984, Rizos and Stolz, 1985; Landau and Hagmaier, 1986]. Similar results are presented in chapter 6.

Table 2.1 summarizes the principal perturbations acting on the GPS trajectory with their magnitudes as a function of arc length. The current GPS satellites orbit approximately 20 000 km above the surface of the earth on a nearly circular orbit, with an inclination of ~64°. At this altitude, the atmosphere density is almost negligible and thus the air drag effect is negligible. However, at this altitude the direct effect of the solar radiation pressure is rather important.

It is clear from Table 2.1 that the accurate modelling of a satellite trajectory is a function of the arc length. For the purposes of this thesis, we have decided to use a short-arc orbit modelling (~6-8 hours) allowing a simple force-field model to respect the 2.5-metre level accuracy in satellite position in order to reach network solution at the ~0.1 ppm level (see eq. 1.1). Thus, the earth's non-central gravitational field, the sun's and moon's gravitational attraction and the direct solar radiation pressure will be taken into account in our equations of motion along with the central part of the earth's gravitational field. The mathematical expression of these perturbing forces as well as the integration technique used will be discussed in Chapter 3.

The next section describes the different approaches used to compute the partial derivatives included in the linearization of the satellite position as a function of the initial

state vector when the dynamical approach is used.

Source	average acceleration (m/sec^2)	perturbation (m)	
		3-hour arc	2-day arc
Earth's non-sphericity			
J_2 term	5×10^{-5}	~ 2 000	~14 000
other harmonics	3×10^{-7}	5 - 80	100 - 1 500
Third body effect			
Sun + moon effects	5×10^{-6}	5 - 150	1000 - 3 000
Tidal effects			
earth tides	1×10^{-9}	----	0.5 - 1.0
ocean tides	1×10^{-9}	----	0.0 - 2.0
Solar pressure			
direct effect	1×10^{-7}	5 - 10	100 - 800
indirect effect (albedo)	1×10^{-9}	----	1.0 - 1.5

Effects of perturbing forces on GPS satellites
(from King et al., 1985)
TABLE 2.1

2.5 Dynamical solution

The improvement problem will be solved by least-squares techniques where observations are involved. These observations, which will be described in Chapter 5, are a function of the station coordinates, satellite coordinates and all other parameters involved in the solution, such as ambiguities, relative clock misalignment, etc. The linearization of the observations as a function of satellite coordinates is straightforward (see Chapter 5), but these satellite coordinates are in turn non-linear functions of the initial state vector of the satellite.

Let us assume for the time being that our epoch state vector (**S**) contains the

initial state of the satellite at the initial epoch (t_o) and one dynamical parameter C_r related to the solar radiation pressure. All the other parameters (the geocentric gravitational constant, GM; the geopotential coefficients, $C_{n,m}$ and $S_{n,m}$, etc.) are assumed to be known with sufficient accuracy:

$$\mathbf{S} = \{x_o, y_o, z_o, x'_o, y'_o, z'_o, C_r\}.$$

The linearization procedure of the satellite trajectory assumes that an a priori orbit $\mathbf{r}_a(t)$ obtained from a state vector **S** must be improved in order to obtain a correct (in a least-squares sense) orbit $\mathbf{r}(t)$ from an improved set of initial conditions **S'**. The linearization can thus be written in the following form [Beutler et al., 1984a]:

$$\mathbf{r}(t) = \mathbf{r}_a(t) + \sum_{i=1}^{7} \left[\frac{\partial \mathbf{r}_a(t)}{\partial s_i} \right] (s_i' - s_i) \qquad (2.14)$$

where the terms s_i and s'_i are elements of the vector **S** and **S'**.

There are two ways to compute the partial derivatives of the satellite position $\mathbf{r}_a(t)$ with respect the state vector **S**: a numerical procedure and an analytical one. The numerical procedure calls for a numerical integration process where the partial derivatives are the solution of second-order differential equations known as variational equations. In orbit problems these partials are therefore known as variational partials. The variational equations have the same relationship to the variational partials as the satellite position vector does to the equations of motion [Martin et al., 1980]. These equations are usually written in matrix form. To do this, let us write equation (2.1) in the following form:

$$\mathbf{r}'' = \nabla U + \mathbf{p}''_r \qquad (2.15)$$

where all the gravitational perturbations as well as the central part of the gravitational field are regrouped and represented in a potential form U, $\mathbf{p}''_r$ being the acceleration introduced by the direct solar radiation pressure effect. All other non-gravitational perturbations have been discarded for the demonstration. By differentiating equation (2.15) with respect to the state vector **S**, we obtain the variational equations in vector form:

$$\frac{\partial \mathbf{r}''}{\partial S} = \frac{\partial}{\partial S}(\nabla U + \mathbf{p}''_r) \tag{2.16}$$

The variational partials ($\partial \mathbf{r}/\partial S$) being a solution of equation (2.16), the similarity to the equations of motion is obvious. It must now be understood that the potential field is only a function of position; thus, the components of the first term of the right-hand side of equation (2.16) can be written as follows:

$$\frac{\partial}{\partial S}\left(\frac{\partial U}{\partial r_i}\right) = \sum_{m=1}^{3}\left(\frac{\partial^2 U}{\partial r_i \, \partial r_m}\right)\frac{\partial r_m}{\partial S} \tag{2.17}$$

It must also be understood that the partials of the solar radiation pressure with respect to the satellite velocity are zero and with respect to the satellite position are negligible [Martin et al., 1980]. Accordingly, the variational equations in matrix form can be written as follows:

$$\mathbf{F} = \mathbf{A}\,\mathbf{X} + \mathbf{K} \tag{2.18}$$

where the matrix **F** represents the left hand-side of equation (2.16):

$$\underset{(3x7)}{\mathbf{F}} = \begin{bmatrix} \frac{\partial x''}{\partial x_o} & \frac{\partial x''}{\partial y_o} & \frac{\partial x''}{\partial z_o} & \frac{\partial x''}{\partial x'_o} & \frac{\partial x''}{\partial y'_o} & \frac{\partial x''}{\partial z'_o} & \frac{\partial x''}{\partial C_r} \\ \frac{\partial y''}{\partial x_o} & \frac{\partial y''}{\partial y_o} & \frac{\partial y''}{\partial z_o} & \frac{\partial y''}{\partial x'_o} & \frac{\partial y''}{\partial y'_o} & \frac{\partial y''}{\partial z'_o} & \frac{\partial y''}{\partial C_r} \\ \frac{\partial z''}{\partial x_o} & \frac{\partial z''}{\partial y_o} & \frac{\partial z''}{\partial z_o} & \frac{\partial z''}{\partial x'_o} & \frac{\partial z''}{\partial y'_o} & \frac{\partial z''}{\partial z'_o} & \frac{\partial z''}{\partial C_r} \end{bmatrix}$$

where the vector {x, y, z, x', y', z', x", y", z"} is the satellite position, velocity and acceleration at epoch (t). The matrix **A** contains the partial derivatives of the potential field U with respect the satellite position at epoch (t):

$$\underset{(3x6)}{\mathbf{A}} = \begin{bmatrix} \frac{\partial^2 U}{\partial x\,\partial x} & \frac{\partial^2 U}{\partial x\,\partial y} & \frac{\partial^2 U}{\partial x\,\partial z} & 0 & 0 & 0 \\ \frac{\partial^2 U}{\partial y\,\partial x} & \frac{\partial^2 U}{\partial y\,\partial y} & \frac{\partial^2 U}{\partial y\,\partial z} & 0 & 0 & 0 \\ \frac{\partial^2 U}{\partial z\,\partial x} & \frac{\partial^2 U}{\partial z\,\partial y} & \frac{\partial^2 U}{\partial z\,\partial z} & 0 & 0 & 0 \end{bmatrix}$$

The matrix **X** contains the variational partials:

$$\underset{(6x7)}{\mathbf{X}} = \begin{bmatrix} \frac{\partial x}{\partial x_o} & \frac{\partial x}{\partial y_o} & \frac{\partial x}{\partial z_o} & \frac{\partial x}{\partial x'_o} & \frac{\partial x}{\partial y'_o} & \frac{\partial x}{\partial z'_o} & \frac{\partial x}{\partial C_r} \\ \frac{\partial y}{\partial x_o} & \frac{\partial y}{\partial y_o} & \frac{\partial y}{\partial z_o} & \frac{\partial y}{\partial x'_o} & \frac{\partial y}{\partial y'_o} & \frac{\partial y}{\partial z'_o} & \frac{\partial y}{\partial C_r} \\ \frac{\partial z}{\partial x_o} & \frac{\partial z}{\partial y_o} & \frac{\partial z}{\partial z_o} & \frac{\partial z}{\partial x'_o} & \frac{\partial z}{\partial y'_o} & \frac{\partial z}{\partial z'_o} & \frac{\partial z}{\partial C_r} \\ \frac{\partial x'}{\partial x_o} & \frac{\partial x'}{\partial y_o} & \frac{\partial x'}{\partial z_o} & \frac{\partial x'}{\partial x'_o} & \frac{\partial x'}{\partial y'_o} & \frac{\partial x'}{\partial z'_o} & \frac{\partial x'}{\partial C_r} \\ \frac{\partial y'}{\partial x_o} & \frac{\partial y'}{\partial y_o} & \frac{\partial y'}{\partial z_o} & \frac{\partial y'}{\partial x'_o} & \frac{\partial y'}{\partial y'_o} & \frac{\partial y'}{\partial z'_o} & \frac{\partial y'}{\partial C_r} \\ \frac{\partial z'}{\partial x_o} & \frac{\partial z'}{\partial y_o} & \frac{\partial z'}{\partial z_o} & \frac{\partial z'}{\partial x'_o} & \frac{\partial z'}{\partial y'_o} & \frac{\partial z'}{\partial z'_o} & \frac{\partial z'}{\partial C_r} \end{bmatrix}$$

and finally the matrix **K** is the direct derivative of the solar radiation pressure with respect to the elements of the vector **S**:

$$\underset{(3x7)}{\mathbf{K}} = \begin{bmatrix} 0 & 0 & 0 & 0 & 0 & 0 & \frac{\partial \mathbf{p}''_{rx}}{\partial C_r} \\ 0 & 0 & 0 & 0 & 0 & 0 & \frac{\partial \mathbf{p}''_{ry}}{\partial C_r} \\ 0 & 0 & 0 & 0 & 0 & 0 & \frac{\partial \mathbf{p}''_{rz}}{\partial C_r} \end{bmatrix}$$

Matrices **A** and **X** can be split into two parts and (2.18) can be rewritten as follows:

$$\mathbf{F} = \mathbf{A}_1\mathbf{X}_1 + \mathbf{A}_2\mathbf{X}_2 + \mathbf{K} \tag{2.19}$$

where $\mathbf{A}_1$ is the first three columns of **A**; $\mathbf{A}_2$ is the three last columns of **A**; $\mathbf{X}_1$ is the first three rows of **X**; and finally $\mathbf{X}_2$ is the three last rows of **X**. This is the form of variational equations presented in Beutler et al. [1984a]. It should be noted that when there is no air drag perturbation, matrix $\mathbf{A}_2$ is a null matrix, i.e. on the right-hand side of the equations of motion the velocity (x', y', z') does not appear. When the numerical approach is used, the variational equations are integrated along with the equations of motion. This integration procedure rigorously propagates the errors of the initial-state vector along the trajectory according to a specific force field. For long-arc integration such a procedure is essential, the GEODYN [Martin et al., 1980] and the PEP [Ash, 1972] program suites making extensive use of this approach.

The second approach is analytical. As mentioned in Section 2.3, the perturbed Keplerian elements can be obtained analytically as a function of the disturbing potential using the Lagrange equations. If such a representation is available, the partial derivatives follow simply by differentiating the system of equations. Moreover, approximations of these partials are easily obtained. It has been shown by Beutler et al. [1984a] that even a Keplerian approximation can be used with short-arc orbit improvement to evaluate the partial derivatives of the satellite position with respect to the initial state vector. This procedure greatly simplifies the implementation of the partials computation without affecting the results when short orbital arcs are used.

The short-arc approach being adopted in our orbit improvement procedure, we decided to used the Keplerian approximation to compute analytically the variational partials. The mathematical development of these partials is given in Section 5.2.5. The integration of the equations of motion is discussed in the next chapter.

3. ORBITAL INTEGRATOR

3.1 Analytical versus numerical methods

As with the variational equations, the equations of motion (2.1) can be integrated numerically or analytically. The principal advantages and disadvantages of each approach have been summarized by Beutler et al. [1984a]:

Numerical methods, advantages:

a) There is no heavy algebra involved, we need only to code a subroutine giving the right-hand side of equation (2.1).
b) Numerical methods are easy to generalize: modelling an additional force merely introduces a new term in equation (2.1).
c) Apart from round-off errors, the approximation can be generated as precisely as desired.

Numerical methods, disavantages:

a) The integration itself is a heavy consumer of computer time.
b) Numerical methods are said to be less transparent.

Analytical method, advantages:

a) The solutions are explicitly given as functions of the unknown parameters. As mentioned earlier, the partials with respect to these unknowns follow simply by differentiating the analytical expression, and simple approximations of partials are easy to compute.

b) Values of the solution for different times are readily available.

Analytical method, disadvantages:

a) Heavy algebra is involved; generalizations are not easy to implement.
b) Many trigonometric functions have to be evaluated.
c) The solutions obtained are always approximate (Keplerian, first-order second-order, ..., nth-order perturbations).

A practical comparison of the two techniques has been performed by the University of Calgary [Nakiboglu et al. 1985]. It has been demonstrated that for short-arc orbit integrations (4 hours), the linear perturbation coupled with a second-order perturbation for e, ω and M were sufficient to respect the one-meter level accuracy in the satellite position (this solution also includes a second-order effect due to J_2). But this analysis showed that from the computer-time point of view, the numerical method is preferable.

One of the most important aspects of the numerical method is that the generalization is very easy to implement: to include a new perturbing force in the force model, a subroutine is simply coded. This means that a very sophisticated force model can be coded in a general program but the final choice for a specific application can be user-selectable.

Although the analytical Keplerian approximation has been chosen for the partial derivatives computation, we have opted for the numerical method to integrate the equations of motion because of the obvious advantages of modularity and the facility of implementation. The computer-time disadvantage of the numerical method is not a major problem with the current computers, since in the overall procedure, as will be explained in Chapter 6, the orbit integration takes only a fraction of the processing time when GPS networks are concerned.

The numerical integration of the equations of motion is performed directly in Cartesian coordinates. This method is known as Cowell's method [Conte, 1963]. Different techniques can be used to perform this integration. Section 3.6 describes our numerical integration technique.

3.2 Equations of motion

As mentioned in Section 2.4, the perturbation accelerations which must be modelled in order to respect the 2.5-metre level for short arcs (~6-8 hours) are the earth's non-central gravitational field, the gravitational effect of the sun and the moon, and the direct effect of solar radiation pressure. For practical purposes, the equations of motion (2.1) can be simplified as follows:

$$\mathbf{r}'' = \mathbf{r}''_g + \left[\mathbf{p}''_g + \mathbf{p}''_s + \mathbf{p}''_m + \mathbf{p}''_{rd}\right] \tag{3.1}$$

where:

- $\mathbf{r}''$ is the total acceleration vector of the satellite,
- $\mathbf{r}''_g$ is the acceleration vector due to the central part of the earth's gravitational field,
- $\mathbf{p}''_g$ is the disturbing acceleration vector due to the non-central part of the earth's gravitational field,
- $\mathbf{p}''_s$ is the disturbing acceleration vector introduced by the sun's gravitational effect,
- $\mathbf{p}''_m$ is the disturbing acceleration vector caused by the moon's gravitational effect,
- $\mathbf{p}''_{rd}$ is the disturbing acceleration vector introduced by the direct effect of solar radiation pressure.

The terms in brackets are the biggest components of equation (2.13). In practice, the terms $\mathbf{r}''_g$ and $\mathbf{p}''_g$ are evaluated together by taking the gradient of the earth's gravitational potential expressed in spherical harmonics. The third-body effects $\mathbf{p}''_s$ and $\mathbf{p}''_m$ are evaluated by the same algorithm using different parameters. Finally, we evaluate the solar radiation pressure by a simple model. All the mathematical expressions used in these computations are given in the subsequent sections.

With Cowell's method of integration, all of these accelerations must be written in a common Cartesian coordinate system, and to respect Newtonian mechanics the adopted system must be inertial, i.e. a non-accelerated system. The next section describes the usual coordinate systems used in orbit computation, and the method of

obtaining an inertial frame for short-arc orbits is discussed.

3.3 Coordinate systems

The most convenient reference system for orbit computation is a system with its origin at the earth's centre of mass, referred to as a geocentric reference system. There are several geocentric coordinate systems, the orientation of some being defined according to the direction of the line pointing toward the vernal equinox (intersecting line of the equatorial plane and the ecliptic), and others being attached to the rotating earth. The most important systems related to orbit computation are the following:

Instantaneous terrestrial system

This is a right-handed orthogonal geocentric system, with the Z axis pointing north along the instantaneous axis of rotation and with the X axis in the equatorial plane pointing toward the Greenwich meridian. The Y axis completes the right-handed sytem. It is a rotating system.

Earth-fixed system

The Earth-fixed or Conventional Terrestrial system has the same characteristics as the instantaneous terrestrial system except that the Z axis is aligned with the mean pole of the earth defined by the CIO (Conventional International Origin), which is the mean position of the instantaneous pole during the period 1900 to 1905. The relation between these two systems is given by the wobble rotation matrix.

True-of-date coordinate system

The true-of-date coordinate system is a right-handed orthogonal geocentric system, with the Z axis pointing along the instantaneous axis of rotation, and the X axis pointing toward the vernal equinox of date. The relation between this system and the instantaneous terrestrial sytem is given by the rotation angle θ, which represents the hour angle of the true equinox of date with respect to the Greenwich meridian as measured in the equatorial plane.

Mean equinox of date system

The true-of-date vernal equinox direction varies with time under the effect of precession and nutation [Mueller, 1969]. The luni-solar precession produces a gyration of the earth's axis which describes a cone with a generating angle of ~23.5° about the pole of the ecliptic, so that the vernal point travels on the ecliptic at a rate of ~50.4" per year making a complete revolution in about 25 800 years [Torge, 1980]. The effect of the planets and the moon introduce a periodic motion of the vernal point in the ecliptic plane as well as in the equatorial plane. This periodic motion is known as nutation (amplitude ~9.2" with a dominant period of ~18.6 years). When the effects of nutation are removed from the true-of-date coordinate system, the resulting system is known as the mean equator and equinox of the date.

The precession effect is removed to relate a mean equinox of date system to another identical system defined with respect to a particular date. For example, most of the astronomical quantities given in the Astronomical Almanac are related since 1984 to the J2000 system, which is a mean equator and equinox system defined for the epoch 12 hours TDB (Barycentric Dynamical Time) on 1 January, 2 000.

Since the instantaneous terrestrial system and the earth-fixed system are not inertial owing to the acceleration introduced by the rotation of the earth, they cannot be used for integration of the equations of motion. Ideally the mean equinox of date (of a particular epoch) would be the best inertial system to use, however, from a practical point of view, over short periods of time (~6-8 hours), the effect of the precession and nutation are negligible (less than the metre level) and the true of date system can be used as the inertial system. Such a simplification has been done by Beutler [1984b].

In our development the inertial system adopted is the true-of-date of the initial epoch of the integration period. Thus, to transform a satellite state vector from our inertial system to the Conventional Terrestrial system (Earth-fixed), only the wobble rotation and the Greenwich Apparent Sidereal Time (GAST) rotation have to be applied. This transformation can be written as follows:

$$\mathbf{r}_{ct} = \mathbf{W}\mathbf{S}\,\mathbf{r}_i \tag{3.2}$$

$$\mathbf{r}'_{ct} = \mathbf{W}\mathbf{S}\,\mathbf{r}'_i + (\mathbf{W}\mathbf{S})'\,\mathbf{r}_i \tag{3.3}$$

where:

$\mathbf{r}_{ct}$, $\mathbf{r}_i$	are the satellite position vectors in the Conventional Terrestrial system and in the inertial system (true-of-date),
$\mathbf{r}'_{ct}$, $\mathbf{r}'_i$	are the satellite velocity vectors in the Conventional Terrestrial system and in the inertial system (true-of-date),
W	is the wobble rotation matrix,
S	is the GAST rotation matrix,
(WS)'	is the time derivative of the product **WS**.

The wobble being considered constant over the integration interval, in our computation **(WS)' = WS'**. Matrices **W** and **S** are given as follows:

$$\mathbf{W} = \begin{bmatrix} 1 & 0 & x_p \\ 0 & 1 & -y_p \\ -x_p & y_p & 1 \end{bmatrix}$$

$$\mathbf{S} = \begin{bmatrix} \cos\theta & \sin\theta & 0 \\ -\sin\theta & \cos\theta & 0 \\ 0 & 0 & 1 \end{bmatrix}$$

θ is the GAST angle, x_p and y_p are the pole coordinates (angular units) and the matrix **S'** is the derivative of **S**. The inverse computation is performed by using the transpose of the rotation matrices since they are orthogonal matrices. The GAST computation is given in Kaplan [1981].

3.4 Mathematical expressions of the perturbing forces

3.4.1 Earth's gravitational field

The usual representation of the earth's gravitational potential field U is given in

the spherical harmonics expansion [Torge, 1980]:

$$U = \frac{GM}{r}\left\{1 + \sum_{n=2}^{\infty}\sum_{m=0}^{n}\left(\frac{a_e}{r}\right)^n P_n^m(\sin\phi)\left[C_{nm}\cos m\lambda + S_{nm}\sin m\lambda\right]\right\} \qquad (3.4)$$

where:

ϕ	is the geocentric latitude;
λ	is the east longitude, in an Earth-fixed system;
r	is the geocentric satellite distance;
GM	is the geocentric gravitational constant;
a_e	is the earth's mean equatorial radius;
$P_n^m(\sin\phi)$	is the associated Legendre function;
C_{nm}, S_{nm}	are the denormalized geopotential coefficients;

The spherical coordinates used in equation (3.4) are related to an Earth-fixed system; therefore the relationship between these coordinates and the inertial satellite coordinates (x, y, z) is given as follows, θ being the GAST angle:

$$\begin{aligned} r &= \sqrt{x^2 + y^2 + z^2} \\ \phi &= \sin^{-1}\left(\frac{z}{r}\right) \\ \lambda &= \tan^{-1}\left(\frac{y}{x}\right) - \theta \end{aligned} \qquad (3.5)$$

The coordinate transformation through equations (3.5) is important since the earth's potential field is not rotationally symmetric [Vanicek, 1973].

The acceleration of a satellite caused by the earth's gravity field is given by the gradient of the potential field U at the satellite position:

$$\begin{aligned} x'' &= \frac{\partial U}{\partial x} = \frac{\partial U}{\partial r}\frac{\partial r}{\partial x} + \frac{\partial U}{\partial \phi}\frac{\partial \phi}{\partial x} + \frac{\partial U}{\partial \lambda}\frac{\partial \lambda}{\partial x} \\ y'' &= \frac{\partial U}{\partial y} = \frac{\partial U}{\partial r}\frac{\partial r}{\partial y} + \frac{\partial U}{\partial \phi}\frac{d\phi}{\partial y} + \frac{\partial U}{\partial \lambda}\frac{\partial \lambda}{\partial y} \end{aligned} \qquad (3.6)$$

$$z'' = \frac{\partial U}{\partial z} = \frac{\partial U}{\partial r}\frac{\partial r}{\partial z} + \frac{\partial U}{\partial \phi}\frac{\partial \phi}{\partial z} + \frac{\partial U}{\partial \lambda}\frac{\partial \lambda}{\partial z}$$

where the related derivatives with respect to the spherical coordinates are the following:

$$\frac{\partial U}{\partial r} = -\frac{GM}{r^2}\left\{1 + \sum_{n=2}^{\infty}\sum_{m=0}^{n}\left(\frac{a_e}{r}\right)^n (n+1)\, P_n^m(\sin\phi)\left[C_{nm}\cos m\lambda + S_{nm}\sin m\lambda\right]\right\} \quad (3.7)$$

$$\frac{\partial U}{\partial \lambda} = \frac{GM}{r}\left\{\sum_{n=2}^{\infty}\sum_{m=0}^{n}\left(\frac{a_e}{r}\right)^n m\, P_n^m(\sin\phi)\left[S_{nm}\cos m\lambda - C_{nm}\sin m\lambda\right]\right\} \quad (3.8)$$

$$\frac{\partial U}{\partial \phi} = \frac{GM}{r}\left\{\sum_{n=2}^{\infty}\sum_{m=0}^{n}\left(\frac{a_e}{r}\right)^n \left(C_{nm}\cos m\lambda + S_{nm}\sin m\lambda\right)\frac{\partial}{\partial \phi}\left[P_n^m(\sin\phi)\right]\right\} \quad (3.9)$$

where the derivative of the Legendre polynomial is:

$$\frac{\partial}{\partial \phi}\left[P_n^m(\sin\phi)\right] = P_n^{m+1}(\sin\phi) - m(\tan\phi)\, P_n^m(\sin\phi). \quad (3.10)$$

The derivatives of the spherical coordinates with respect to the Cartesian coordinates are straightfoward (with $r_1 = x$, $r_2 = y$ and $r_3 = z$):

$$\begin{aligned}
\frac{\partial r}{\partial r_i} &= \frac{r_i}{r} \\
\frac{\partial \phi}{\partial r_i} &= \frac{1}{\sqrt{x^2+y^2}}\left[\frac{-z r_i}{r^2} + \frac{\partial z}{\partial r_i}\right] \\
\frac{\partial \lambda}{\partial r_i} &= \frac{x}{y^2+x^2}\left[\frac{\partial y}{\partial r_i} - \frac{y}{x}\frac{\partial x}{\partial r_i}\right]
\end{aligned} \quad (3.11)$$

The geopotential coefficients that have been used in this work are those of the

GEM-L2 solution given in Melbourne et al. [1983]; the GM and a_e constants are those related to this specific solution. The GEM-L2 coefficients published are the normalized coefficients; the denormalized coefficients have been obtained by applying the following factor [Lambeck and Coleman, 1983]:

$$C_{nm} = \left[\frac{(n-m)!\ (2n+1)\ (2-\delta_m)}{(n+m)!} \right]^{1/2} \bar{C}_{nm} \qquad (3.12)$$

$\bar{C}_{nm}$ being the normalized coefficients, the same relation is valid for $\bar{S}_{nm}$ and S_{nm}, δ_m is the Kronecker delta function; $\delta_m = 1$, for $m = 0$ and $\delta_m = 0$, for $m \neq 0$.

These expressions have been programmed in a FORTRAN subroutine GRAVI, which calls the subroutine LEGEN to evaluate the associated Legendre functions and the subroutine IRTV to retrieve the geopotentiel coefficients. The coefficients are denormalized by a separate subroutine DENOR. The output of the subroutine GRAVI is the vector $(\mathbf{r}''_g + \mathbf{p}''_g)$ of equation (3.1) in our inertial system.

3.4.2 Third-body effect

The perturbing acceleration introduced by a third body is easily described in a Cartesian coordinate system (see Fig. 3.1). The acceleration is proportional to the force exerted on the satellite by the third body minus the acceleration of the geocentre due to the gravitational forces exerted on the earth by the same third body [Nakiboglu et al., 1985]. In a vectorial form, the acceleration is given as follows:

$$\mathbf{r}''_T = GM_T \left[\frac{(\mathbf{r}_T - \mathbf{r}_s)}{|\mathbf{r}_T - \mathbf{r}_s|^3} - \frac{\mathbf{r}_T}{|\mathbf{r}_T|^3} \right] \qquad (3.13)$$

where:

$\mathbf{r}''_T$	is the perturbing acceleration vector introduced by the third body,
GM_T	is the third body gravitational constant,
$\mathbf{r}_T$	is the geocentric position vector of the third body,
$\mathbf{r}_s$	is the geocentric position vector of the satellite.

In this formulation, only the central part of the third body's gravitational field is

taken into account; for short integration interval (6-8 hours) at GPS satellite altitudes the non-central part can be neglected. Thus, the perturbed acceleration can be directly computed in the inertial system since the orientation of the disturbing mass is not important.

The geocentric position vector of the sun is computed using a modified version of the subroutine SUN [Beutler, 1984b]. The original version of this subroutine computes the sun's position in the mean equator of 1950.0 system using Simon Newcomb's tables of the sun. This modification gives the sun's position in the mean equator of computation's date system; thus to obtain the position in our true-of-date inertial system, the nutation rotation matrix is simply applied. The nutation model used (IAG 1980) can be found in Kaplan [1981] and Wahr [1981].

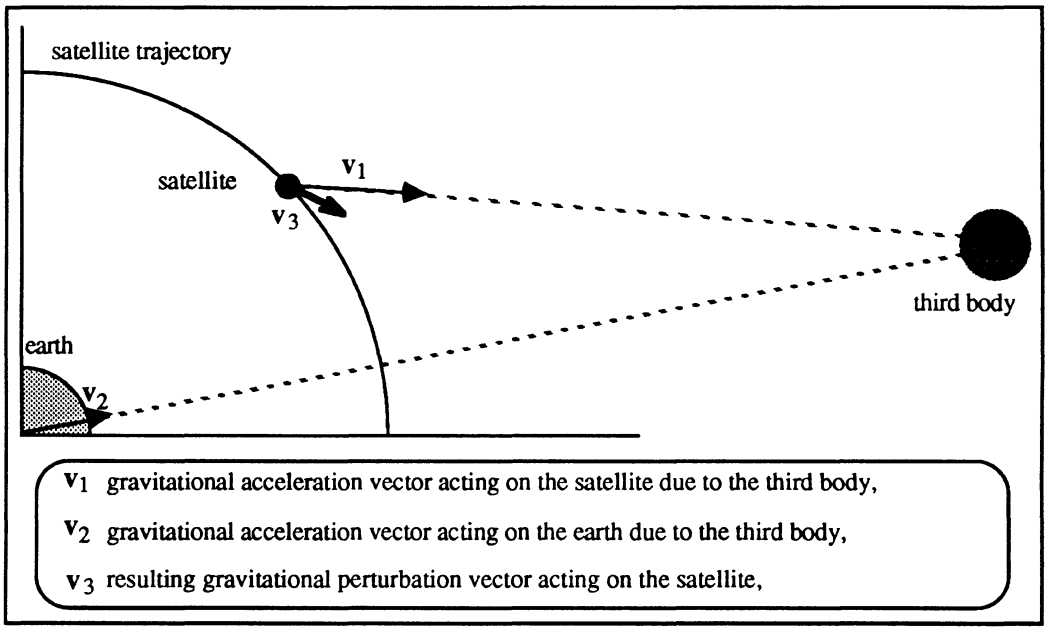

Third body disturbing acceleration
FIGURE 3.1

The true-of-date moon position is obtained directly using the subroutines MOON and MONTSO [Beutler, 1984b]. The gravitational constant GM_T for the moon and the sun are from Melbourne et al. [1983]. A subroutine THBOD has been coded to compute the disturbing accelerations introduced by the sun and the moon. The

acceleration vectors $\mathbf{r}''_s$ and $\mathbf{r}''_m$ of equation (3.1) are thus computed by the subroutine THBOD with appropriate values as input (i.e, GM_m or GM_s and $\mathbf{r}_m$ or $\mathbf{r}_s$); the output vector is in the same system as the input vector.

3.4.3 Solar radiation pressure

The disturbing effect of solar radiation pressure is the most difficult perturbation to model for GPS satellites. The acceleration is a function of different parameters which are themselves difficult to model; the solar radiation pressure P_s is not constant and may vary by about 7% over a year [King et al., 1985]; the mass (m) of the satellite varies after each manoeuvre when fuel is consumed; the satellite being of irregular shape, the area (A) facing the sun varies as the satellite moves in its orbit; and the reflectivity (C_r) properties of the different components of the GPS satellite are different. A model which would take into account all of these characteristics is very difficult to work out.

The usual approximation of this problem is a simple model (cannonball model) which represents the direct effect of the solar radiation pressure on a spherical satellite of constant reflectivity factor (C_r) in the sun-satellite direction:

$$\mathbf{r}''_{rd} = - \nu \; P_s \; C_r \; \frac{A}{m} \; \frac{(\mathbf{r}_{sun} - \mathbf{r}_s)}{|\mathbf{r}_{sun} - \mathbf{r}_s|} \tag{3.14}$$

where:

$\mathbf{r}_{sun}$ is the geocentric sun position vector,

$\mathbf{r}_s$ is the geocentric satellite position vector,

ν is the eclipse factor ($0 < \nu < 1$) which is the fraction of the sun's disk covered by the earth as seen from the satellite,

all the other terms being previously defined.

The "unknown" constants P_s (Newton/m^2), C_r (unitless), and A/m (m^2/kg) of equation (3.14) are often grouped together in one term usually known as the direct solar radiation pressure parameter [Beutler et al., 1986]:

$$\mathbf{r}''_{rd} = - \nu \cdot p_0 \cdot \mathbf{e}_0 \tag{3.15}$$

where:

p_0 is the direct solar radiation pressure parameter,

$\mathbf{e}_0$ is unit vector pointing from the satellite to the sun.

Owing to the uncertainties about the parameter p_0, it is a usual procedure to estimate it in the solution along with the six initial conditions of the satellite. The nominal value for p_0 is ~ 1.0×10^{-7} m/s^2 [Van Dierendonck et al., 1980]. This value can vary up to 20% [Beutler et al., 1986]. As will be shown in Chapter 6, for short-arc lengths of ~6-8 hours, a constant value p_0 (at ± 10%) can be used without problem if the 2.5-metre level accuracy in the satellite position is acceptable. Thus, in our development there is no estimation of solar radiation pressure parameters.

As mentioned in Section 2.4, the so-called Y-axis bias introduces a perturbed acceleration other than in the sun-satellite direction of the order of 10^{-9} m/sec^2. The magnitude of this acceleration being so small, it is completly unnecessary to take it into account in our force model for short-arc modelling.

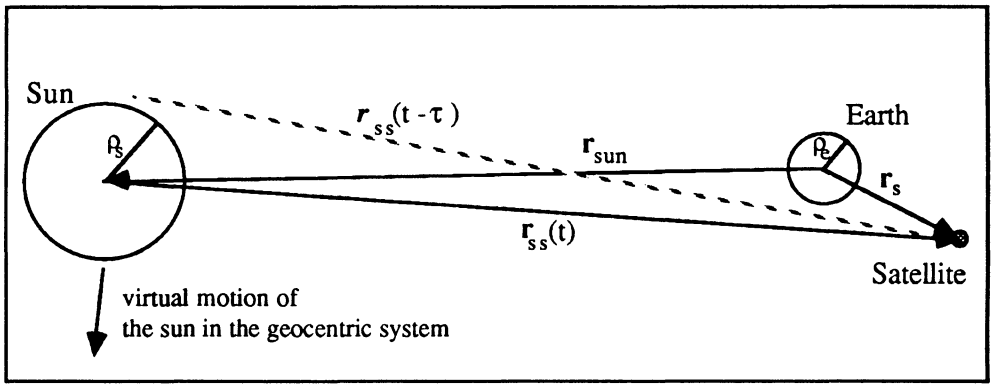

Relative positions of sun-earth-satellite for penumbra factor calculation
FIGURE 3.2

The penumbra factor ν of equation (3.14) and (3.15) has a certain importance in the integration process. The factor ν must gradually change between 0 and 1 when entering and leaving shadow zones in order to smooth the abruptness for reasons of numerical integration stability in addition to the fact that things happen this way in nature [Ash, 1972]. We have implemented a modification of the penumbra factor by R. Reasenberg [Ash, 1972] in our orbital integrator.

According to Fig. 3.2, when the magnitude of the sun-satellite vector $\mathbf{r}_{ss}$ is

smaller than the magnitude of the sun-earth vector $\mathbf{r}_{sun}$, the penumbra factor ν is equal to 1 (satellite in full sunlight). Otherwise, we first account for the virtual motion of the sun in the geocentric coordinate system for the light travel time τ, i.e. the photons, which perturb the satellite at time t originate from the sun at time $(t - \tau)$. Thus the effective sun position must be computed at time $(t - \tau)$. The symbol c being the speed of light, the light travel time τ is:

$$\tau \approx \frac{|\mathbf{r}_{ss}|}{c} \tag{3.16}$$

Let us call the corrected sun-satellite vector $\boldsymbol{r}_{ss}$, and let us define the projection L of the earth-satellite vector $\mathbf{r}_s$ on the sun-satellite vector $\boldsymbol{r}_{ss}$ as follows:

$$L = \frac{\mathbf{r}_s \cdot \boldsymbol{r}_{ss}}{|\boldsymbol{r}_{ss}|} \tag{3.17}$$

Let us define the the closest approach d of the vector $\boldsymbol{r}_{ss}$ to the centre of the earth:

$$d = \left| \mathbf{r}_s - L \frac{\boldsymbol{r}_{ss}}{|\boldsymbol{r}_{ss}|} \right| \tag{3.18}$$

With ρ_s being the sun's radius, we have the angular radius of the sun k_s seen from the satellite:

$$k_s = \frac{\rho_s}{|\boldsymbol{r}_{ss}|} \tag{3.19}$$

If ρ_e is the earth's radius, the factor ν will obviously be equal to 1 as long as the following condition is respected:

$$d \geq \rho_e + L k_s \tag{3.20}$$

Otherwise the disks of the sun and the earth intersect as seen from the satellite, and the fraction of the apparent sun disk must be evaluated.

The tangent of the angular radius of the earth k_e as seen from the satellite can be approximated as:

$$k_e \approx \frac{\rho_e}{L} \tag{3.21}$$

and the tangent of the angle between the sun-satellite vector r_{ss} and the earth-satellite vector $\mathbf{r}_s$, is:

$$s \approx \frac{d}{L} \tag{3.22}$$

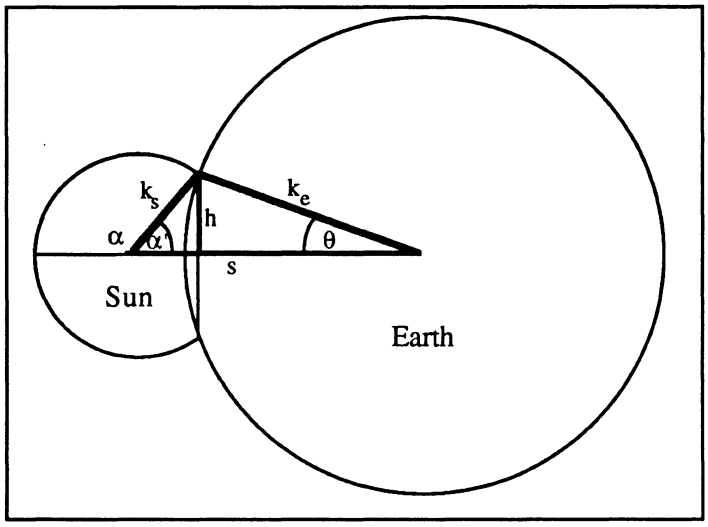

Sun and earth disks as seen from the satellite
FIGURE 3.3

Referring to Fig. 3.3, the following parameters are defined:

$$\theta = \cos^{-1}\left(\frac{k_e^2 + s^2 - k_s^2}{2k_e s}\right)$$

$$h = k_e \sin\theta$$

$$\alpha' = \sin^{-1}\left(\frac{h}{k_s}\right)$$

$$\alpha = \pi - \alpha' \tag{3.23}$$

Afterwards, the intersecting section of the sun and the earth disks are divided as

shown in Fig. 3.4, with the areas of the figures given by:

$$A_1 = \alpha k_s^2$$

$$A_2 = s\,h$$

$$A_3 = \theta k_e^2 \qquad (3.24)$$

where α and θ are in radians. From Fig. 3.4 the non-overlapped area A of the small disk (the sun) is:

$$A = A_1 + A_2 - A_3 . \qquad (3.25)$$

And finally the penumbra factor ν is defined as follows:

$$\nu = \frac{A}{\pi r_s^2} \qquad (3.26)$$

The sun's disk completly disappears when $k_e - k_s \geq s$ (see Fig. 3.3).

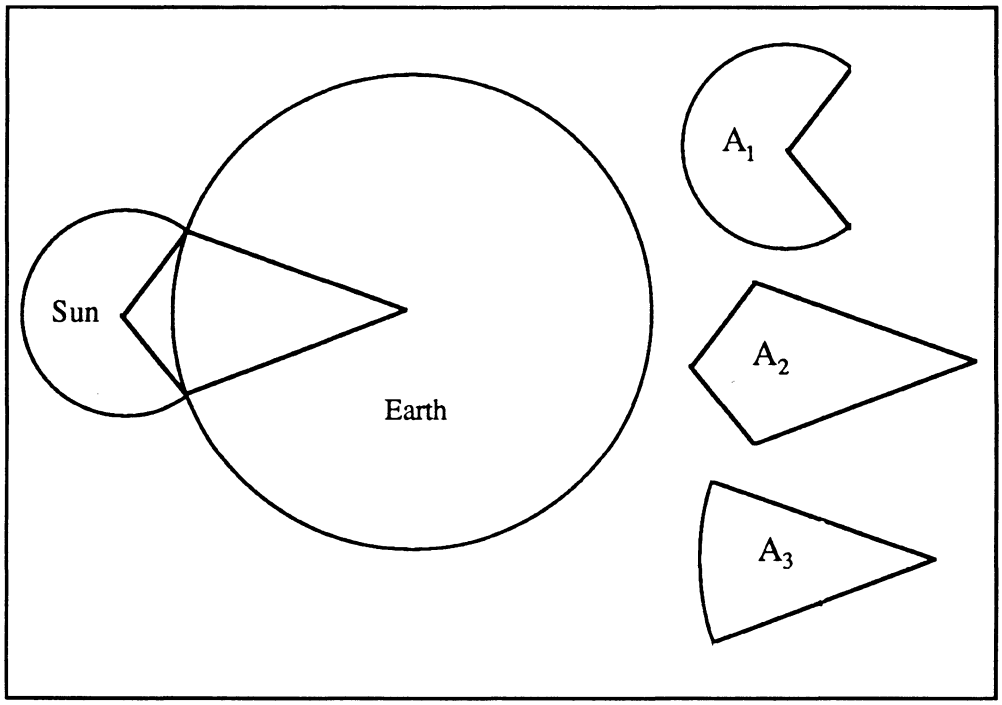

Decomposition of the earth and sun disk intersection
FIGURE 3.4

This model can easily be extended for interplanetary spacecraft where all planets can be taken into account (see Ash, 1972). The solar radiation pressure computation has been coded in a subroutine SOLPR, which calls the subroutine ECLIP for the penumbra factor computation. The sun's position is computed by the modified subroutine SUN described earlier.

3.5 Computation of initial conditions

The initial state of the satellite, which is the starting point of the integration process, can be obtained in different ways: from a set of osculating elements, from a tabular ephemeris like the Macrometer® T-files, from a set of precise ephemerides [Remondi, 1986], or from a set of broadcast messages.

With a code-tracking receiver, the last option is the most accessible to the user. We have opted for this source of information to obtain our initial state vectors. Since the accuracy of the satellite position and velocity computed from broadcast messages is a function of the difference between the computation time and the reference time t_{oe} [Van Dierendonk et al., 1980], we have developed a utility program to merge all the broadcast messages recorded at different sites during a campaign in order to have as complete a set of broadcast messages as possible. This procedure is certainly not necessary for small networks since all stations record almost the same information, but for large networks, all satellites do not rise and set at the same time, and thus, one receiver frequently records more (or different) messages than another one.

This output file is used afterwards to compute the initial state vectors by searching for the ephemeris with the closest reference time. Integration from a state vector (x_o, y_o, z_o, x'_o, y'_o, z'_o) is also possible in order to enable re-integration of a corrected trajectory from an improved state vector. The procedure for computing satellite position and velocity from broadcast messages can be found in Van Dierendonck et al. [1980] or Wells et al. [1986].

The initial conditions computation is managed by the subroutine INTCD, whereas the computation of the satellite positions and velocities from broadcast messages is managed by subroutine SATCP.

3.6 Numerical integrator

Numerical techniques for integration are divided into two groups: the single-step and the multi-step procedures. For example, the Runge-Kutta approach is a single-step procedure, whereas predictor-corrector type numerical integrators are multi-step procedures.

In orbit integration problems, the predictor-correctors are usually preferred over the single-step method since fewer evaluations of the differential equations (right-hand side of 3.1) are required. For example, a simple differential equation of the form $y' = f(x,y)$ can be solved using a single-step Runge-Kutta procedure [Hamming, 1962] of the form:

$$
\begin{aligned}
y_{i+1} &= y_i + \frac{1}{6}(k_1 + 2k_2 + 2k_3 + k_4) \\
k_1 &= h\, f(x_i, y_i) \\
k_2 &= h\, f(x_i + h/2\,,\, y_i + k_1/2) \\
k_3 &= h\, f(x_i + h/2\,,\, y_i + k_2/2) \\
k_4 &= h\, f(x_i + h\,,\, y_i + k_3)
\end{aligned}
\tag{3.27}
$$

where h is the integration step size.

Since this specific fourth-order Runge-Kutta method involves four evaluations of the differential equation f, it is not an economic solution. A fourth-order predictor-corrector formula for the same function f can be written as follows:

$$
y^p_{i+1} = y_i + h\sum_{n=0}^{3} B_{i-n}\, f(x_{i-n}\,,\, y_{i-n}) \tag{3.28}
$$

$$
y^c_{i+1} = y_i + h\sum_{n=0}^{3} A_{i-n+1}\, f(x_{i-n+1}\,,\, y_{i-n+1}) \tag{3.29}
$$

where the coefficients B and A are specific coefficients for the predictor (3.28) and the corrector (3.29) formulas, h being the step size [Moursund and Duris, 1967]. A procedure to derive the coefficients A and B for different types of predictor-corrector formulas is well described by Velez and Maury [1970]. With the multi-step formulas, the solution is obtained iteratively. First a value y^p_{i+1} is computed with the predictor

formula. This value is then used in the corrector formula to compute the corrected value y^c_{i+1}. Iteration is then performed with the corrector until convergence is reached. With an appropriate step size, three evaluations of the function f generally will be suffucient (2 iterations with the corrector). The four initial values (y) required to start the procedure can be obtained from a single-step integrator (like Runge-Kutta) or using a special starting procedure as will be described later (if we take into account the initial condition (y_o), only three other values have to be computed).

For fourth-order integrators the difference between the single- and multi-step procedure is not so obvious, but for high-order formulas the benifit of the predictor-corrector formulas becomes obvious, since only two or three iterations are usually necessary to reach convergence.

The numerical integrator chosen for the solution of our initial value problem is an eleven-point multi-step predictor-corrector formula. Our formulation uses a Störmer predictor and a Cowell corrector [Velez and Maury, 1970]. This formulation takes advantage of the specific force model described earlier. In the force model described in Section 3.4 the velocity vector **r'** does not appear on the right-hand side of equation (3.1). In this case, the three second-order differential equations can be directly integrated instead of separating them into six first-order differential equations as is usually done. The predictor is given in the following form:

$$\mathbf{r}(t) = 2\,\mathbf{r}(t\text{-}h) - \mathbf{r}(t\text{-}2h) + h^2 \sum_{i=0}^{10} \xi_i\, \mathbf{r}''(t\text{-}(1+i)h) \qquad (3.30)$$

whereas the corrector is:

$$\mathbf{r}(t) = 2\,\mathbf{r}(t\text{-}h) - \mathbf{r}(t\text{-}2h) + h^2 \sum_{i=0}^{10} \beta_i\, \mathbf{r}''(t - ih) \qquad (3.31)$$

where:

h	is the step size,
r(t)	is the satellite position at epoch (t),
r"(t)	is the satellite acceleration at epoch (t),
ξ_i	are the predictor coefficients (see Appendix 1),
β_i	are the corrector coefficients (see Appendix 1).

Equation (3.30) and (3.31) require 10 starting values, in addition to the initial

conditions, to undertake the integration process. These values are obtained iteratively using the starting procedure of Velez and Maury [1970]. The initial conditions being at epoch (t_o), solutions are sought at times (t_{-5}, t_{-4}, . . ., t_{-1}, t_1, . . .,t_5); the starter uses the following set of equations:

$$\mathbf{r}(t_o + Kh) = f_J(\mathbf{r}''(t_{-5}), \mathbf{r}''(t_{-4}), ...\mathbf{r}''(t_o), ...\mathbf{r}''(t_5)) \qquad (3.32)$$

where:

h	is the step size,
K	is an integer value varying as $-5 \le K \le -1$ and $1 \le K \le 5$, representing 10 different equations, 5 before the initial epoch (t_o) and 5 after,
f_J	represents 10 different functions for $10 \ge J \ge 6$ and $4 \ge J \ge 0$, where $J = 5 - K$.

The vectors $\mathbf{r}(t)$ and $\mathbf{r}''(t)$ being the position and the acceleration vector at epoch (t), the functions f_J are defined as follows:

$$\mathbf{r}(t_o + Kh) = \mathbf{r}(t_o) + K\,h\,\mathbf{r}'(t_o) + h^2 \sum_{i=0}^{10} \alpha_{Ji}\,\mathbf{r}''(t_o + Kh + (J-i)h) \qquad (3.33)$$

$\mathbf{r}'(t_o)$ being the initial velocity. Ten sets of coefficients α_{Ji} are required to solve the 10 different sets of equations (see Appendix 1). These 10 different functions are evaluated until convergence is reached. The initial values required to start this procedure are obtained from a two-body problem as described in Chapter 2. The numerical integration is managed by the subroutine NRINT, whereas the starting values computation is managed by subroutine INITV. The subroutine START and COWEL have been specially coded for the starting and the predictor-corrector procedure.

3.7 Approximation of the orbit

The numerical integration produces a set of satellite positions at a specific epoch which does not not necessarily correspond to the time tag of the observations to be processed. Different interpolation procedures can be used to obtain satellite positions at specific epochs from a tabular ephemeris. To solve this problem efficiently, we decided to approximate the tabular ephemeris by a set algebraic polynomials. We did not

see the benifit of using Chebychev polynomials. Although the Chebychev polynomials are more stable at higher degree, we decided to use algebraic polynomials at lower degree over small segments by dividing orbital arcs into segments of 1.5 to 2 hours. Our orbit approximation is given as follows:

$$r_j = A^i_{j,0} + \sum_{k=1}^{n} A^i_{j,k} \left(\frac{t - t_{io}}{\Delta t_i} \right)^k \qquad (3.34)$$

where:

n	is the order of the polynomial,
j	is one of the three components of the satellite position vector (j=1, 2, 3),
i	represents a specific segment of the orbital arc,
t_{io}	is the reference time associated with the segment i (if t_1 is the first epoch of the segment i and t_2 the last, then we have $t_{io} = (t_1 + t_2)/2$),
$A^i_{j,k}$	are the polynomial coefficients (k) associated with the segment (i) and the component (j),
Δt_i	is the normalization factor (associated to segment i) used to avoid numerical problems (if t_1 is the first epoch of the segment i, then we have $\Delta t_i = t_{io} - t_1$).

The orbital arcs have to be divided into segments of 1.5 or 2.0 hours to maintain sub-metre precision in the satellite positions. This means that for an orbital arc of 10 hours with a segmentation of 2 hours there will be 15 different polynomials (five for each component). For a polynomial of degree n, 15 (n+1) coefficients will represent the orbit; for example if n=7, there will be 120 parameters, which is quite acceptable. With the broadcast ephemeris representation, the same orbital arc will require 150 parameters if we assume no satellite clock corrections (15 parameters per message, one message per hour). In order to have continuous piece-wise polynomials, two common data points are used to approximate two adjacent segments.

The polynomial coefficients are estimated by least-squares approximation. At each integration step a set of normal equations (A^TA), and three sets of vectors (A^TW_j) are updated by the subroutine ATAP2. After the integration of one segment, three sets

of coefficients ($A^i_{j,k}$) are estimated. The partitioning of an orbital arc into different segments is performed by the subroutine NRINT using input parameters. The polynomial degree (up to 9) is user-defined.

These coefficients represent the orbit in a true-of-date system. Thus for each orbital arc, the earth's rotation parameters, which must be used to recover the coordinates in an Conventional terrestrial system, are stored on a disk file along with the coefficients.

3.8 Improvement of initial conditions

The idea for the following procedure comes from Beutler et al. [1984a]. It concerns the adjustment of the initial conditions using broadcast satellite positions as pseudo-observations. As mentioned in Section 3.5, the initial conditions are computed using the closest message as possible to the initial epoch. Owing to the limited accuracy of each separate broadcast message, it is possible for the initial state vector to be offset from the overall broadcast trajectory. A few metres or a few (m/sec) errors in the initial state vector can yield an integrated trajectory offset (from the broadcast trajectory) by several ten metres after a few hours' integration.

Assuming the broadcast trajectory to have an accuracy of 25-50 metres, it would be interesting to adjust the integrated trajectory to the broadcast one. This procedure, at this stage, is an opportunity to avoid an iterative process in the final adjustment with the GPS double-difference phase observations.

To do this, a series of satellite positions is generated at 15 minute intervals using the broadcast messages; afterwards, following the procedure described in Section 2.5, the initial conditions are improved using broadcast satellite positions as pseudo-observations. Although the number of iterations is user-defined, usually one iteration is sufficient to reach convergence. From the residuals (integrated trajectory minus broadcast trajectory), in terms of along-track, across-track and radial direction, this preliminary improvement procedure is obviously important, since large offsets between the two trajectories exists after the first integration.

The satellite positions (pseudo-observations) are computed with the subroutine INTCD; the subroutine ADJUS proceeds to the least-squares adjustment. The partial derivatives used in this adjustment are described in Section 5.2.5.

3.9 Program ORDAP

All the developments presented in this chapter have been regrouped in a FORTRAN 77 program ORBDAP (ORBital DAta Preprocessor). The list of the subroutines involved in this program is given in Appendix 2. The processing is controlled by a file giving all the necessary input parameters, such as the force field selection, the integration parameters for segmentation, the polynomial degree, the earth orientation parameters, the time start and time end for each satellite involved in the observations, the broadcast file name or the osculating element file name.

The current version of the software does not access earth orientation parameter files such as IRIS (International Radio Interferometric Surveying) files. These values (x_p, y_p, UT1-UTC) have to be input manually in the control file for the specific observation session. In a future version, such improvement would worthwhile.

The output of the program is a file including all coefficients of each segment for all satellites in a true-of-date system; the file includes as well the earth orientation parameters for subsequent transformation in the Earth-fixed system. The initial conditions for each satellite are output in a separate file. The progam also generates an alphanumeric output file for analysis; it includes a summary of the options used and all the residuals (of the preliminary adjustment) for each satellite after each iteration. Appendix 3 gives an example of such output. Fig. 3.5 depicts ORDAP's procedure in a flow chart.

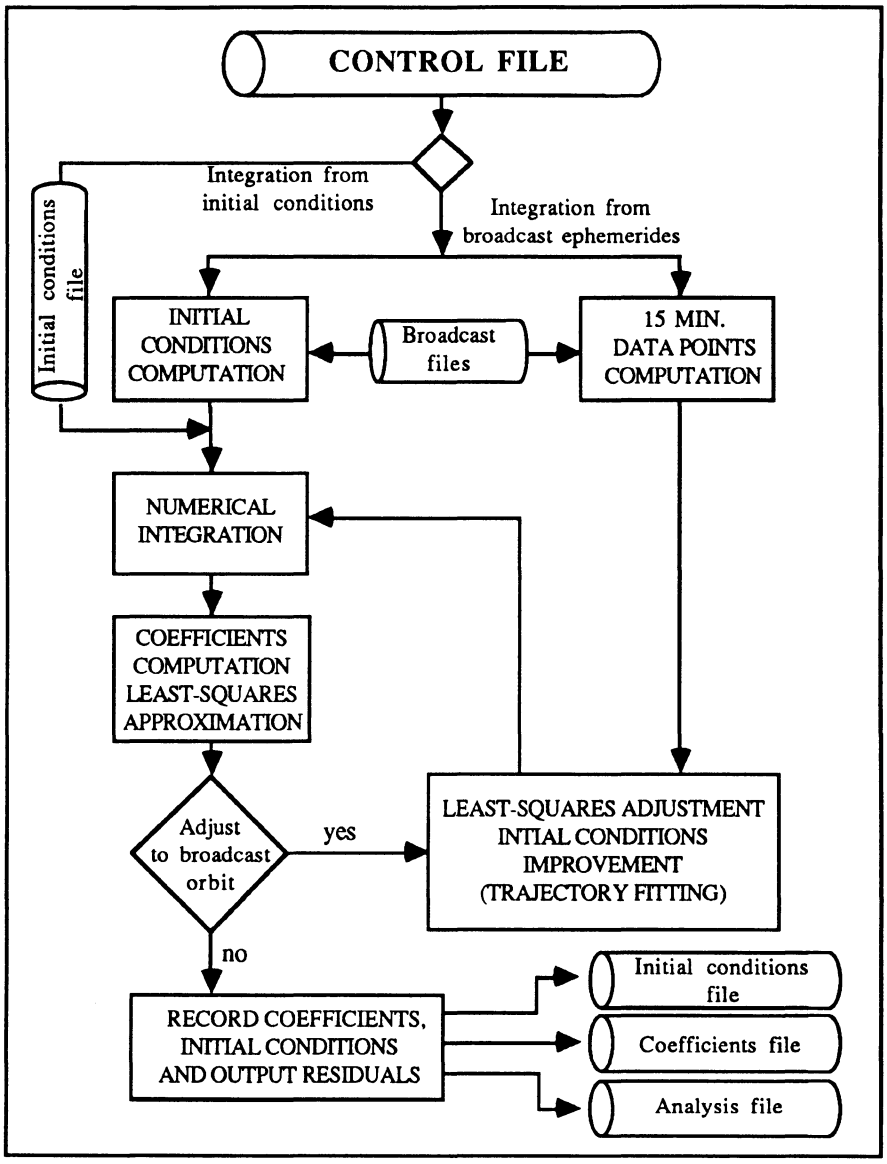

Orbital data pre-processor flow-chart
FIGURE 3.5

4. OBSERVATIONS PRE-PROCESSING

4.1 General approcah

The way observations are pre-processed varies from one piece of software to another. With DIPOP 2.0, the UNB GPS software, the principal tasks to be performed at the pre-processing stage, are to remove all cycle slips and bad observations, to form the double-difference observables and to compute satellite positions and velocities. Ionospheric and tropospheric calibration is done during the least-squares final adjustment.

The HPBT data set, being extensively corrupted by cyle slips, the zero-order polynomial procedure of the first generation TI 4100 UNB pre-processor to evaluate cycle slips [Vanicek et al., 1985] was not adequate for solving our problem. Therefore, we wrote a procedure which solves this problem automatically, to some extent.

We first wrote a routine EXTR3 to reformat the HPBT observation files [Scott et al., 1986] in the UNB GPS observations data format. Afterwards, a progam SINGLE was written to form the inter-satellite single-differences, and to compute the satellite positions from a set of broadcast messages or from a set of coefficients obtained from the ORDAP program previously described. The output files are then corrected for cyle slips by the CSLIP program, which produces pseudo-clean single-difference files. This first correction is usually good at the one to three cycle level depending on the data gaps accompanying the cycle slips. Afterwards, the DOUBLE program uses two single-difference files (inter-satellite), combining them in one double-difference file. The remainding cycle slips in this double-difference output file are then corrected again by the program CSLIP.

Since the differencing of the raw phases is a straightfoward procedure, the next sections are dedicated to the cycle slips problem.

4.2 Cycle slips definition

The GPS carrier phase observation used to compute precise geodetic positions is the difference between the phase of the received carrier signal of a GPS satellite and the phase of a local oscillator within the receiver. It is often called the carrier beat phase. Measurements of the carrier beat phase can be either "complete instantaneous phase measurements" or "fractional instantaneous phase measurements". The distinction between the two is that the former includes the integer number of cycles of the carrier beat phase since the initial phase measurement, and the latter is a number between zero and one cycle [Wells, 1985].

The carrier beat phase recorded by the GPS receiver is usually the "complete instantaneous phase measurement". Once the satellite signals have been acquired by the receiver, the whole number of cycles are tracked and counted as the satellite moves on its orbit. By definition, the initial phase measurements are ambiguous by an integer number of cycles. Therefore, as long as the receiver keeps phase lock on the incoming satellite signals, the initial (unknown) phase measurement, which is an integer number of cycles, is the same over a particular observing session. These unknown biases (one for each satellite) or ambiguities are introduced in the least-squares estimation as phase parameters.

Sometimes, for different reasons, the receivers lose lock and reacquire the signal during the same observing session. The major reasons for such a break in the recorded data can be caused by both problems inside the tracking hardware and environmental causes, i.e. obstruction of the line of sight, multipath, ionospheric effect, etc. [Langley and Parrot, 1987]. After reacquisition of the signal, the fractional phase measurement is the same as if tracking had been maintained; however, the initial (integer) ambiguity takes a different value. This sudden change in ambiguity is evidenced by a sudden jump in the recorded phase data. This occurrence is known as a "cycle slip"; if cycle slips are not repaired (i.e. if the new integer number introduced in the phase measurement observations is not corrected) each cycle slip introduces a new phase ambiguity parameter, which must be solved in the least-squares solution.

The task of our CSLIP program is to repair these phase breaks or cycle slips as fully as possible; otherwise a new phase ambiguity is introduced in the main processor for each uncorrected cycle slip. The next section describes the algorithm used to detect the cycle slips.

4.3 Cycle slip detection

The algorithm that is described here is based on dual-frequency phase observations on L1 and L2. Goad [1985] gives an example of this algorithm to detect cycle slips in a raw-data file. To begin with, let us write the raw phase observation equation [Kleusberg et al., 1985]:

$$\lambda\phi_i^k(t_{i\beta}) = c \cdot (dt_\beta^k - dt_{i\beta}) - \rho_i^k - dI_i^k - dT_i^k + \lambda \cdot (df \cdot t_{i\beta} + N_i^k + A^k - A_i) \qquad (4.1)$$

where:

$\phi_i^k(t_{i\beta})$	is the carrier beat phase observation related to receiver i and satellite k,
$t_{i\beta}$	is the observation epoch β on receiver time scale,
N_i^k	is the initial carrier beat phase ambiguity related to satellite k and receiver i,
λ	is the carrier wavelength,
c	is the vacuum speed of light,
dt^k_β	is the satellite time offset at epoch β,
$dt_{i\beta}$	is the receiver time offset at epoch β,
ρ_i^k	is the geometric signal path length between satellite k at the transmitting time (different than $t_{i\beta}$) and receiver i,
dI_i^k	is the ionospheric phase delay,
dT_i^k	is the tropospheric phase delay,
df	is the offset from the nominal satellite oscillator frequency,
A_i	is the initial receiver oscillator phase (receiver i),
A^k	is the initial satellite oscillator phase (satellite k).

For the single-difference observation (inter-satellite) the following equation is obtained:

$$\lambda\phi_i^{kl}(t_{i\beta}) = c \cdot (dt_\beta^{kl}) - \rho_i^{kl} - dI_i^{kl} - dT_i^{kl} + \lambda \cdot (N_i^{kl} + A^{kl}) \qquad (4.2)$$

the superscript "1" representing the second satellite. For double-difference observations the equation is as follows:

$$\lambda\phi_{ij}^{kl}(t_{i\beta}) = -\rho_{ij}^{kl} - dI_{ij}^{kl} - dT_{ij}^{kl} + \lambda \cdot N_{ij}^{kl} \qquad (4.3)$$

In equation (4.2), the receiver clock term is cancelled out, but we still have the satellite clock term. In equation (4.3) all clock parameters are cancelled out.

As mentioned earlier, cycle slips appear like sudden jumps in the raw data series; with dual-frequency measurements, cycle slips can occur at either frequency L1 or L2, or both. This means that if equation (4.1) is written for L1 and L2 separately, the ambiguity parameters $N_i^k{}_{L1}$ or $N_i^k{}_{L2}$ (or both) take new values at each epoch t_p where a cycle slip occurred. The problem is the same with single- or double-difference phase observations.

If the equation (4.3) is written for L1 and L2 and they are differenced, the following result is obtained:

$$\lambda\phi_{ij}^{kl}(t_{i\beta})_{L1} - \lambda\phi_{ij}^{kl}(t_{i\beta})_{L2} = -dI_{ij\,L1}^{kl} + dI_{ij\,L2}^{kl} + \lambda_{L1}N_{ij\,L1}^{kl} - \lambda_{L2}N_{ij\,L2}^{kl} \qquad (4.4)$$

In this equation, all clock terms cancel out, and the tropospheric term also drops out as the tropospheric delay is not frequency dependent. Since the terms $N_{ij}^{kl}{}_{L1}$ and $N_{ij}^{kl}{}_{L2}$ should remain constant during the whole observing session (assuming no cycle slips), the variations in this time series will come from the difference in the ionospheric delay on L1 and L2. Equation (4.4) can be written in the same way for single-difference phase observations (with one clock term).

With single- and double-difference phase observations, the time series generated by equation (4.4) produces curves with high-frequency noise at the centimetre level (or below). Kleusberg [1986] investigated this kind of data series for observations spanning 2 hours on 13- and 40-km baselines in the Ottawa area. All of the produced

residual plots present a total variation of about 20 centimetres for the two hours of data.

As we have seen, if a cycle slip occurs at time (t_p) of magnitude $C_{ij}^{kl}{}_{L1}$ cycles in L1 and $C_{ij}^{kl}{}_{L2}$ cycles in L2, the resulting time series generated by equation (4.4) will show a discontinuity of $\lambda_{L1}C_{ij}^{kl}(t_p)_{L1} - \lambda_{L2}C_{ij}^{kl}(t_p)_{L2}$ at epoch (t_p).

This characteristic is used to detect the cycle slips. The difference in the time series (4.4) epoch-to-epoch is tracked, and if the difference is greater than a certain tolerance, a cycle slip is suspected at this epoch on L1, L2, or both. The weakness of this approach is that if the combination $\lambda_{L1}C_{ij}^{kl}(t_p)_{L1} - \lambda_{L2}C_{ij}^{kl}(t_p)_{L2}$ is below the tolerance, the cycle slip cannot be detected. An example of this problem would be a jump of 19 cycles in L2 and 24 cycles in L1, with a wavelength of ~24 cm for L2 and ~19 cm for L1; the resulting combination would be close to zero. The probability of encountering such a combination is rather low. This detection can be performed either on single- or double-difference files.

The proposed detection algorithm is probably the best existing approach to detect cycle slips in dual-frequency, double-difference observables. Using the same approach, the cycle slips can be detected in undifferenced as well as single-difference (inter-station) dual-frequency data with the same degree of confidence. For single-frequency observations in double-difference mode it has been shown by Parrot [1988] that the observables (with data interval up to 60 seconds) can be predicted with acceptable confidence level to detect the cycle slips at the sub-cycle level (the algorithm compared the predicted against the observed values). This approach was generalized to include all of the kinds of single-frequency observables (undifferenced, single- and double-difference). It has been shown that the succesful cycle slip resolution to the sub-cycle is directly related to the rate of data acquisition. Some other investigators used triple-difference residuals to detect cycle slips [Lachapelle et al., 1988].

4.4 Cycle slip correction

To correct a cycle slip, the observation data series in the vicinity of the slip is approximated by a pair of step-wise continuous algebraic polynomials with a step occurring at the cycle slip. The first and higher order terms of the polynomials have identical coefficients, with the difference of the zero-order terms corresponding to the number of slipped cycles. One estimate is evaluated on L1 and another is evaluated on

L2. In order to obtain better results in our estimation process, the theoretical observations are removed from the recorded observations; this yields a times series with small variations.

With inter-satellite single-difference observations, the time series generated by equation (4.2) is used to estimate cycle slips; a resolution at the sub-cycle level is not guaranteed, owing to the noise introduced by the clock term. However, it should be noted that the effect of the satellite clock term in equation (4.2) is smaller than the effect of the receiver clock term present in the inter-station single-difference, and thus most of the cycle slips (but not all) can be resolved with observations of type (4.2).

After a first correction in a single-difference file, the double-difference observations represented by equation (4.3) are formed from two "pseudo-clean" single-difference files. In equation (4.3) all the clock terms are cancelled out, and the estimation of the cycle slips, by the simple algebraic polynomial, usually gives a resolution at the sub-cycle with a high level of confidence.

In order to obtain a fast algorithm, the algebraic polynomial is fitted to the data only around the cycle slip; it uses between 3 and 10 (user selectable) good data points before and after the cycle slip.

As described in Section 4.1, a cycle slip is usually evidenced as a sudden jump in the recorded carrier phase data. But for various reasons, sometimes in the data there is a series of consecutive outliers which introduce gaps in the time series. When gaps occur, it is more difficult to obtain a good estimate of the cycle slip. Some processing with our algorithm has shown that a gap of about 10 min. can be very well bridged without problem when 30-second data points are used in the double-difference observations. Gaps longer than 10 to 15 minutes can be difficult to correct .

The weakness of our approach is that when many breaks occur in a very short time span, the algorithm deletes some observations and creates artificial gaps; this problem can be avoided to some extent by using fewer than 10 data points before and after each break. Fig. 4.1 describes this problem. When a gap in a data series is longer than a threshold value (user-defined), instead of correcting the cycle slips, we introduce a new phase ambiguity in the main processor adjustment of the observations.

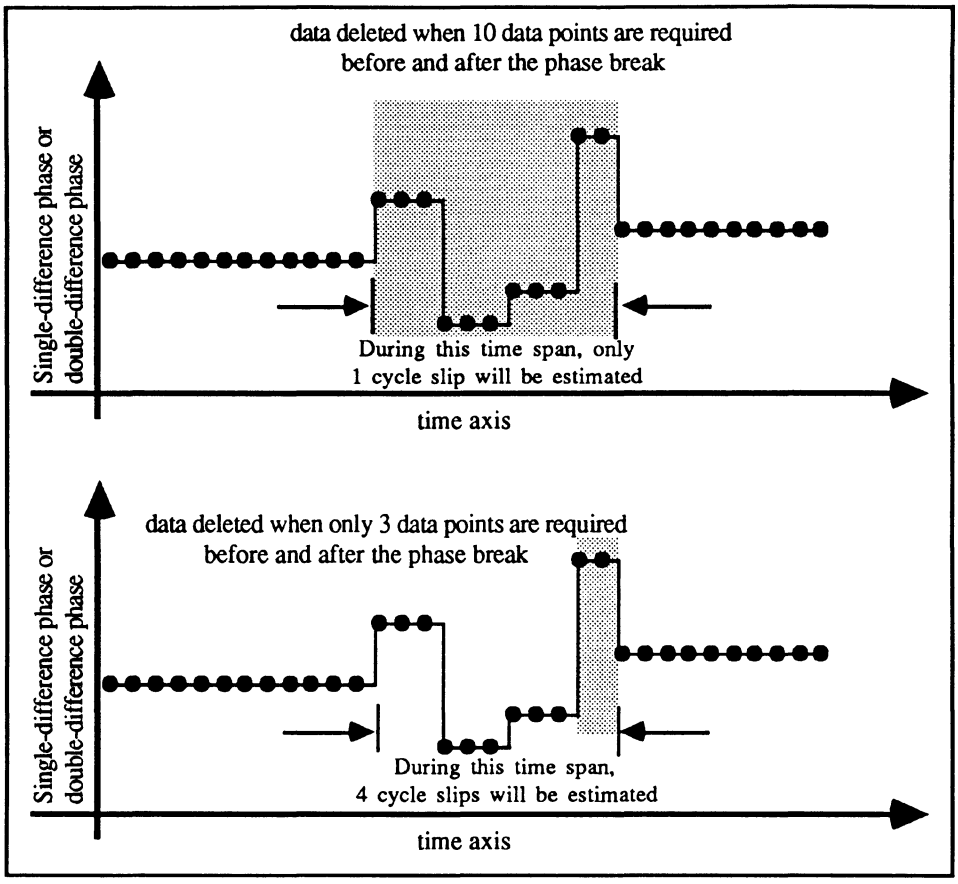

Observations deleted by the
cycle-slip correction algorithm
FIGURE 4.1

4.5 Practical considerations

New phase ambiguities are introduced in the main processor simply by introducing a "pseudo-satellite" number in the observations file. All data for a particular satellite recorded after an "unfixable cycle" slip is assigned a new satellite identification number. In this way, the least-squares estimation procedure will estimate a phase ambiguity for this pseudo-satellite as it does for all the others. The pseudo-satellites are introduced by the CSLIP program only when double-difference observation files are input. For example, if at an epoch t_x, we have the satellite pairs (6-8) and (8-9), and a gap occurs at this time in the data series (6-8), then the satellite pairs (6-28) and (28-9)

will be formed after the gap. Here we are dealing with double-difference observations, which means it is impossible to known on which satellite the gap has really occured. The program always selects the last satellite of the pair to apply the pseudo-satellite number. The reference satellite algorithm used in DIPOP [Vanicek et al., 1985] allows such a procedure. The pseudo-satellites are always created by adding the constant 20 to the satellite PRN number. Such a consistent procedure is important since in the final least-squares adjustment the observations of pseudo-satellite 28 must be recognized as observations from satellite PRN number 8 in order that the partial derivatives computation with respect to the initial conditions of satellite 8 be correctly carried out.

It should also be mentioned that since our a priori ambiguities are applied on double-difference observations, they are all linearly independent of one other; thus the reference satellite algorithm used in DIPOP cannot be applied if there is one satellite pair number (e.g. 6-11) which is dependent on two other satellite pair numbers (e.g. 6-8 and 8-11). The simplest way to overcome this problem is to introduce a pseudo-satellite number to destroy this dependence (i.e. replace 6-11 by 6-31). This is an artificial way to estimate double-difference ambiguities for each satellite pair, which is required when double-difference ambiguities are applied instead of inter-station single-difference ambiguities. Such editing must be done manually by the operator, all the other operations being automatic.

According to the pre-processing that has been done, the automatic procedure to detect and correct cycle slips succeeds in ~95-98% of the cases even with very corrupted data. The pre-processing is completed by processing the data baseline by baseline with an a priori orbit (held fixed) in order to analyze the residuals plot to see if any cycle slips remain. When cycle slips remain, they are fixed manually by means of an interactive program using the epoch number of occurrence and the magnitude of the break in terms of cycles. The remaining cycle slips, if there are any, are usually of the order of one cycle.

To conclude this section, it should be mentioned that the program SINGLE and DOUBLE can differentiate the data of one site from the data of up to nine other sites simultaneously; the CSLIP program can process up to 10 files sequentially. All of these programs are controlled by command files.

Fig. 4.2 depicts our pre-processing procedure. While decoding the raw data, a scenario file is generated for each observation file in order to facilitate the selection of the

reference satellite required in DIPOP to handle the ambiguities estimation [Vanicek et al., 1985]. An a priori station coordinates file is required by the cycle slip editor in order

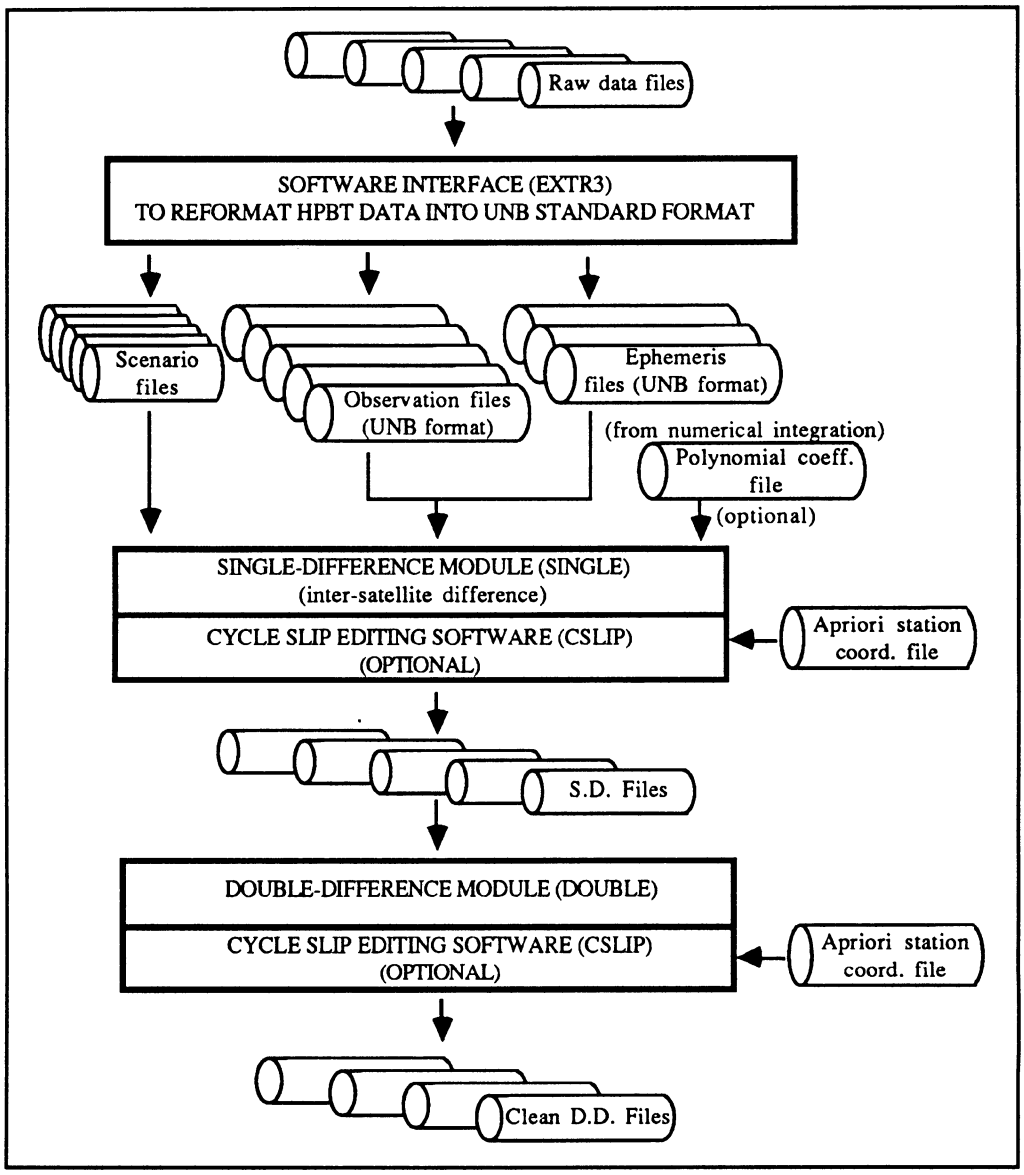

Pre-processor flow chart
FIGURE 4.2

to remove the orbit dynamics from the observations prior to fitting the algebraic polynomial to the data series (for cycle slip estimation). Removing orbital motion yields smoother data series. Appendix 4 gives a list of the subroutines involved in these programs.

5. MODELLING GPS OBSERVABLES AND RELATED DERIVATIVES

5.1 Observation equation

The current model implemented in the DIPOP 2.0 GPS software accommodates the so-called double-difference observables. Observations from codeless as well as code receivers can be processed without problem. However, a slightly different approach is used for code receiver observations where the advantage of timing information is taken into account. To understand the difference between both approaches, let us recall equation (4.1):

$$\lambda\phi_i^k(t_{i\beta}) = c \cdot (dt_\beta^k - dt_{i\beta}) - \rho_i^k - dI_i^k - dT_i^k + \lambda \cdot (df \cdot t_{i\beta} + N_i^k + A^k - A_i) \qquad (5.1)$$

In this equation, the range ρ^k_i must be computed at transmission time $(t_{i\beta} - \tau_\beta - dt_{i\beta})$ where τ_β is the exact signal travel time and $dt_{i\beta}$ is the receiver clock misalignment with respect to the GPS time t^{GPS}_β (i.e. $t_{i\beta} = t^{GPS}_\beta + dt_{i\beta}$). The value $dt_{i\beta}$ being small, the range ρ^k_i is usually expanded in a Taylor's series as follows:

$$\rho_i^k = \rho_i^k(t_{i\beta} - \tau_\beta - dt_{i\beta}) = \rho_i^k(t_{i\beta} - \tau_\beta) + \dot\rho_i^k(t_{i\beta} - \tau_\beta) \cdot (- dt_{i\beta}) \qquad (5.2)$$

Replacing $(t_{i\beta} - \tau_\beta)$ by a subscript α, substituting (5.2) in (5.1) and after doubly differencing the equation between satellite k and l with station i and j, the following is obtained:

$$\lambda\phi_{ij}^{kl}(t_{i\beta}) = - \rho_{ij\alpha}^{kl} - dI_{ij}^{kl} - dT_{ij}^{kl} + \lambda N_{ij}^{kl} - \dot\rho_{i\alpha}^{k} \cdot (- dt_{i\beta})$$
$$+ \dot\rho_{j\alpha}^{k} \cdot (- dt_{j\beta}) + \dot\rho_{i\alpha}^{l} \cdot (- dt_{i\beta}) - \dot\rho_{j\alpha}^{l} \cdot (- dt_{j\beta}) \qquad (5.3)$$

The satellite clock misalignments (dt^k_β and dt^l_β) do not appear in equation (5.3). As we will see, these terms have to be taken into account when code observations are used to recover satellite positions at transmission time. When phase observations are concerned it is the frequency accuracy and stability of the satellite clocks during the satellite pass which is important. In DIPOP, it is assummed that the satellite clocks do not contribute measurably to the double-difference observables [Vanicek et al., 1985]. The receiver clock misalignment problem is handled as a relative clock synchronization. The relative synchronization is simply obtained by setting the term $dt_{i\beta}$ at zero. Equation (5.3) can now be rewritten as follows:

$$\lambda\phi^{kl}_{ij}(t_{i\beta}) = (-\dot{\rho}^{\,k}_{j\alpha} + \dot{\rho}^{\,l}_{j\alpha}) \bullet dt_{j\beta} - dI^{kl}_{ij} - dT^{kl}_{ij} - \rho^{kl}_{ij\alpha} + \lambda N^{kl}_{ij} \qquad (5.4)$$

If $\Delta t_{ij} = dt_{j\beta}$ and an error ε associated with the observation is added, the basic model equation used in DIPOP for the reduction of carrier phase observations is obtained:

$$\lambda\phi^{kl}_{ij}(t_{i\beta}) = (-\dot{\rho}^{\,k}_{j\alpha} + \dot{\rho}^{\,l}_{j\alpha}) \bullet \Delta t_{ij} - dI^{kl}_{ij} - dT^{kl}_{ij} - \rho^{kl}_{ij\alpha} + \lambda N^{kl}_{ij} + \varepsilon \qquad (5.5)$$

where Δt_{ij} will be referred to as the relative clock synchronization error of receiver j with respect to receiver i.

For the squaring-type receiver, equation (5.5) is used with half of the carrier wavelength as effective wavelength. The signal travel time τ needed to compute satellite positions is computed iteratively using positions at receiving time as a priori values.

Data from code-correlating receivers are usually pre-processed using the timing information of the P-code data. The P-code is used to recover the exact transmission time corresponding to each receiver time tag in order to compute satellite coordinates. For example, let us assume that the reception time of a signal at receiver i is ($t^{GPS}_\beta + dt_{i\beta}$) and the time when this signal left the satellite k is ($t_\beta^{GPSk} + dt^k_\beta$) where $dt_{i\beta}$ and dt^k_β are receiver and satellite clock misalignement, t^{GPS}_β and t_β^{GPSk} being the GPS time of reception and transmission. The resulting P-code observation will be ($t^{GPS}_\beta - t_\beta^{GPSk} + dt_{i\beta} - dt^k_\beta$). Using the broadcast clock parameters, the major part of the term dt^k_β can be removed from the P-code observation which can be subtracted afterwards from the reception time ($t^{GPS}_\beta + dt_{i\beta}$) to recover the transmission time t^{GPSk}_β. This is the DIPOP procedure for removing the clock term in equation (5.5) when P-code observations are available.

Some other procedures use a single-point positioning solution to estimate a term $dt_{i\beta}$ (which is usually modelled by a low degree polynomial) for each receiver. These terms can be used afterwards to cancel the clock term in the observation equation.

As we will see in chapter 6, our data set from the HPBT campaign was corrupted by some timing problems which did not allow us to take advantage of the P-code data. We had no choice but to process the TI 4100 data as codeless data with observation equation (5.5) including a clock term. Thus, we decided to use equation (5.5) as a standard model for our GPS double-difference carrier phase reduction.

5.2 Partial derivatives

5.2.1 Station coordinates

The partials with respect to the station coordinates are obtained in a straightforward way. In equation (5.5), the station coordinates are in the term ρ^{kl}_{ij}; if the station coordinates are denoted by the vector **R** and if we drop the epoch tag ($t_{i\beta}$) the partials can be written:

$$\frac{\partial \lambda\phi^{kl}_{ij}}{\partial \mathbf{R}_i} = \frac{\partial \lambda\phi^{kl}_{ij}}{\partial \rho^{kl}_{ij}} \cdot \left[\frac{\partial \rho^{kl}_{ij}}{\partial \rho^{k}_{ij}} \cdot \frac{\partial \rho^{k}_{ij}}{\partial \rho^{k}_{i}} \cdot \frac{\partial \rho^{k}_{i}}{\partial \mathbf{R}_i} + \frac{\partial \rho^{kl}_{ij}}{\partial \rho^{l}_{ij}} \cdot \frac{\partial \rho^{l}_{ij}}{\partial \rho^{l}_{i}} \cdot \frac{\partial \rho^{l}_{i}}{\partial \mathbf{R}_i} \right] \tag{5.6}$$

where :

$$\begin{aligned} \rho^{kl}_{ij} &= \rho^{k}_{ij} - \rho^{l}_{ij} \\ \rho^{k}_{ij} &= \rho^{k}_{i} - \rho^{k}_{j} \\ \rho^{l}_{ij} &= \rho^{l}_{i} - \rho^{l}_{j} \\ \rho^{m}_{n} &= \sqrt{(X_n - x^m)^2 + (Y_n - y^m)^2 + (Z_n - z^m)^2} \end{aligned} \tag{5.7}$$

with m = k, l and n = i, j , the partials are as follows:

$$\frac{\partial \lambda \phi_{ij}^{kl}}{\partial \mathbf{R}_i} = -\mathbf{e}_i^k + \mathbf{e}_i^l$$

$$\frac{\partial \lambda \phi_{ij}^{kl}}{\partial \mathbf{R}_j} = \mathbf{e}_j^k - \mathbf{e}_j^l \qquad (5.8)$$

where $\mathbf{e}^m{}_n$ is the unit vector in station-satellite (n-m) direction. These partials are obviously computed with station and satellite coordinates in the same reference system.

5.2.2 Clock synchronization

In DIPOP the relative receiver clock synchronization error is modelled by a first order algebraic polynomial:

$$\Delta t_{ij} = A_o + A_1(t - t_o) \qquad (5.9)$$

where A_o represents the relative clock offset, and A_1 the relative clock drift, t_o is a reference time corresponding to the first epoch of observation. The partials are then derived as follows:

$$\frac{\partial \lambda \phi_{ij}^{kl}}{\partial A_o} = \frac{\partial \lambda \phi_{ij}^{kl}}{\partial \Delta t_{ij}} \cdot \frac{\partial \Delta t_{ij}}{\partial A_o} = (-\dot{\rho}_j^k + \dot{\rho}_j^l) \qquad (5.10)$$

$$\frac{\partial \lambda \phi_{ij}^{kl}}{\partial A_1} = \frac{\partial \lambda \phi_{ij}^{kl}}{\partial \Delta t_{ij}} \cdot \frac{\partial \Delta t_{ij}}{\partial A_1} = (-\dot{\rho}_j^k + \dot{\rho}_j^l) \cdot (t - t_o) \qquad (5.11)$$

The option of estimating the coefficients A_o and A_1 is user-selectable.

5.2.3 Phase ambiguity

It is the inter-station single-difference ambiguties $N^k{}_{ij}$, $N^l{}_{ij}$ which are estimated in DIPOP; moreover, it is a relative estimate which is performed since one satellite ambiguity is set at zero (reference satellite). A double-difference ambiguities estimation would be possible as well.

Since the double difference ambiguity in equation (5.5) is given as follows:

$$N_{ij}^{kl} = N_{ij}^{k} - N_{ij}^{l} \tag{5.12}$$

the partials are given by:

$$\frac{\partial \lambda \phi_{ij}^{kl}}{\partial N_{ij}^{k}} = \frac{\partial \lambda \phi_{ij}^{kl}}{\partial N_{ij}^{kl}} \cdot \frac{\partial N_{ij}^{kl}}{\partial N_{ij}^{k}} = \lambda \tag{5.13}$$

$$\frac{\partial \lambda \phi_{ij}^{kl}}{\partial N_{ij}^{l}} = \frac{\partial \lambda \phi_{ij}^{kl}}{\partial N_{ij}^{kl}} \cdot \frac{\partial N_{ij}^{kl}}{\partial N_{ij}^{l}} = - \lambda \tag{5.14}$$

In DIPOP the signs of equation (5.13) and (5.14) are inverted; the estimated ambiguities are simply of opposite sign. For a squaring type receiver, these partials are scaled as half of the carrier wavelength.

For dual-frequency data, a linear ionospheric free combination is used in order to remove the bulk of the dispersive ionospheric delay [Vanicek et al., 1985; Kleusberg, 1986]. In this case the ambiguity term of equation (5.5) is a product of a real number and an integer number:

$$\frac{c^2}{f_{L1}^2 - f_{L2}^2} \cdot \left(\frac{N_{ijL1}^{kl}}{\lambda_{L1}} - \frac{N_{ijL2}^{kl}}{\lambda_{L2}} \right) = \frac{77}{2329} \lambda_{L1} \left(77\, N_{ijL1}^{kl} - 60\, N_{ijL2}^{kl} \right) \tag{5.15}$$

where:

f_{L1} is the L1 frequency 1575.42 MHz,

f_{L2} is the L2 frequency 1227.60 MHz.

When this linear combination is used, the term in parenthesis on the right-hand side of equation (5.15) is estimated. Although this term is an integer by definition, it is very sensitive to small changes in the ambiguity terms on L1 and L2. For example, if the ambiguities $N_{ij}{}^{kl}{}_{L1} = 10$ and $N_{ij}{}^{kl}{}_{L2} = 5$, the estimated ambiguity term (from 5.15) should be (77*10 - 60*5) = 470. If for some reasons (multipath effects, orbit accuracy, internal tracking errors, etc.) the real estimated ambiguities for each frequency cannot be better than $N_{ij}{}^{kl}{}_{L1} = 10.08$ and $N_{ij}{}^{kl}{}_{L2} = 4.91$, which are very close to integer values, the estimated value (from 5.15) will be 481.56. This is quite far from the expected value

(470). Thus, it is almost impossible to resolve the ambiguity from the estimated ambiguity term of equation (5.15). In all network solutions presented in chapter 6 we used the ionospheric free linear combination with real estimated values.

5.2.4 Tropospheric zenith delay

This is a parameter that we have implemented in our new version of DIPOP. This parameter is in fact a correction applied to the modified Hopfield model [Wells, 1974] used in DIPOP 2.0. The tropospheric delay dT^{kl}_i, at site i, can be written as follows [Santerre, 1987]:

$$dT_i^{kl} = (1 + \kappa_i) \cdot dTo_i^{kl} \qquad (5.16)$$

where:

dTo^{kl}_i	is the single-difference tropospheric correction computed according to the modified Hopfield model,
κ_i	is the parameter of interest, a corrective term to the computed delay at sites i (scale factor).

This corrective term κ_i can be viewed as a correction applied to the tropospheric zenith delay. Since κ_i is a constant value we assume that this parameter will absorb, to some extent, the constant unmodelled part of the relative tropospheric zenith delay by the surface meteorological data. This can include the malfunctioning of the meteorological devices or will simply allow us to use standard meterological data without too many problems (when there is no meteorological data available).

This estimate being a constant, if standard meteorological data are used at sites where meteorological conditions vary significantly (during the observation period), the results might be doubtful. On the other hand, if the temperature, pressure and relative humidity are rather constant at sites, the estimation of this parameter may be useful if the standard meteorological values used are far from the real surface meteorological data. For widely varying meteorological conditions, a linear (or higher degree) model or the estimation of scale parameters at every hour should be investigated. The in depth study of tropospheric refraction not being within the scope of this thesis, we opted for the

zero-order model.

In our model, one tropospheric parameter can be estimated on demand at each site involved in a baseline or a network solution. The double-difference tropospheric delay of equation (5.5), at each of the sites, can be written as follows:

$$\begin{aligned} dT_{ij}^{kl} &= dT_i^{kl} - dT_j^{kl} \\ dT_i^{kl} &= dT_i^{k} - dT_i^{l} \\ dT_j^{kl} &= dT_j^{k} - dT_j^{l} \end{aligned} \tag{5.17}$$

The partial derivatives follow from (5.5), (5.16) and (5.17):

$$\frac{\partial \lambda\phi_{ij}^{kl}}{\partial \kappa_i} = \frac{\partial \lambda\phi_{ij}^{kl}}{\partial dT_{ij}^{kl}} \cdot \frac{\partial dT_{ij}^{kl}}{\partial dT_i^{kl}} \cdot \left[\frac{\partial dT_i^{kl}}{\partial dT_i^{k}} \cdot \frac{\partial dT_i^{k}}{\partial \kappa_i} + \frac{\partial dT_i^{kl}}{\partial dT_i^{l}} \cdot \frac{\partial dT_i^{l}}{\partial \kappa_i} \right] \tag{5.18}$$

A similar equation is written for κ_j, and finally we have:

$$\frac{\partial \lambda\phi_{ij}^{kl}}{\partial \kappa_i} = - dTo_i^{k} + dTo_i^{l} \tag{5.19}$$

$$\frac{\partial \lambda\phi_{ij}^{kl}}{\partial \kappa_j} = dTo_j^{k} - dTo_j^{l} \tag{5.20}$$

with $dTo^m{}_n$ being the modified Hopfield correction applied on the range between satellite m and receiver n.

5.2.4 Satellite initial state vector

The partials with respect to the satellite initial state vector S are obtained as follows:

$$\frac{\partial \lambda \phi_{ij}^{kl}}{\partial s_i^n} = \frac{\partial \lambda \phi_{ij}^{kl}}{\partial \mathbf{r}^n} \cdot \frac{\partial \mathbf{r}^n}{\partial s_i^n} \tag{5.21}$$

where n = k or l, whereas the s_i (i=1,2, . . ,6) represents the six Keplerian elements of the initial state vector **S**. The first part of the right-hand side of equation (5.21) is obtained with equation (5.6) replacing **R** by **r**:

$$\frac{\partial \lambda \phi_{ij}^{kl}}{\partial \mathbf{r}^k} = -\mathbf{e}_j^k + \mathbf{e}_i^k \tag{5.22}$$

$$\frac{\partial \lambda \phi_{ij}^{kl}}{\partial \mathbf{r}^l} = \mathbf{e}_j^l - \mathbf{e}_i^l \tag{5.23}$$

The second part of the partials is obtained with the aid of equations (2.10) and (2.11):

$$\begin{bmatrix} x \\ y \\ z \end{bmatrix}_{\text{inertial}} = R_3(-\Omega)\, R_1(-i)\, R_3(-\omega) \begin{bmatrix} a(\cos E - e) \\ a(1 - e^2)^{1/2} \sin E \\ 0 \end{bmatrix} \tag{5.24}$$

Using equations (2.3), (2.4) and (2.5) the eccentric anomaly E can be expressed in the following way:

$$E = \sqrt{\frac{GM}{a^3}} \cdot (t - T) + e \sin E \tag{5.25}$$

Equations (5.24) and (5.25) are the basic equations needed to derive the partial of the inertial satellite position **r**(t) with respect to the initial six Keplerian elements defined in the same inertial system.

To derive the partials let us write equation (5.24) as a product of two matrices $\mathbf{f}_1$ and $\mathbf{f}_2$:

$$\mathbf{r}(t) \;=\; \mathbf{f}_1(i\,,\omega\,,\Omega\,)\;\bullet\;\mathbf{f}_2(a,e\,,E\,) \tag{5.26}$$

$\mathbf{f}_1$ being the first three terms of equation (5.24) and $\mathbf{f}_2$ the last term in brackets of the same equation. According to this simple form, the partials with respect to an element s_i can be written as follows:

$$\frac{\partial \mathbf{r}}{\partial s_i} \;=\; \mathbf{f}_1 \bullet \frac{\partial \mathbf{f}_2}{\partial s_i} \;+\; \frac{\partial \mathbf{f}_1}{\partial s_i} \bullet \mathbf{f}_2 \tag{5.27}$$

Since $\mathbf{f}_1$ and $\mathbf{f}_2$ are not functions of the same elements there will always be only one term on the right-hand side of equation (5.27). Another simplification can be introduced when we realize that the third element of the (3x1) matrix $\mathbf{f}_2$ is zero. This implies that the (3x3) matrix $\mathbf{f}_1$ can be reduced to a (3x2) matrix. By performing the matrix multiplication and dropping the third column the following is obtained:

$$\mathbf{f}_1 = \begin{bmatrix} \cos\Omega\cos\omega - \sin\Omega\cos i\sin\omega & , -\cos\Omega\sin\omega - \sin\Omega\cos i\cos\omega \\ \sin\Omega\cos\omega - \cos\Omega\cos i\sin\omega & , -\sin\Omega\sin\omega + \cos\Omega\cos i\cos\omega \\ \sin i\sin\omega & , \sin i\cos\omega \end{bmatrix} \tag{5.28}$$

The partials of $\mathbf{f}_1$ with respect to ω, Ω and i, are derived directly:

$$\frac{\partial \mathbf{f}_1}{\partial \omega} = \begin{bmatrix} -\cos\Omega\sin\omega - \sin\Omega\cos i\cos\omega & , -\cos\Omega\cos\omega + \sin\Omega\cos i\sin\omega \\ -\sin\Omega\sin\omega + \cos\Omega\cos i\cos\omega & , -\sin\Omega\cos\omega - \cos\Omega\cos i\sin\omega \\ \sin i\cos\omega & , -\sin i\sin\omega \end{bmatrix} \tag{5.29}$$

$$\frac{\partial \mathbf{f}_1}{\partial \Omega} = \begin{bmatrix} -\sin\Omega\cos\omega - \cos\Omega\cos i\sin\omega & , \sin\Omega\sin\omega - \cos\Omega\cos i\cos\omega \\ \cos\Omega\cos\omega - \sin\Omega\cos i\sin\omega & , -\cos\Omega\sin\omega - \sin\Omega\cos i\cos\omega \\ 0 & , 0 \end{bmatrix} \tag{5.30}$$

$$\frac{\partial \mathbf{f}_1}{\partial i} = \begin{bmatrix} \sin\Omega \sin i \sin\omega & , & \sin\Omega \sin i \cos\omega \\ -\cos\Omega \sin i \sin\omega & , & -\cos\Omega \sin i \cos\omega \\ \cos i \sin\omega & , & \cos i \cos\omega \end{bmatrix} \tag{5.31}$$

Dropping the last element of the column matrix $\mathbf{f}_2$, the following is obtained:

$$\mathbf{f}_2 = \begin{bmatrix} a\ (\cos E - e) \\ a\ (1 - e^2)^{1/2} \sin E \end{bmatrix} \tag{5.32}$$

E being a function of a, e and T, the partials of $\mathbf{f}_2$ with respect to these three elements can be written in the following way:

$$\frac{\partial \mathbf{f}_2}{\partial a} = \begin{bmatrix} (\cos E - e) - a \sin E \cdot \dfrac{\partial E}{\partial a} \\ (1 - e^2)^{1/2} \sin E + a\ (1 - e^2)^{1/2} \cos E \cdot \dfrac{\partial E}{\partial a} \end{bmatrix} \tag{5.33}$$

$$\frac{\partial \mathbf{f}_2}{\partial e} = \begin{bmatrix} -a\ (1 + \sin E \cdot \dfrac{\partial E}{\partial e}) \\ a\left(\dfrac{-e}{(1 - e^2)^{1/2}}\right) \sin E + a\,(1 - e^2)^{1/2} \cos E \cdot \dfrac{\partial E}{\partial e} \end{bmatrix} \tag{5.34}$$

$$\frac{\partial \mathbf{f}_2}{\partial T} = \begin{bmatrix} -a \sin E \cdot \dfrac{\partial E}{\partial T} \\ a\,(1 - e^2)^{1/2} \cos E \cdot \dfrac{\partial E}{\partial T} \end{bmatrix} \tag{5.35}$$

The partials of the eccentric anomaly E with respect to the three elements a, e and T are:

$$\frac{\partial E}{\partial a} = -\frac{3}{2} \cdot \sqrt{\frac{GM}{a^3}} \cdot \frac{1}{a} \cdot \frac{(t - T)}{(1 - e \cos E)} \tag{5.36}$$

$$\frac{\partial E}{\partial e} = \frac{\sin E}{(1 - e \cos E)} \tag{5.37}$$

$$\frac{\partial E}{\partial T} = -\sqrt{\frac{GM}{a^3}} \cdot \frac{1}{(1 - e \cos E)} \tag{5.38}$$

The partials of the satellite positions $\mathbf{r}(t)$ with respect to the Keplerian elements can now be obtained according to equation (5.27):

$$\frac{\partial \mathbf{r}}{\partial a} = \mathbf{f}_1 \cdot \frac{\partial \mathbf{f}_2}{\partial a} \tag{5.39}$$

$$\frac{\partial \mathbf{r}}{\partial e} = \mathbf{f}_1 \cdot \frac{\partial \mathbf{f}_2}{\partial e} \tag{5.40}$$

$$\frac{\partial \mathbf{r}}{\partial T} = \mathbf{f}_1 \cdot \frac{\partial \mathbf{f}_2}{\partial T} \tag{5.41}$$

$$\frac{\partial \mathbf{r}}{\partial \omega} = \frac{\partial \mathbf{f}_1}{\partial \omega} \cdot \mathbf{f}_2 \tag{5.42}$$

$$\frac{\partial \mathbf{r}}{\partial \Omega} = \frac{\partial \mathbf{f}_1}{\partial \Omega} \cdot \mathbf{f}_2 \tag{5.43}$$

$$\frac{\partial \mathbf{r}}{\partial i} = \frac{\partial \mathbf{f}_1}{\partial i} \cdot \mathbf{f}_2 \tag{5.44}$$

These equations have been spelled out in Langley et al. [1984] and coded in a Univeristy of Berne subroutine RPART. In their equations (4.22), (4.23) and (4.24)

which are our equations (5.36) (5.37) and (5.38), the following equivalence has been used:

$$\frac{a}{r} = \frac{1}{(1 - e \cos E)} \tag{5.45}$$

where r is the magnitude of the vector **r**(t).

In Langley et al. [1984] a minus sign was omitted in their equation (4.24). It is obviously a typing mistake since the equation is correctly coded in subroutine RPART. In their equations set (4.25), the second part of the right-hand side of the equation related to $\partial \mathbf{r}/\partial e$ (our equation 5.34) a minus sign related to the eccentricity e also was omitted. In subroutine RPART, the sign is also missing. This mistake introduces only few centimetres of error in the improved satellite positions when a good a priori value of the eccentricity e is known (close to 10^{-6}). A corrected version of RPART is used in our new version of DIPOP to compute these partials.

5.3 Actual DIPOP adjustment approach

The first version of DIPOP (1.0) has been well described in Vanicek et al. [1985], Santerre et al. [1985] and Langley et al. [1986a], whereas the second version (2.0) is described in Santerre et al. [1987]. This section describes the main idea behind the nuisance parameters elimination approach that is an important feature of DIPOP.

In the sequential least-squares parametric adjustment used in DIPOP, the estimated parameters are divided into parameters of interest (station coordinates) and nuisance parameters (biases), which are all other parameters contributing to the observation equations.

The observations are also divided into several independent groups or sessions where a session is characterized by a common set of nuisance parameters. In the current DIPOP (2.0) version, a session is defined by all the observations related to a specific baseline vector where common nuisance parameters are clock synchronization terms and phase ambiguities. It should be noted that in network mode, this definition assumes no correlation between simultaneous double-difference observables formed by different pairs of receivers.

The observations within a session are divided into sequences. A sequence is a

unit of the sequential adjustment. The algorithm is such that a sequence can be just one epoch (one observation) or may cover a complete session.

To understand this approach, let us define the following example; we have three receivers (2 independent baselines) simultaneously observing 4 satellites over two different observation sessions (2 different days). This collected data can be organized in a solution involving 3 stations (A, B, C: 9 coordinates) as parameters of interest plus 8 clock parameters (2 by baseline over 2 sessions) and 16 ambiguties (4 by baseline over 2 sessions) as nuisance parameters. The schematic design matrix of this problem for a conventional least-squares batch solution is given in Fig. 5.1. Since there are 4 satellites observed, 3 independent double-difference observables are formed and each line of a block session (observation related to a specific baseline) of Fig. 5.1 represents all observations pertaining to a specific double-difference observable. Thus, black squares represent non-zero sub-matrices (nx1) whereas empty squares are zero sub-matrices. Such a representation is used by Mikhail and Ackerman [1976] to study the computational efficiency of large least-squares problems.

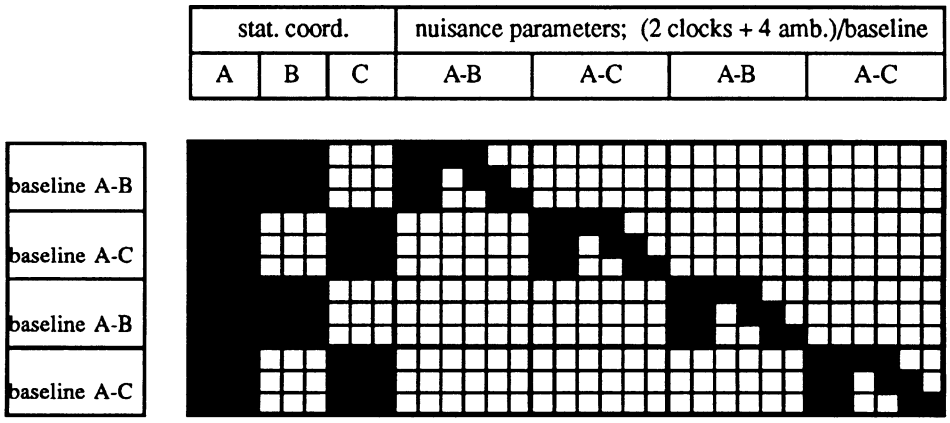

Design matrix for classical least-squares batch solution
(solution for 3 receivers, 2 observation sessions,
4 satellites, 2 clocks/baseline)
FIGURE 5.1

Assuming that we fix station A with an appropriate P_x matrix, the schematic normal equation matrix ($A^TPA + P_x$) from the design matrix of Fig. 5.1 is given in Fig.

5.2 where black squares represent non-zero elements whereas empty squares are zero elements). This result is obtained with an identity matrix P, i.e. no correlation between observations of different baselines is taken into account. The elimination algorithm used in DIPOP is based on the special form of the matrix presented in Fig. 5.2. Since there is no correlation between nuisance parameters from one baseline to another, the adjustment

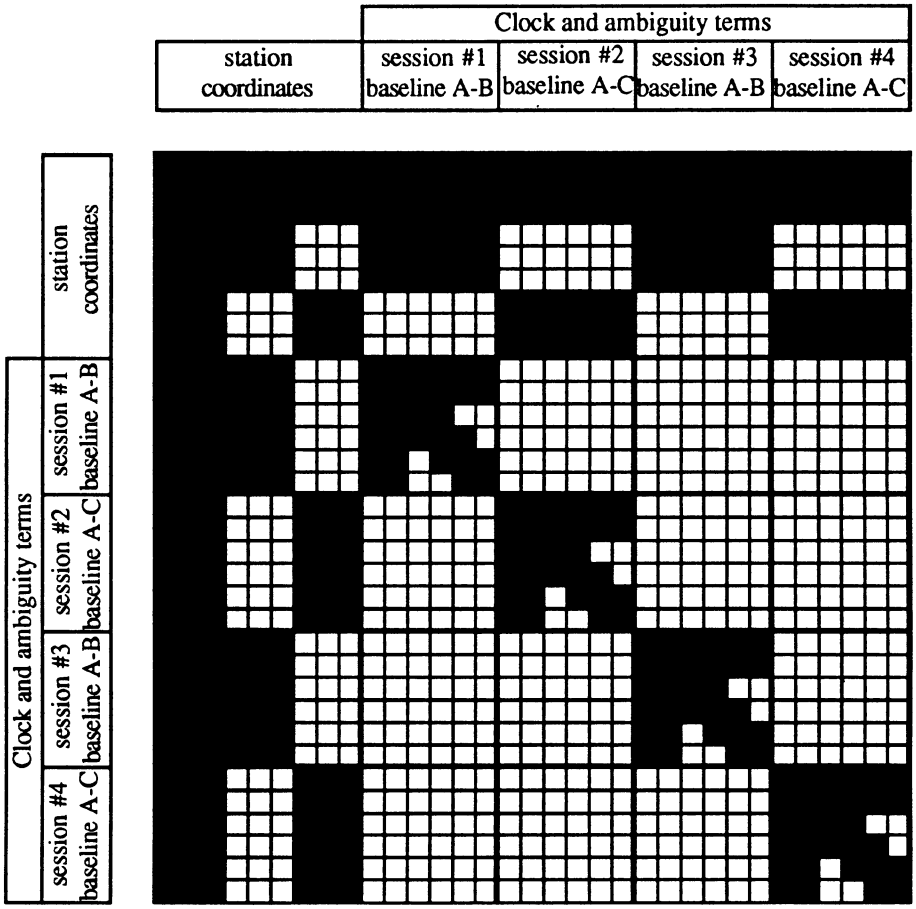

Normal equations ($A^TPA + P_x$) associated with
the design matrix of Fig. 5.1 (P = identity matrix)
FIGURE 5.2

may process the observations of each baseline sequentially by rigourously eliminating the nuisance parameters from the normal equations (related to station coordinates) after

all observations pertaining to a specific baseline have been processed. From this procedure, a baseline vector can be defined as a specific session. This approach is a powerful tool by which to reduce the memory storage requirement. For a specific number of station coordinates, an unlimited number of sessions can be processed in a network mode since the observations from one more session do not increase the storage requirement. The algorithm of this sequential least-squares adjustment is described in detail in Vanicek et al. [1985].

Although the correlation between simultaneous observations of different baseline vectors cannot be easily taken into account when a session is defined as baseline, the correlation between double-difference observations of the same baseline can be handled without problem. This option is part of DIPOP 2.0.

If an orbit improvement is to be implemented in DIPOP 2.0, the current definition of a session must be modified since the orbital parameters are common to all observations pertaining to a specific orbital arc. The next section describes the principal modifications that we performed to handle this situation.

5.4 Principal DIPOP modifications

We introduced three different types of modification in DIPOP 2.0, the most important being the modifications related to the orbit improvement. Some other modifications, as mentioned earlier, were done to improve the observations modelling, and finally modifications for data handling were done.

The major modification which was implemented in order to obtain orbit improvement capability was the redefinition of a session. All the internal bookkeeping was redesigned to produce a flexible organization of the observations in different session spans. Although our orbit modelling was designed for short-arc orbits of ~6-8 hours, as long as the memory is not a limiting factor, a session can be extended up to several days. Following this new definition, when orbital parameters must be estimated, we will refer to an "orbital session" as the unit of the nuisance parameters elimination algorithm. This orbital session is defined by the arc length generated by the numerical integrator. Although this session reorganization is necessary for an orbit solution, it will allow (in future development) the correlation between all simultaneous observations as described

in Beutler et al. [1987b] to be taken into account. Owing to the major changes in most of the array dimensions, the program DPDIM [Santerre et al.,1987], which creates the include file containing the DIPOP dimension parameters needed during the complilation of the main and post-processor, was modified.

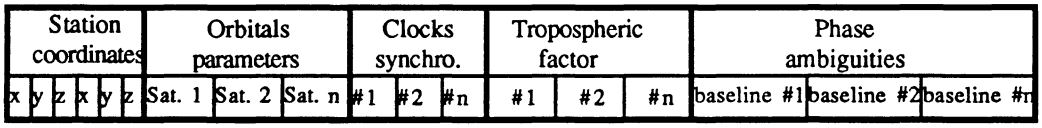

New partitioning of parameters within the design matrix
FIGURE 5.3

The algorithm of the sequential least-squares adjustment was not modified. The elimination is now performed after each orbital session. We only reorganized the design matrix; the new partitioning of the parameters within the matrix is presented in Fig. 5.3. In our new version the following options are possible:

1. pure orbit improvement, where only orbital parameters and ambiguities have to be estimated; all stations are fixed,
2. simultaneous solution, where orbital parameters and all station coordinates are estimated along with ambiguities (free-network solution),
3. simultaneous solution, where orbital parameters and some of the stations coordinates are estimated along with ambiguities; some stations are held fixed (fiducial network solution),
4. standard geodetic solution where only station coordinates are to be estimated along with ambiguities (fixed-orbit solution),
5. option to estimate clock synchronization parameters for code or codeless receivers for each receiver pair pertaining to a baseline,
6. option to estimate a tropospheric scale factor at each site involved in a session,
7. the set of orbital parameters to be estimated is user defined; one to six parameters can be estimated,
8. a preliminary observation elevation angle cutoff can be applied on the input data.

With the exception of the ambiguity parameters, all estimated values can be constrained by a diagonal P_x matrix. Although the standard geodetic solution (fixed

orbit) can be obtained through an appropriate P_x matrix, there is an option where the estimation of orbital parameters is not included (no partials are computed).

In DIPOP 2.0, the input data files for code and codeless receivers contain different types of information; the first contains the satellite positions at transmission time, whereas the second contains the satellite positions and velocities at the reception time. Since the input data is different in each case, the partials are computed by two different subroutines. We have unified this approach. In our new version the input data for code and codeless receivers are the same, and in both cases the partials computation is managed by the same subroutine EQOBS. Moreover, the new input file contains only the double-difference phase observations, the satellite positions and velocities being computed during the processing using polynomial coefficients obtained from a separate file (coefficients previously computed by the orbital pre-processor). In such an approach, a wavelength factor is to be provided in order to scale the effective carrier wavelength properly. The elimination of satellite coordinates in the input files reduces the data storage by approximatly 50%.

The computation of satellite positions and velocities during the processing stage has obvious advantages. First the observations data preprocessing can be performed with any kind of a priori orbit to produce definitive clean input data files; second if an iteration, or simply a re-evaluation of a baseline with an improved orbit is required, the original observations data do not need to be re-preprocessed with the new orbital information: only an updated set of polynomial coefficients (obtained by the orbital pre-processor) must be provided to the main processor along with the same observation input files. This is important since the pre-processing is time-consuming.

The post-processor program, which analyzes the adjustment results, was also modified to take into account all the new parameters and the new session definition. The command file, which controls all the selected options for a specific run, was redesigned as well. An example of the new control file is presented in Appendix 5.

A flow chart of the general procedure to obtain an orbit solution with our package is presented in Fig. 5.4. As mentioned in the introduction we tested our development with observations from the March 1985 HPBT data set. These results are presented in the next chapter.

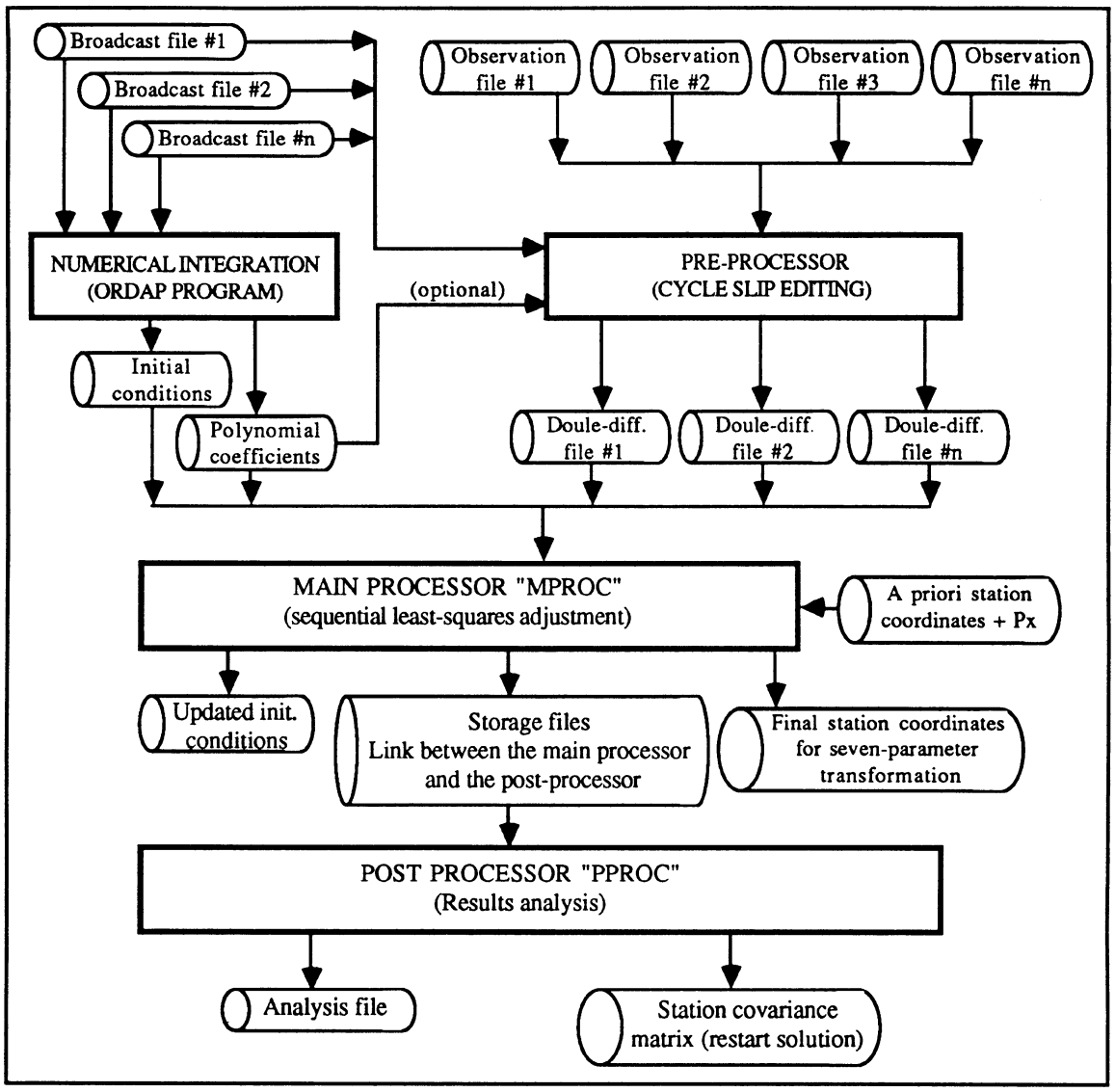

Flow chart of modified DIPOP version
FIGURE 5.4

6. RESULTS

6.1 Data set description

As mentioned in the introduction, the Jet Propulsion Laboratory (JPL) in conjunction with 17 other institutions conducted a high-precision baseline test (HPBT) in the spring of 1985 in order to evaluate the capability of GPS for crustal dynamics studies [Davidson et al., 1985].

Between 29 March and 5 April, dual-frequency GPS receivers were operated at 10 sites in the continental U.S. (see Fig. 6.1). All 10 sites were occupied by Texas Instruments TI 4100 receivers. At two sites (Mojave and Big Pine) JPL's SERIES-X receivers were also operated and at Westford, Richmond, and Fort Davis, Air Force Geophysical Laboratory dual-frequency receivers were additionally operated. The receivers were used with a variety of frequency standards: hydrogen masers, cesium, rubudium as well as receiver internal oscillators. Water-vapour radiometers were operated at three of the sites in California: Hat Creek, Mojave and Big Pine.

The GPS satellites were visible over the continental U.S. during two daily windows, one from about 3 hours to 11 hours UT, when satellites PRN 4, 6, 8, 9, 11, 12, 13 were visible, and one from about 17 hours to 21 hours, when only satellites 8, 9, 11 and 12 were briefly visible. The consecutive sessions have been numbered 0 through 15 with the major sessions being even-numbered [Langley et al., 1986b].

At the ARL (Applied Research Laboratory at Austin) and NSWC (Naval Surface Weapons Center at Dahlgren) sites, the TI 4100 receivers were operated throughout the test with external cesium beam-tube frequency standards. At Mammoth Lakes an external rubidium standard was used. At the Westford, Richmond, and Fort Davis VLBI sites, the hydrogen maser standard was always used. And for the two days on which the

Point Mugu receiver participated, the internal crystal oscillator of the receiver was used. At Mojave, Big Pine and Hat Creek a variety of frequency standards were used on an alternating basis. A summary of the observation sessions as well as the frequency standards related to the TI 4100 receivers is presented in Fig. 6.2 [Langley et al., 1986b].

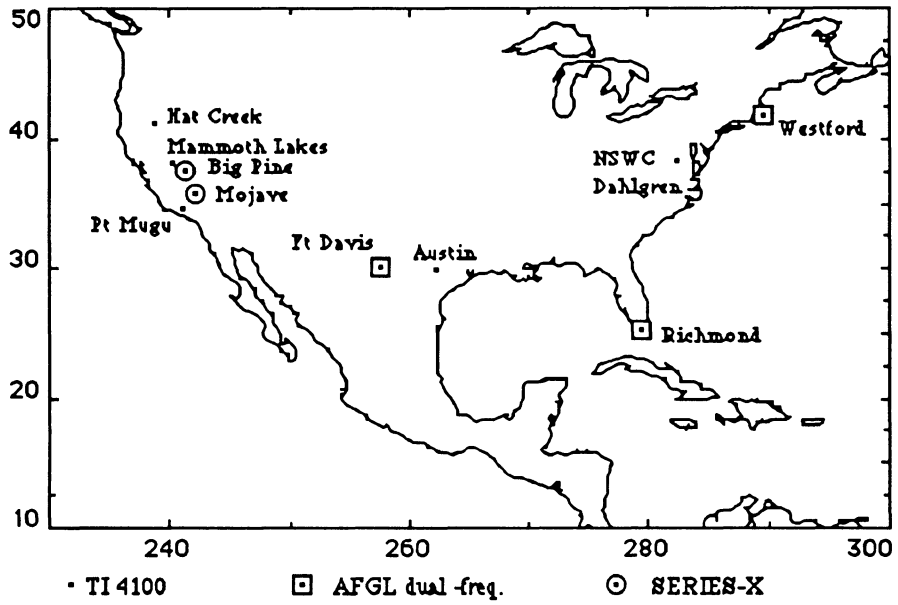

Spring 1985 Hight Precision Baseline Test (HPBT) site locations
FIGURE 6.1

This HPBT test was specially designed to include orbit improvement using GPS observations from VLBI sites, tropospheric correction including estimates of wet-path delay based on water-vapor radiometer (WVR) observations and ionospheric correction based on dual-frequency carrier-phase observations [Ware et al., 1986].

The HPBT data set is then designed perfectly to demonstrate the capability of our software to obtain highly accurate station coordinates by estimating orbital parameters since the coordinates of six of the ten stations of the network are accurately known from VLBI observations (stations Mojave, Westford, Richmond, Fort Davis, Hat Creek and Big Pine). The WGS72 VLBI coordinates have been obtained from Langley [1987]. They are those used by the Bernese group in their preliminary analysis

of the HPBT campaign. This coordinate set differs by a rotation angle of 0.54 arcsec. around the Z axis from those published by Kroger [1986]. Table 6.1 lists the VLBI coordinates (including the GPS antenna eccentricities) in the WGS72 system that we have used as a basis of comparison.

Since our approach is designed for short orbital arc we have decided, to demonstrate the correctness of our algorithms, to process only a subset of the HPBT TI 4100 data set instead of processing the data from the whole campaign. We have selected the first four full (9 stations) TI 4100 sessions as a subset, numbered 02, 04, 06 and 12 (see Fig. 6.2).

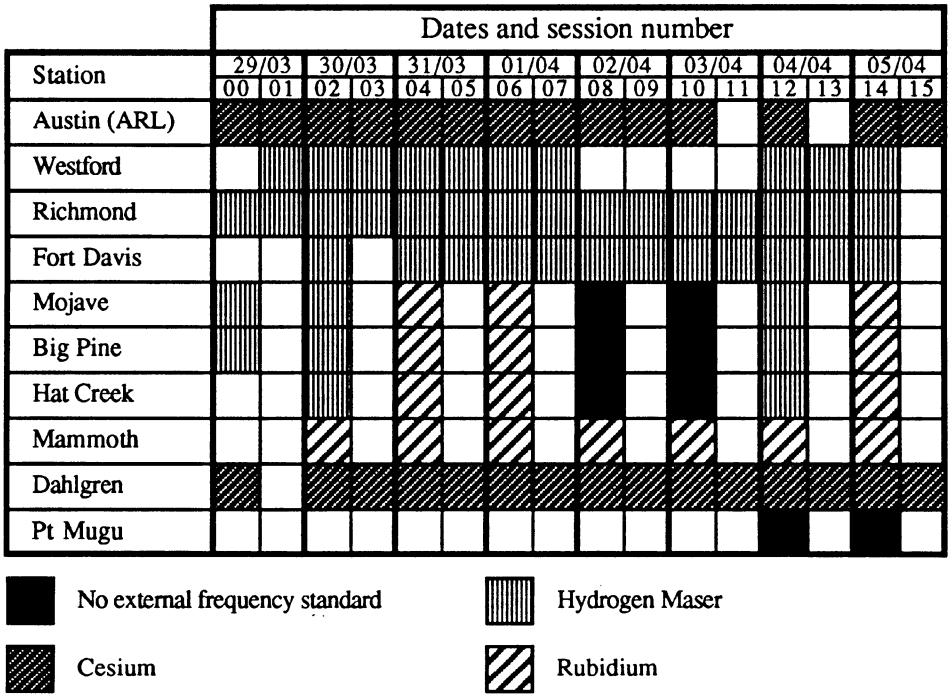

TI 4100 observation schedule
(from Langley et al., 1986b)
FIGURE 6.2

6.2 Test descriptions

We have performed different kinds of tests in order to assess our software development. We will present the most interesting ones in the following sections. The

first series of tests are related to our orbit integrator; we produced some plots to see the different effects of the perturbing forces on the GPS satellites as described in Section 2.4. These plots were produced to assess the correct implementation of the perturbing force models as well as to represent graphically the complexity of the force field required for orbital arc modelling up to 2 days.

SITE	Monument inscription	X	Y	Z
Big Pine	(BP ARIES 3)	-2409654.7415	-4478261.9504	3838638.7329
Fort Davis	(HARVARD RM 4 1980)	-1324205.7179	-5332056.0713	3232043.6300
Westford	(OCP 3 NOAA TM NOS NGS21)	1492398.4454	-4457293.8953	4296819.2655
Hat Creek	(LM NO. 1 M)	-2523882.5946	-4123573.0094	4147719.3431
Mojave	(MOJAVE NCMN NO.3 1983)	-2356576.1550	-4646565.1052	3668427.6533
Richmond	(TIMER 1962)	961302.9852	-5674057.1094	2740563.8693

WGS72 VLBI coordinates (metre)
TABLE 6.1

The second test series is related to the data subset described in the previous section. After the baseline by baseline pre-processing, we first combined all double-difference observations in a fixed-orbit network solution (NETFX) in order to obtain an idea of the broadcast ephemerides accuracy. The rms of the coordinate residuals between our solution and the VLBI WGS72 coordinates was used to judge the accuracy of the broadcast ephemerides.

This estimated broadcast orbit accuracy was used subsequently as a priori constraints (through the P_x matrix) in a free-network solution (NETFR), where all station coordinates are free to adjust along with the orbits. The quality of the network solution was evaluated through a seven-parameter transformation (see Appendix 6) using VLBI coordinates as fixed stations. The same network adjustment was performed in a fiducial network mode (NETFD) where the VLBI stations Westford, Richmond, Fort Davis and Hat Creek were held fixed by means of the P_x matrix. Afterwards, the fiducial approach was used to perform an independent solution for each day involved in the network (02FD, 04FD, 06FD, 12FD). These 4 independent results were used to evaluate the day-to-day network repeatability as well as the internal network accuracy. The characteristics of these solutions appear in Table 6.2.

Finally, we solved for pure orbit solutions using station Westford, Richmond, Fort Davis and Hat Creek as fiducial sites. The improved orbit was subsequently used to process some baselines.

The data from the Westford station recorded in session 04 have been discarded since only few data points were recorded. For sessions 02, 06 and 12, all the observations were differenced with respect to observations from Westford (8 baselines/per day) whereas all data from session 04 were differenced with Hat Creek observations (7 baselines).

As mentionned in Chapter 5, during the HPBT campaign, there was a malfunctioning of the internal receiver software since large clock offsets were found in the TI 4100 data by the Bernese group [Beutler et al., 1986]. The clock offsets obtained from the double-difference phase solutions were not consistent with the same offsets obtained from point positioning (P-code). One of the possible reasons to explain this problem is the non-synchronization of the P-code and the phase measurement, i.e. the two different observations were not observed at the same time although they were recorded with an identical time tag. The DIPOP 2.0 version not being able to estimate these offsets for code receiver data, we were obligated, as mentioned in Section 5.1 to generalize the clock estimation procedure in the software. We thus estimated two clock parameters (offset and drift) for each baseline involved in our solutions. We found clock synchronization offsets of up to 6 milliseconds (see Appendix 7).

Solution	Total # obs.	Number of parameters					Total # parameters
		coord.	amb.	clock	tropos.	orbit	
NETFX	41 168	24	229	62	35	0	350
NETFR	41 168	27	229	62	35	168	521
NETFD	41 168	15 *	229	62	35	168	509
02FD	9 214	15 *	58	16	9	42	140
04FD	10 000	12 *	54	14	8	42	130
06FD	10 772	15 *	59	16	9	42	141
12FD	11 182	15 *	58	16	9	42	140

* Fiducial solution with 12 station coordinates fixed by means of P_x matrix

Different GPS solutions
TABLE 6.2

Seven satellites were observed during each session, and thus (7-1 = 6) ambiguities usually had to be estimated for each baseline, i.e. 48 ambiguities for a session involving 9 stations (8 independent baselines) and 42 for a session involving 8 stations (7 independent baselines). In Table 6.2 there are more ambiguity parameters than the minimum required. This large number of ambiguity parameters is explained by the pseudo-satellites introduced in the solution because of gaps in the data series caused by cycle slips or the necessity to destroy, as mentioned in Section 4.5, the linear dependency between each satellite pair involved. Needless to say that these additional unknowns along with the clock parameters weaken our solutions substantially.

Because we did not have access to surface meteorological data, we decided to solve for a tropospheric scale factor at each station using standard values of meteorological data as a priori values. To be on the safe side with the tropospheric model, we used a cut-off satellite elevation angle of 20° for each solution.

Although the argument of perigee and the time of perigee passage are highly correlated, we decided to solve for 6 parameters for each orbital arc. The selection of the orbital constraints used in the solution will be discussed later.

It should be mentioned that all subroutines that we have developed, to generate our results, are coded in FORTRAN 77 language and all our processing has been performed on the MicroVAX minicomputer of an Intergraph series 250 system.

6.3 Numerical integrator test

This section has been included in order to assess the correct implementation of the force model described in Section 3.4. We proceeded as explained in Section 2.4. We generated a reference trajectory using a complete force model including the earth's geopotential coefficients up to degree and order 8, the third-body effect of the sun and the moon and our simple solar radiation force model. From this reference trajectory, each component of the force model can be easily analyzed graphically.

Although the numerical integrator has been designed to be used for short-arc orbits owing to the specific force model used, the integrator can easily generate a 2-day arc-length trajectory. We obtained from the broadcast ephemerides (from session 02) a

set of osculating elements for satellite PRN 8 at the osculating epoch 46154.1250 MJD (modified Julian date) to integrate a 2-day reference orbital arc. The osculating elements at the epoch are:

$$
\begin{array}{lcl}
a & = & 26\,561\,740.4 \text{ m} \\
e & = & 0.004\,1338 \\
i & = & 63.25^\circ \\
\Omega & = & 148.29^\circ \\
\omega & = & -23.93^\circ \\
T & = & 46154.1059
\end{array}
$$

We first investigated the effect of the higher-order geopotential coefficients, i.e coefficients higher than degree and order 4. We then generated a trajectory with all perturbing forces where the geopotential model was truncated to the degree and order 4. Afterwards, this trajectory was compared at each 10-min. interval (over 48 hours) with the reference trajectory previously described. Fig. 6.3 gives the effect of this truncation in terms of radial, along-track and across-track errors. Clearly, a (4,4) model is not sufficient for short-arc modelling of 6-8 hours when half-metre accuracy level is required, since the total error reach up to 0.60 metres after 6 hours. But if a 0.1 ppm solution is sought, according to equation (1.1), a 2.5-metre accuracy in satellite positions is sufficient and a (4,4) model can be adequate. It can be shown in the same way [Landau and Hagmaier, 1986] that a (8,8) model is sufficient to integrate a 6-day arc at the sub-metre accuracy level.

In the same way we plotted the combined effect of the gravitational attraction of the sun and the moon. Fig 6.4 shows the residuals of this comparison. The third-body effects along with the moon and sun positions computation seems to be correctly implemented since our results correlate with those of Table 2.1. After 3 hours of integration we accummulated a total error up to 132 metres and after two days integration the error reached up to 2750 metres, the along-track component being the most affected.

The solar pressure model correlates as well with the results of Table 2.1. The Fig. 6.5 shows the errors introduced in a trajectory when the solar radiation pressure is not modelled. After 3 hours we accumulated up to 5.5 metres of errors and after two days the error reached up to 480 metres for this specific trajectory.

The force model being well implemented, we can now explain why we do not

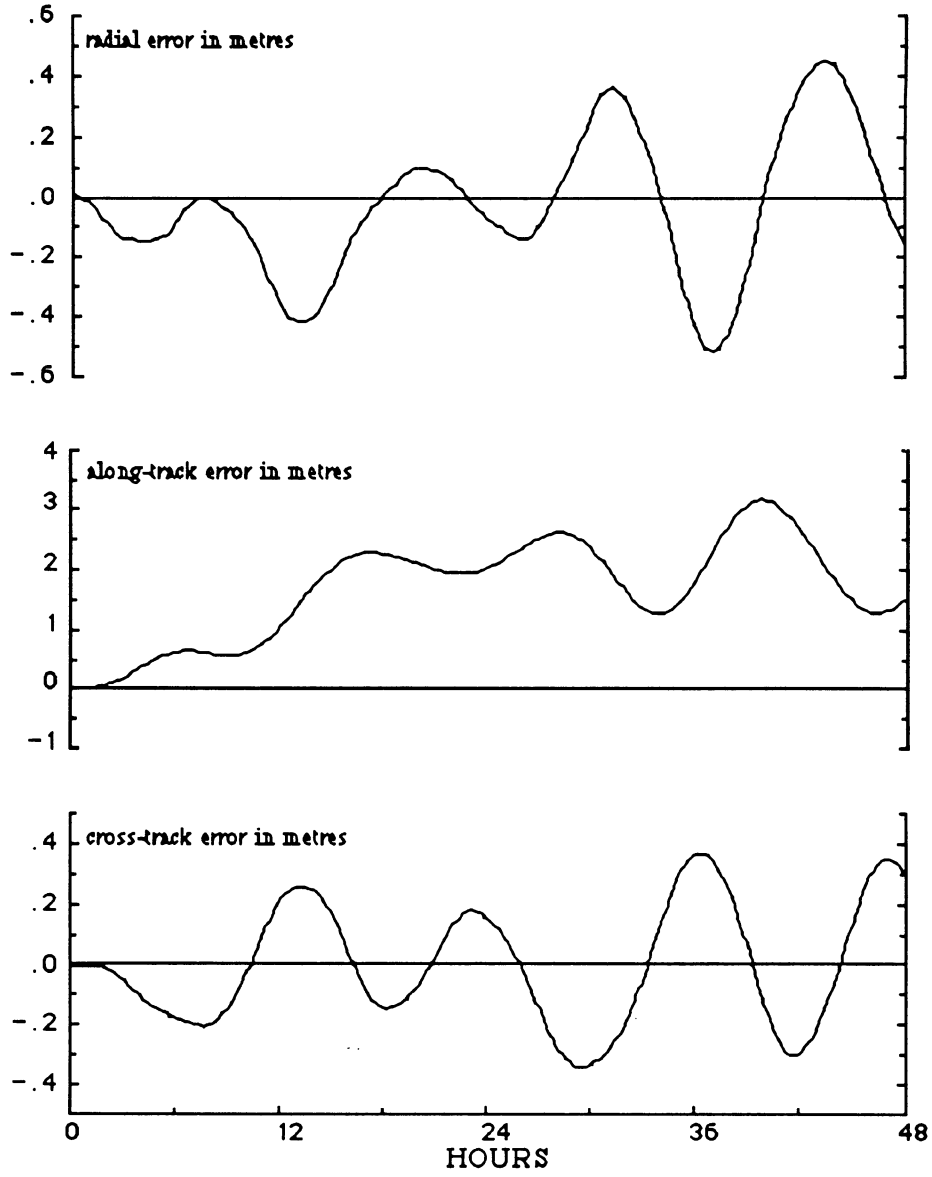

Influence of spherical harmonics of degree and order greater than 4 on satellite's position
FIGURE 6.3

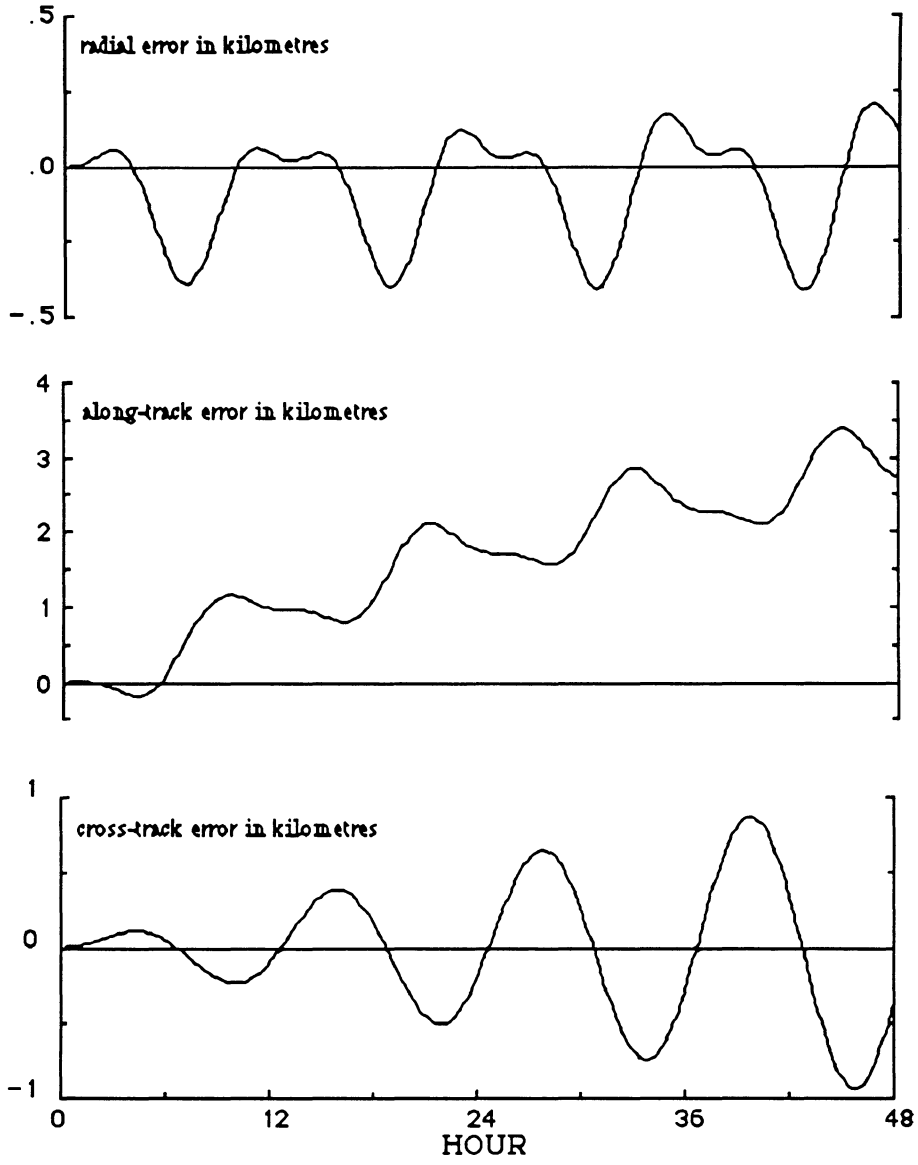

Influence of the gravitational attraction of the sun and
the moon on satellite's position
FIGURE 6.4

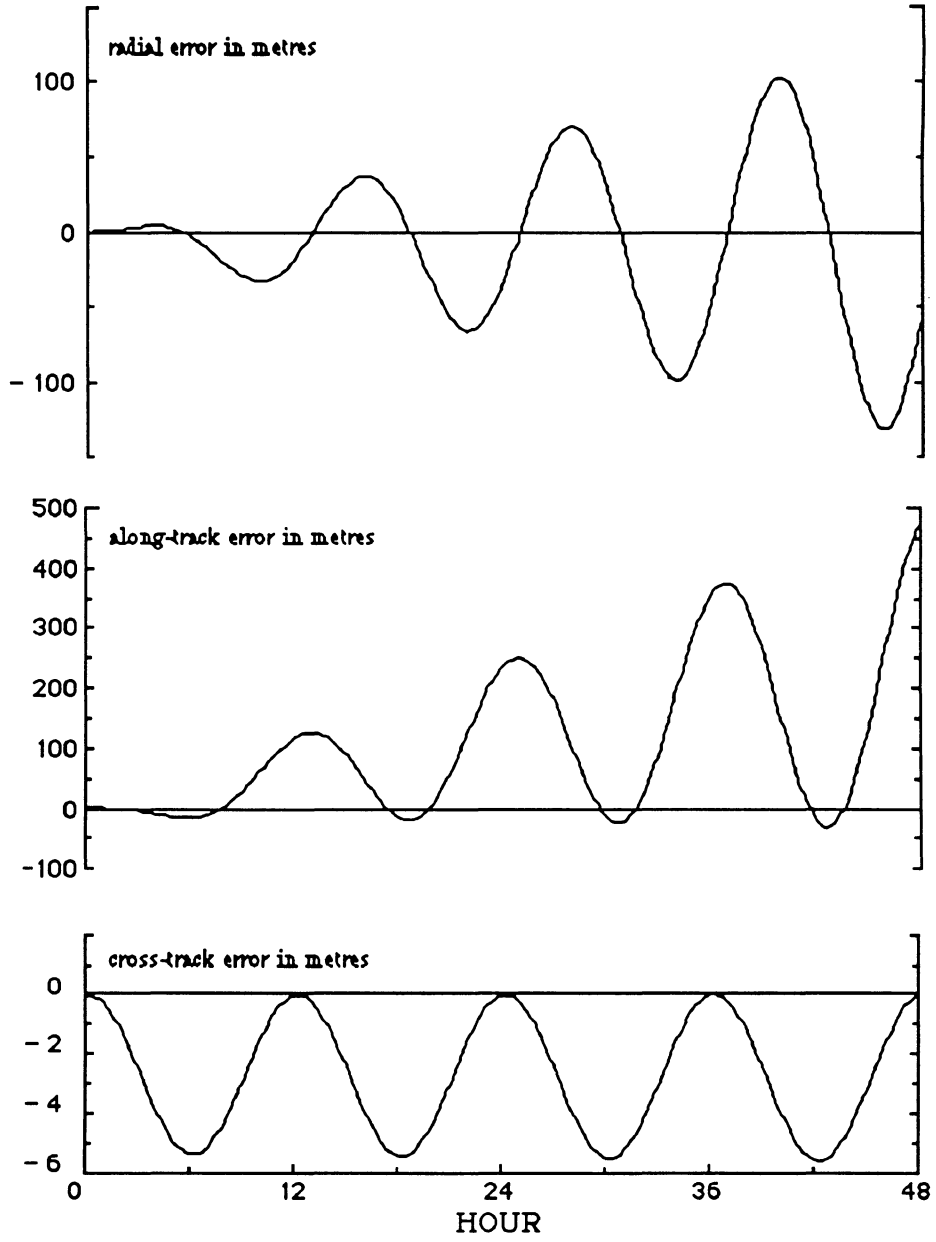

Influence of the solar radiation pressure
on satellite's position
FIGURE 6.5

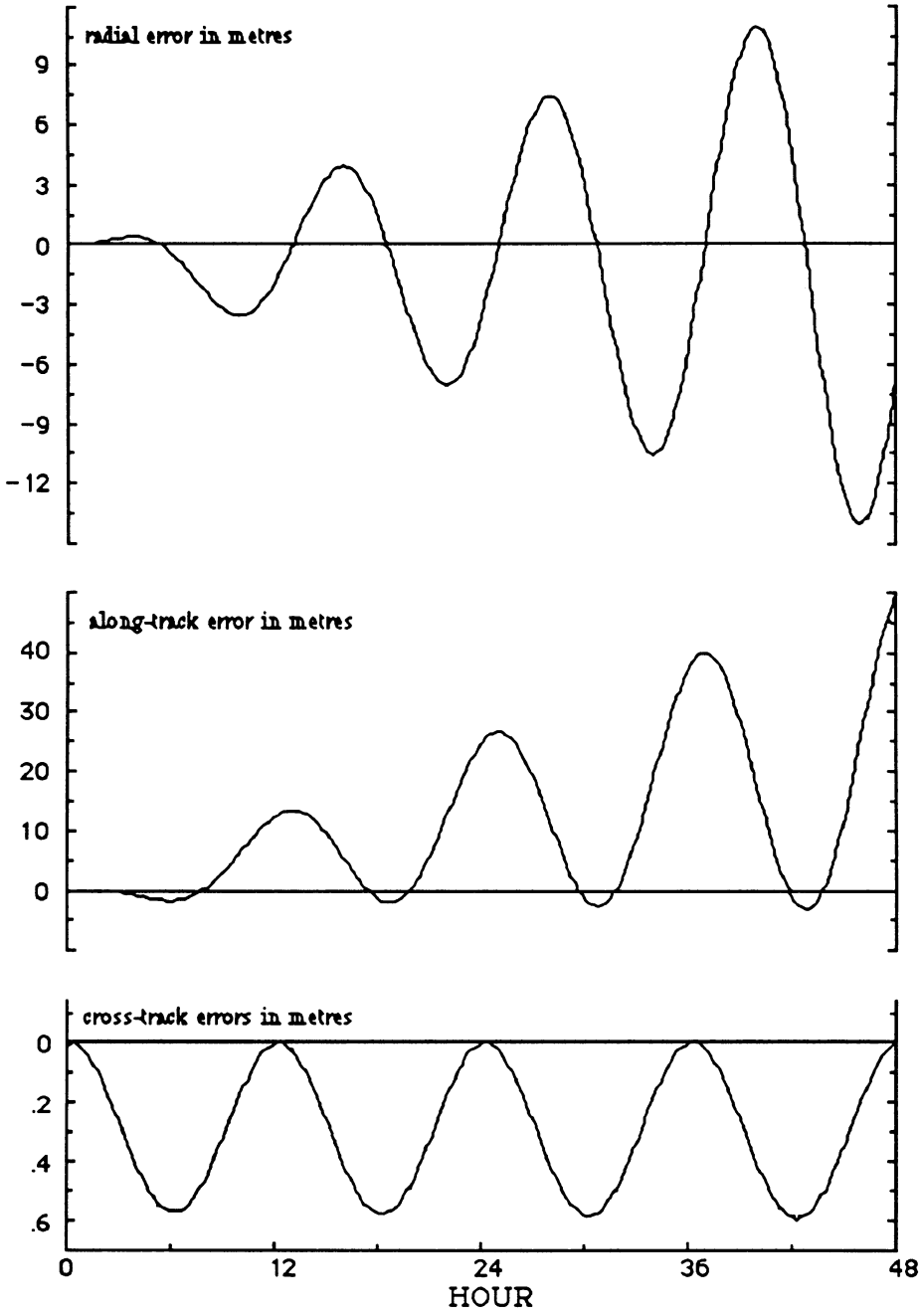

Influence on satellite's position of a direct solar radiation pressure coefficient in error by 10%
FIGURE 6.6

estimate any solar radiation parameters along with our orbital parameters. Beutler et al. [1986] in their preliminary analysis of the HPBT campaign estimated the direct solar radiation parameter along with the orbital parameters. A cursory analysis of their results shows that the estimated values for each satellite vary between 0.83 and 1.02 ($x10^{-7}$ m/sec^2). Thus, we can say that the direct solar radiation pressure parameters for this campaign can be evaluated as $0.94 \times 10^{-7} \pm 10\%$. We investigated the effect of an error of 10% in the solar radiation pressure parameter. These results are shown in Fig. 6.6. The effect is simply one order of magnitude less than the total effect illustrated in Fig. 6.5. For 4 hours of integration the 2.5-metre accuracy level is well maintained; after 7 hours of integration the accumulated errors can reach up to 1.85 m, which is, to a certain extent, acceptable since only satellite PRN 11 has to be integrated over 7 hours (for this specific campaign), all other satellites being integrated for arc-lengths of about 4 hours. However, it is clear from this plot that for arc-lengths longer than 8 hours a solar radiation pressure parameter p_o (see equation 3.15) has to be estimated (for each satellite) if the 2.5-metre level is sought in the satellite positions. The negligible effect of estimating solar radiation pressure parameters over short-arcs has also been pointed out by different authors [Williams, 1986; Beutler et al., 1986].

According to this latest result, all trajectories were integrated with a value of 0.94×10^{-7} m/sec^2 as solar radiation pressure parameter. The integrator is organized in such a way that up to 10 orbital sessions can be integrated sequentially in one run. Using an appropriate step size, the integration of 7 arcs per day over 4 days, including a preliminary improvement (see Section 3.8), takes no more than 40 minutes on our MicroVAX (when a preliminary improvement is required, the integration is performed twice for each satellite).

6.4 Network solutions

We have computed a fixed orbit solution (NETFX) using integrated trajectories adjusted to the broadcast ephemerides as fixed orbit (see Section 3.8). The difference between the "adjusted-integrated" trajectories and the broadcast ephemerides is usually at the metre level, Fig. 6.7 gives an example of these residuals. A significant discontinuity is observed between an old message (AODE = 28 hrs) and a fresh one (AODE = 2.8

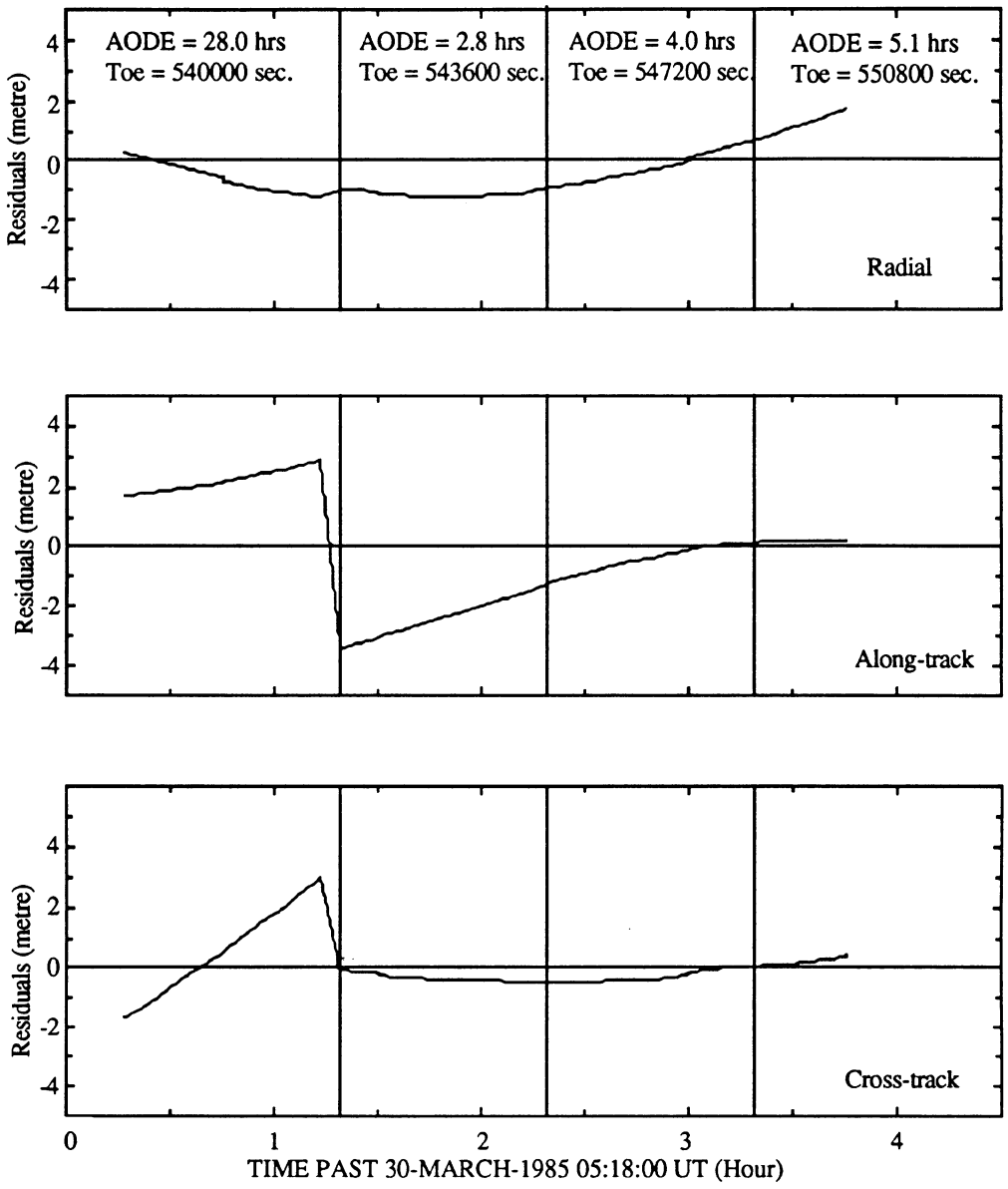

Residuals of the adjustment of the integrated orbit
to the broadcast ephemerides (PRN 9)
FIGURE 6.7

hrs). This example demonstrates why the broadcast ephemerides have to be smoothed prior to use. Since our data set has been collected in 1985, it should be mentioned that all our computations were performed using the WGS72 GM value.

The ionosphere-free combination of L1 and L2 was used in this solution and in all subsequent solutions. For this specific solution, the Westford station was held fixed at the sub-millimetre level through the P_x matrix. The quality of the broadcast ephemerides are as expected. Table 6.3 gives the difference between the NETFX solution and the VLBI coordinates.

Since baselines of up to 4 000 km are involved in the network, the horizontal components of our solution are at the ~ 0.7 ppm relative accuracy level whereas the vertical components are good at the 1.5 ppm level. Without Richmond these values drop to 0.3 and 0.8 ppm. Our results demonstrated the better agreement of the horizontal components when using the broadcast ephemerides. The vertical component is usually 2 or 3 times worse than the horizontal components. Table 6.3 also shows the effect of the better north-south coverage of the current constellation; the latitude is usually better resolved.

Site	North (m)	East (m)	Height (m)
Big Pine	-0.311	-1.371	-3.794
Fort Davis	-0.186	0.007	-2.426
Hat Creek	0.269	-2.254	-1.782
Mojave	-0.108	-1.171	-3.261
Richmond	0.313	-7.276	-10.518
Rms of horizontal residuals	2.62 m		
Rms of vertical residuals	6.02 m		

Difference between fixed-orbit GPS
solution and the VLBI WGS72 coordinates
TABLE 6.3

According to equation (1.1), a relative accuracy of the order of 0.7 ppm results in an orbital error of ~16 m. We used this simple approach to constrain the orbital parameters in the free network solution.

It should be noted that we are talking here about average errors and it may be posssible that some orbits are worse than others. We selected the following a priori constraints to be applied on each orbital element (through the P_x matrix); the induced orbit errors are given in parentheses:

a	=	2 m	(2 m)
e	=	1.0×10^{-7}	(~3 m)
i	=	0.02 arcsec.	(~3 m)
Ω	=	0.02 arcsec.	(~3 m)
ω	=	0.02 arcsec.	(~3 m)
T	=	0.004 sec.	(~15 m)

These a priori weights are similar to those used by Beutler et al. [1987a]. The selected a priori weight for the time of perigee passage was selected to be larger only to be on the safe side, since the largest portion of the error is usually along-track. The selection of the orbital parameter a priori weights have been investigated by Beutler et al. [1987a]. It was clearly shown that a priori weights ranging between 0.1 and 10 times the values previously selected do not significantly affect the final results.

This a priori orbital information was then used to constrain 6 initial conditions per satellite in a free-network solution (NETFR) where all stations were constrained within 100 metres in x, y and z coordinates. Table 6.4 gives the results of the seven-parameter transformation between our free-network solution and the WGS72 VLBI coordinates.

These results are very interesting: horizontal components have improved by a factor of ~20 with respect to the fixed orbit solution whereas the vertical component has improved by almost two orders of magnitude. The better north-south resolution is still well observed. Considering that the network is of the order of 4 000 km, this solution is well below the 0.1-ppm accuracy level. However, there are two significant translation parameters (on x and z axis) which may reflect the poor capacity of phase observations for absolute positioning. There is also a slight scale factor and two small rotation angles between the coordinte sets. Table 6.4 demonstrates, to a certain extent, the correct implementation of the orbit improvement process.

To verify the orbital constraints effect, we have relaxed by a factor of 2 the constraints used previously. The agreement of this new solution with VLBI coordinates

was ~ 0.12 m in the horizontal components and ~ 0.10 m in the vertical component. This result corroborated the Beutler conclusions mentioned previously.

Residuals of the transformation (GPS-VLBI in metres)			
Site	North	East	Height
Big Pine	-0.015	-0.006	0.057
Fort Davis	0.004	-0.116	0.071
Westford	0.201	0.102	0.053
Hat Creek	-0.049	0.130	-0.092
Mojave	0.043	0.047	-0.054
Richmond	-0.152	-0.120	-0.034

rms of horizontal residuals	0.11 m	
rms of vertical residuals	0.07 m	
Translation of x axis	10.54 ±	0.19 m
Translation of y axis	3.73 ±	0.27 m
Translation of z axis	6.88 ±	0.35 m
Rotation around x axis	0.02 ±	0.02 arcsec.
Rotation around y axis	-0.08 ±	0.01 arcsec.
Rotation around z axis	-0.05 ±	0.01 arcsec.
Scale factor	0.07 ±	0.03 ppm.

Seven-parameter transformation between GPS free-network solution and the VLBI WGS72 coordinates
TABLE 6.4

In our fiducial network test, we left the orbits almost free to adjust since the coordinates of 4 network stations were held fixed. The following a priori weights on the orbit initial conditions were used in our fiducial solution (NETFD):

a	=	50 m
e	=	2.0×10^{-5}
i	=	1.0 arcsec.
Ω	=	1.0 arcsec.
ω	=	1.0 arcsec.
T	=	0.250 sec.

The Westford, Richmond, Fort Davis and Hat Creek stations were held fixed. The quality of the solution can be checked by looking at the results for the other two

VLBI sites Mojave and Big Pine. Table 6.5 gives the difference of the estimated coordinates with the VLBI WGS72 coordinates. The discrepancies at Mojave and Hat Creek are of the same order of magnitude as the residuals of Table 6.4, which suggests that free-network and fiducial network approaches have almost the same capabilities to solve the orbit improvement problem to recover accurate relative coordinates. However, as far as the stability of the reference frame is concerned, the fiducial approach is certainly more stable than the free-network approach.

Site	North	East	Height
Big Pine	0.014	-0.077	0.056
Mojave	0.067	-0.012	-0.091

Discrepancy between fiducial solution and VLBI WGS72 coordinates (metre)
TABLE 6.5

Solution	rms (cm)
Orbit fixed	49.04
Free network	1.92
Fiducial network	1.92

Rms of double-difference phase residuals
TABLE 6.6

Table 6.6 gives the rms of double-difference phase residuals for each network solution; the large rms of the fixed orbit solution is simply due to large systematic trends in the double-difference residuals introduced by the orbital errors. Fig. 6.8 illustrates such trends using 3 hours of data (epoch interval = 30 seconds). When orbital parameters are estimated, the rms drops significantly by a factor of 30 which means that the systematic trends greatly disappear. Fig. 6.9 shows the double-difference residuals of the same observations using an improved orbit integrated from a set of initial conditions obtained from the fiducial solution.

The agreement of the NETFR and NETFX solutions with respect the VLBI WGS72 coordinates being ~ 0.1 ppm, or even below, it would be interesting to compare

these two solutions at non-fiducial sites. This comparison is summarized in Table 6.7; VLBI stations Mojave and Big Pine, which were left free in the fiducial solution are also part of this comparison. The free-network coordinates used in this comparison are those obtained after transformation with VLBI WGS72 coordinates (transformation of Table 6.4).

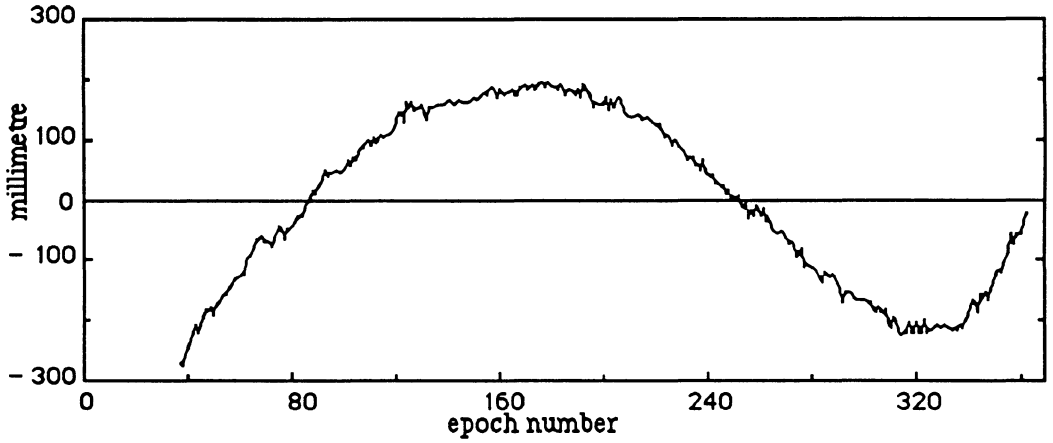

Double-difference residuals satellite 6-8 (L1+L2),
Hat Creek - Fort Davis, session 04.
Solution using broadcast derived orbit
FIGURE 6.8

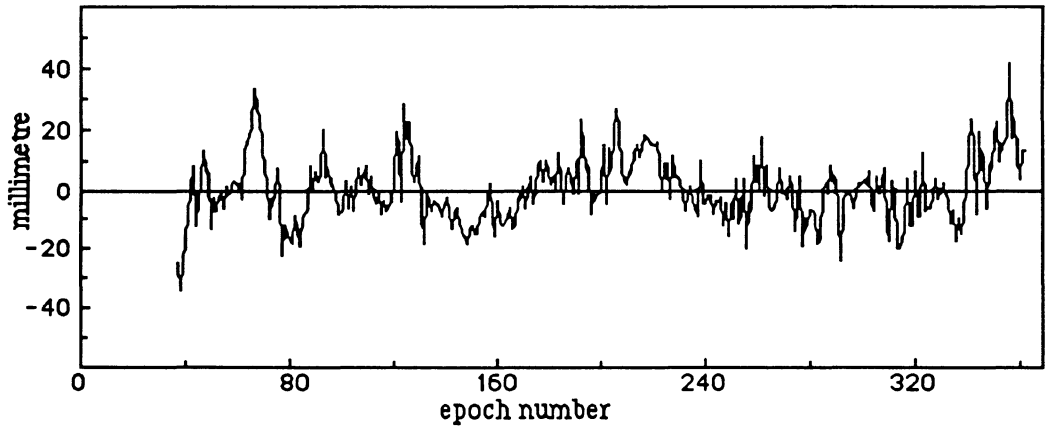

Double-difference residuals satellite 6-8 (L1+L2),
Hat Creek - Fort Davis, session 04.
Solution using improved orbit
FIGURE 6.9

The rms of the comparison is roughly 7 cm (in the three components), which means that the agreement between the two solutions is better than 0.05 ppm level. We also compared the baselines derived from each solution with the VLBI-derived baseline length. We restrained this comparison to the baselines where double-difference observables were formed, i.e. only baselines including Westford and Hat Creek are compared. The results are shown in Table 6.8.

Site	North	East	Height
Dahlgren	0.128	0.033	-0.049
Austin	0.008	-0.148	0.032
Big Pine	-0.029	0.071	0.002
Mammoth	-0.033	0.083	-0.010
Mojave	-0.025	0.059	0.036

Discrepancy (metre) between fiducial solution and free-network solution at non-fiducial sites
TABLE 6.7

Baseline	length	SOLUTION					
		NETFX		NETFR		NETFD	
	(km)	diff. (m)	ppm	diff. (m)	ppm	diff. (m)	ppm
HY - RC	2 045.6	0.608	0.30	0.406	0.20	-.---	-.--
HY - FD	3 135.6	-0.503	0.16	0.265	0.08	-.---	-.--
HY - BP	3 928.9	0.145	0.04	0.116	0.03	0.079	0.02
HY - HT	4 032.9	1.363	0.34	-0.067	0.02	-.---	-.--
HY - MJ	3 904.5	0.051	0.01	0.026	0.01	-0.045	0.01
HT - RC	4 065.7	-7.625	1.88	-0.183	0.05	-.---	-.--
HT - FD	1 933.4	1.547	0.80	-0.228	0.12	-.---	-.--
HT - BP	484.1	0.817	1.69	-0.108	0.22	-0.053	0.11
HT - MJ	728.8	0.688	0.94	-0.134	0.18	-0.068	0.09

HY Westford (Haystack) HT Hat Creek FD Fort Davis
RC Richmond MJ Mojave BP Big Pine

Baseline comparison with respect to VLBI derived baselines
TABLE 6.8

The results of Table 6.8 probably give a better idea of the real accuracy of our solutions. First, as it has been pointed out by Beutler et al. [1987a] and Delikaraoglou [1987], the agreement of the shortest baselines is slightly worse. This effect is less apparent in the fiducial solution since one end of the baseline was held fixed (Hat Creek); thus, the baseline accuracy represents, to a certain extent, the accuracy of the coordinates of the other end of the baseline. The relative accuracy of the shortest baselines is usually worse than the longest ones since biases which are independent of the baseline length (such as tropospheric effects) magnify the relative accuracy over small vectors [Beutler et al., 1987c; Delikaraoglou, 1987], i.e., 0.25 m error on 2 500 km baseline represents only 0.1ppm relative accuracy whereas the same error on a 250 km baseline represents 1.0 ppm relative accuracy.

According to Table 6.8, the orbit-fixed solution relative accuracy is at the 0.7 ppm level (average) as we expected in horizontal. The fiducial network is at 0.06 ppm level wereas the free network solution is at 0.10 ppm (average). The fiducial network seems to be of better quality than the free-network solution, but as mentioned previously in the fiducial solution one end of the baseline is fixed, as opposed to the free-network solution where coordinate errors of two stations contribute to the relative baseline errors.

Thus, as far as relative accuracy is concerned, it is difficult to conclude from Table 6.8 that the fiducial approach is better than the free-network solution. The only disadvantage that we can point out about the free-network approach is that the final solution is not well aligned with the adopted reference system (the reference system is not stable) and a small scale factor exists, which means that these coordinates cannot be used directly with coordinates derived from the adopted reference frame. The free-network coordinates have to be transformed before any manipulation, whereas the fiducial-network coordinates can be used directly with those in the adopted reference system.

The complete output listing of our fiducial network solution is presented in Appendix 7. Appendix 8 presents the difference between improved orbits from this solution with respect to a priori orbits (for March 30).

In almost all our baseline results using a priori orbits (integrated orbits adjusted to broadcast ephemerides) the rms of double-difference phase residuals which include PRN 4 (e.g. 12-4, 13-4) were always larger (by a factor of 2 or more) than all other

satellite pairs. These large systematic phase residuals may explain the larger orbital residuals of satellite PRN 4 in Appendix 8.

In Table 6.9 we summarize the coordinates of the non-fiducial sites of this solution (NETFD) along with their formal errors. Although the estimated coordinate errors represent 1 sigma, they are still too optimistic. The same estimated errors for the free-network solution are larger by approximately two orders of magnitude. But in that case, they are too pessimistic. This can be explained easily by the poor capacity of the double-difference observables for absolute positioning (the large translation parameters of Table 6.4 is also a demonstration of this weakness). However, in both cases, when these errors are translated into north, east and height components, the north components are systematically of better quality than the east components (see Appendix 7). This is usually attributed, as we mentionned earlier, to the superior north-south coverage provided by the present constellation [Abbot et al., 1986].

Site	X	Y	Z
Big Pine	-2409654.826 ± 0.007	-4478261.945 ± 0.006	3838638.778 ± 0.006
Mojave	-2356576.115 ± 0.008	-4646564.999 ± 0.008	3668427.655 ± 0.006
Dahlgren	1123313.689 ± 0.010	-4882071.059 ± 0.012	3934412.026 ± 0.013
Austin	-740328.391 ± 0.008	-5457067.648 ± 0.008	3207239.691 ± 0.006
Mammoth	-2444443.598 ± 0.007	-4428696.329 ± 0.006	3875726.899 ± 0.005

Fiducial network solution (metre)
(non-fiducial sites)
TABLE 6.9

To conclude this section, we can say, according to Tables 6.4, 6.5 and 6.8 that our software has the capability, for short-arc orbits, to achieve the 0.1 ppm level over long baselines in both approaches, fiducial and free-network mode. The next section is devoted to the daily solution repeatability.

6.5 Day-to-day repeatability

Since the fiducial approach yields solutions that are well aligned in the reference system, we selected this approach to present a day-to-day repeatability. To test the accuracy of the coordinate repeatability, we tabulated the difference between the coordinates of the non-fiducial stations Big Pine and Mojave with their VLBI WGS72 positions. The results are shown in Table 6.10; network values have been also included. These results can be seen as a measure of the external accuracy of the solution. In session 04, Mojave was used as a fiducial point since the Westford station was not used. The effect of a new fiducial configuration at session 04 can easily be observed on the north-south and the vertical component of station Big Pine. Fig. 6.10 represents the situation in diagrammatic form.

Site	Session	North	East	Height
Big Pine	02	0.029	-0.077	-0.029
Big Pine	04	-0.026	-0.074	0.142
Big Pine	06	0.010	-0.121	0.066
Big Pine	12	0.012	-0.092	0.104
Big Pine	(fid.-network)	0.014	-0.077	0.056
Mojave	02	0.079	0.003	-0.141
Mojave	04	-.---	-.---	-.---
Mojave	06	0.070	-0.141	-0.090
Mojave	12	0.064	-0.006	-0.045
Mojave	(fid.-network)	0.067	-0.012	-0.091

Fiducial daily solutions with respect to
VLBI WGS72 positions (metre)
TABLE 6.10

The internal accuracy of the fiducial network solution can be verified, to a certain extent, by comparing the daily solutions with our network solution. The difference in the coordinate components obtained in the daily solutions and the overall network solution is a measure for the impact of the unmodelled effects [Kleusberg and Wanninger, 1987]. Table 6.11 presents this comparison. The different fiducial configuration in session 04 is the biggest systematic effect that can be outlined. It is very

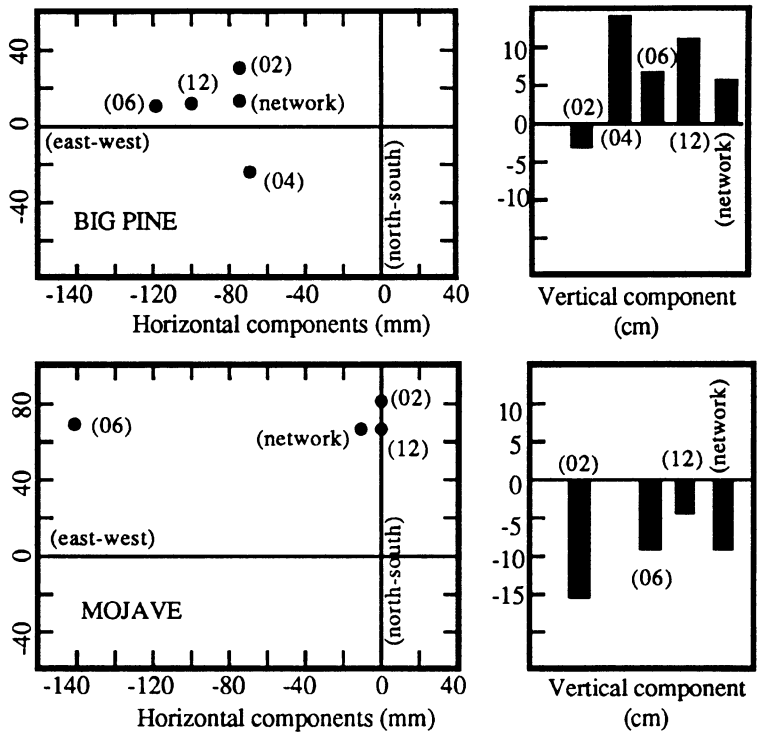

Graphical representation of Table 6.10
FIGURE 6.10

well observed especially at Dahlgren, which is really outside the area covered by the Richmond, Fort Davis, Mojave and Hat Creek stations. If we exclude the Dahlgren determination of session 04, the internal accuracy of the coordinates is below the 10-centimetre level, which means an internal accuracy (and daily repeatability) of the order of ~ 0.03-ppm level.

The same comparison can be performed on the baseline repeatability. Table 6.12 summarizes the relative baseline accuracy with respect to VLBI-derived baselines, whereas Table 6.13 summarizes the relative internal accuracy (with respect to our fiducial network solution) of the same baselines plus all other baselines including non-fiducial sites.

Site	Session	North	East	Height
Big Pine	02	0.014	0.000	-0.085
Big Pine	04	-0.040	0.003	0.087
Big Pine	06	-0.005	-0.044	0.011
Big Pine	12	-0.002	-0.015	0.049
Mojave	02	0.012	0.015	-0.050
Mojave	04	-.---	-.---	-.---
Mojave	06	0.003	-0.129	0.000
Mojave	12	-0.003	0.006	0.046
Dahlgren	02	0.004	0.007	0.021
Dahlgren	04	0.376	0.595	-0.069
Dahlgren	06	-0.041	0.082	0.143
Dahlgren	12	0.018	-0.067	-0.142
Austin	02	-0.010	0.016	-0.007
Austin	04	0.060	0.034	-0.027
Austin	06	0.009	-0.012	-0.018
Austin	12	-0.009	0.006	-0.038
Mammoth	02	0.007	-0.004	-0.075
Mammoth	04	-0.041	0.016	0.046
Mammoth	06	-0.007	-0.052	0.049
Mammoth	12	0.002	0.004	0.037

Daily solutions (non-fiducial sites) with respect
to our fiducial network solution (metre)
TABLE 6.11

According to Table 6.12, the relative accuracy of the shortest baselines are worse than those obtained in the network solution. This suggests that some baseline independent biases (e.g. atmospheric biases) can be averaged out over long observation periods. For the longest baseline the repeatability is still below the 0.1-ppm level. The good agreement of the HT-BP baseline for session 04 is probably due to the addition of the Mojave station, in the fiducial configuration, which is very close to Big Pine.

Baseline	length (km)	SESSION 02	04	06	12
HY - BP	3 928.9	0.01	-.---	0.03	0.03
HY - MJ	3 904.5	0.02	-.---	0.02	0.01
HT - BP	484.1	0.14	0.03	0.15	0.12
HT - MJ	728.8	0.10	-.---	0.19	0.08

HY Westford (Haystack) HT Hat Creek
MJ Mojave BP Big Pine

Daily baseline comparison (in ppm) with respect to
VLBI derived baselines
TABLE 6.12

The most interesting result is the internal accuracy. Over long baselines (> 1 000 km) the daily baseline repeatability (average) is at the 0.01 ppm level, whereas for the shortest baselines it is at the ~ 0.05 ppm level (average).

Baseline	length (km)	SESSION 02	04	06	12
HY - BP	3 928.9	0.008	-.---	0.011	0.007
HY - MJ	3 904.5	0.008	-.---	0.028	0.003
HY - NS	669.3	0.011	-.---	0.027	0.037
HY - AR	2 678.0	0.003	-.---	0.000	0.003
HY - MM	3 959.4	0.006	-.---	0.016	0.002
HT - BP	484.1	0.031	0.079	0.041	0.009
HT - MJ	728.8	0.007	0.093	0.097	0.011
HT - NS	3 731.3	0.003	0.109	0.035	0.029
HT - AR	2 417.4	0.007	0.005	0.008	0.001
HT - MM	416.4	0.025	0.107	0.046	0.004

HY Westford (Haystack) HT Hat Creek MM Mammoth
MJ Mojave NS Dahlgren (NSWC)
BP Big Pine AR Austin

Daily baseline comparison (in ppm) with respect to
our fiducial network solution
TABLE 6.13

In order to assess our development further, we will compare the repeatability of a 484-km and a 4 000-km baseline computed with an orbit obtained from a pure orbit improvement solution.

6.6 Repeatability using improved orbit

We used the POLARIS Westford, Fort Davis and Richmond stations together with Hat Creek as fiducial sites to produce a pure-orbit improvement solution. Observations from session 02, 06 and 12 were combined in a fiducial network to produce three independent sets of short-orbital arcs. The solved-for parameters of this solution were one tropospheric scale factor for each station, one relative clock offset and one relative clock drift for each baseline, the ambiguities and 6 orbital parameters for each satellite. Session 04 was not used since there was not enough data recorded at Westford to be combined with the other stations.

The improved set of initial conditions for each arc were integrated over a few hours. Afterwards, these trajectories were used to solve a short baseline of 484-km between Big Pine and Hat Creek and a 4 000-km baseline between Westford and Mojave. This test will further assess the modelling of our orbital integrator.

Site	Session	North	East	Height
Big Pine	02	0.199	-0.011	0.271
Big Pine	06	0.270	-0.059	0.375
Big Pine	12	0.191	-0.100	0.263
Mojave	02	0.129	-0.018	0.083
Mojave	06	0.131	-0.005	0.334
Mojave	12	0.202	0.122	0.388

Daily coordinate repeatability (metre) using an improved orbit.
Comparison with WGS72 VLBI coordinates
TABLE 6.14

For this baseline processing, we solved for two clock parameters, for the ambiguties and for three station coordinates for each baseline. Coordinates of Westford and Hat Creek were held fixed. The coordinate and baseline comparisons are with

respect to the WGS72 VLBI coordinates. Table 6.14 gives the coordinate comparison whereas Table 6.15 gives the baseline comparison.

The coordinate repeatability accuracy for the short baseline is of the order of 0.5 ppm. For the long baseline, the repeatability accuracy is of the order of 0.05-ppm. As far as baseline repeatability is concerned, the short baseline repeats at the 0.5 ppm level, the long baseline repeats well below the 0.05-ppm level.

The results on the shortest baseline are worse still. This is not surprising since the coordinate discrepancies of Table 6.14 are of the same order either for the long or the short baseline, suggesting an unmodelled constant effect. The estimation of a tropospheric scale factor did not really improve the results on the long baseline. For the short baseline, the results were slightly worse. Since the tropospheric model was unable to remove a portion of this effect, if the unmodelled effect is from the troposphere, we must assume that the meteorological conditions at Big Pine or Hat Creek or both stations were not constant during the observation period.

Baseline	length (km)	SESSION 02	06	12
HY - MJ	3 904.5	0.00	0.01	0.02
HT - BP	484.1	0.37	0.55	0.46

HY Westford (Haystack) HT Hat Creek
MJ Mojave BP Big Pine

Daily baseline repeatability (in ppm) using improved orbit.
Comparison with respect to VLBI derived baselines
TABLE 6.15

We can conclude from the results of Table 6.14 and 6.15 that the force model of our orbital integrator is satisfactory since the solutions obtained with the integrated orbit are of the same order of magnitude than those obtained in our fiducial network solution.

7. CONCLUSIONS AND RECOMENDATIONS

We have demonstrated in two different ways that a simple force model including the earth's gravitational field up to degree and order 4, the gravitational attraction of the sun and the moon and a simple solar radiation pressure model are sufficient to integrate precise short orbital arcs of ~6-8 hours. The plots generated in Section 6.3 showed that such a model over 6-8 hours can preserve the 2.5-metre accuracy in the satellite's position if the solar radiation constants are known at ±10%. Results of Section 6.6 are consistent with this assumption, since results of 0.05 ppm (over a long baseline) and ~0.4 ppm (over a short baseline) were obtained in baseline length when solutions were computed with integrated orbits from improved initial conditions. The results on the longest baseline are a better measure of the relative accuracy. From these results we can conclude that the orbital integrator program ORDAP is operating well and can be used without problem to generate precise short-arc orbits.

From our subset of the HPBT campaign, we have demonstrated the correct implementation of the orbital parameter estimation using a Keplerian approximation to compute partial derivatives with respect to the initial state vector.

From a fixed-orbit network adjustment over 4 days, using integrated orbits with initial conditions derived from broadcast ephemerides, we have realized that the broadcast ephemerides were of good quality. The rms of the coordinate residuals (between GPS and VLBI) has shown a network accuracy of 0.7 ppm in horizontal components and 1.5 ppm in the vertical component.

When the same network is processed in free-network mode, where orbital

parameters are estimated along with all station coordinates, the improvement in the solution is significant. First, the rms of double-difference phase residuals of our network solution dropped from 49 cm to roughly 2 cm, which means that most of the systematic trends in the double-difference residuals have disappeared. Second, the general agreement at the VLBI sites has improved by a factor of 20 in horizontal components and by two order of magnitude in the vertical component, which implies a solution at the 0.1-ppm level and even below in the station coordinates.

A network solution in a fiducial mode has produced results compatible at the 0.05-ppm level, in the coordinates, with the free-network solution, suggesting that both solutions are almost equivalent. With the exception of short baselines, the comparison with VLBI-derived baselines is at at the 0.1-ppm accuracy level for the free-network solution, whereas the fiducial-network-derived baselines compare at slightly better than the 0.1 ppm level.

Although free-network and fiducial network solutions seem to provide equivalent results, it has been shown that the free-network approach is not very stable in a short-arc mode as far as the reference frame is concerned.

The day-to-day fiducial adjustment solution repeatability was surprisingly good. The coordinate comparisons with the WGS72 VLBI station coordinates were still at the 0.1-ppm level. The internal fiducial network accuracy has been evaluated using results of the daily solutions. The coordinate comparison showed an agreement of the order of 0.05-ppm. From the day-to-day repeatability, it has been pointed out, from the solution of session 04, that the fiducial network configuration has a significant effect on the results. The day-to-day baseline comparison with VLBI vectors were still below the 0.1-ppm level for long baselines, whereas the shortest baseline repeated at the 0.15-ppm level. The internal baseline comparison (with respect to our global fiducial network solution) is rather amazing; over long baselines the repeatability is well below the 0.05 ppm level.

According to these tests, there is some evidence, that our fiducial and even our free-network solutions are at the ~ 0.1 ppm level. However, we believe that a better pre-processing of the observations will strengthen the solution considerably, since, in our pre-processing, artificial phase breaks had to be introduced in order to eliminate the linear dependency between satellite pairs (see Section 4.5). It is clear that our pre-processing was done correctly, but it is also clear that this is not the optimum

procedure.

At the time of writting this thesis, a new dual-frequency pre-processor, to be used along with the DIPOP 2.0 main processor, was under development at the University of New Brunswick. If this new pre-processor is to be used with our new DIPOP version, some modifications will have to be made to ensure compatibility with the new version. The most important will be the output modification, which is very easy to implement. Since data validation can be done without problem with the broadcast ephemerides, the implementation of orbit computation from coefficients is not really necessary.

We also suggest introducing a single point positioning solution at the pre-processing stage in order to produce a priori station coordinates as well as a clock alignment verification. A more general pre-processor to detect cycle slips should also be developed in order to preprocess single-frequency observations as well as dual-frequency observations.

As far as orbits are concerned, the next step to be undertaken will be to extend the orbital length capability of the developed software. First, the force model will have to be completed (depending on the arc length sought) with some other forces. With the numerical integration approach, this will be straightfoward. The more important modification will be to introduce the least-squares process one solar radiation parameter for each satellite, and if orbital arcs longer than 2 days are sought, two other parameters will have to be estimated for each satellite in order to take into account the Y-axis bias. The subroutine EQOBS in our software will also have to be modified in order to accept these new partial derivatives. Although these estimations have not been implemented in our version of DIPOP, there is provision in the arrays for these future parameters. The definition of the inertial system will also have to be reviewed since some simplifications have been used owing to the short-arc approach.

As far as the DIPOP least-squares filter is concerned, the development of an algorithm to compute the weight matrix of simultaneously observed double-differences from n (>2) receivers to m (>1) satellites should be investigated (the case of n=2 is already implemented). This improvement will be a major modification of the sequential procedure since all simultaneous observations will have to be loaded into memory simultaneously.

Although the extension of the arc length will not improve the results

significantly, it will certainly provide a more stable reference frame from the orbit point of view. One of the advantages of the longer orbital-arc approach is the large decrease in the number of the parameters involved in the solution.

Our DIPOP modifications along with an optimum pre-processor can now be used to investigate:

- the limit of the orbit-improvement capability as far as network size is concerned,
- the sensitivity of a solution as a function of the fiducial network configuration,
- the benefit of including the pseudo-range observations in a pure orbit solution.

REFERENCES

Abbot, R. I., Y. Bock, C. C. Counselman III, and R. W. King (1986)."GPS orbit determination." *Proceedings of the Fourth International Geodetic Symposium on Satellite Positioning*, Vol. 1, pp. 271 - 272.

Ash M.E.(1972). "Determination of earth satellite orbits." Technical Note 1972-5, Massachusetts Institute of Technology, Cambridge, MA.

Beutler G., D. A. Davidson, R. B. Langley, R. Santerre, P. Vanicek, D. E. Wells (1984a). "Some theoretical and practical aspects of geodetic positioning using carrier phase difference observations of GPS satellites." Department of Surveying Engineering Technical Report No. 109, University of New Brunswick, Fredericton, Canada.

Beutler, G. (1984b). "GPS carrier phase difference observation software." Department of Surveying Engineering Technical Memorandum TM-2, University of New Brunswick, Fredericton, Canada.

Beutler G., W. Gurtner, I. Bauersima, R.B. Langley (1985). "Modelling and estimating the orbits of GPS satellites." *First International Symposium on Precise Positioning with Global Positioning System - Positioning with GPS-1985,* U.S. Dept. of Commerce, NOAA, Rockville, Md., pp. 99-111.

Beutler G., W. Gurtner, M. Rothacher, T. Schildknecht, I. Bauersima (1986). "Determination of orbits using double difference carrier phase observations from regional networks." *Proceedings of the Fourth International Geodetic Symposium on Satellite Positioning*, Vol. 1, pp. 319-335.

Beutler G., I. Bauersima, W. Gurtner, M. Rothacher, T. Schildknecht (1987a). "Evaluation of the 1984 Alaska Global Positioning System campaign with the Bernese GPS software.", *JGR*, Vol. 92, No. B2, pp. 1295-1303.

Beutler G., I. Bauersima, W. Gurtner, and M. Rothacher, (1987b), "Correlations between simultaneous GPS double difference carrier phase observations in the multistation mode: Implementation considerarions and first experiences." *Manuscripta geodaetica*, 12, pp. 40-44.

Beutler G., I. Bauersima, S. Bottom, W. Gurtner, M. Rothacher and T. Schildknecht (1987c). "Accuracy and biases in the geodetic application of the Global Positioning System". Paper presented at the IUGG XIX General Assembly, Vancouver, Canada, 9-22 August.

Cain, J.D. (1986). "Macrometry surveys - A summary of results." *Proceedings of the Fourth International Geodetic Symposium on Satellite Positioning*, Vol. 1, pp. 419-429.

Collins, J. and A. Leick (1985). "Analysis of macrometer networks with emphasis on the Montgomery (PA) county survey." *First International Symposium on Precise Positioning with Global Positioning System - Positioning with GPS-1985,* U.S. Dept. of Commerce, NOAA, Rockville, Md., pp. 667-691.

Colombo, O. L. (1986). "Ephemeris errors of GPS satellites." *Bulletin Géodésique*, 60, pp. 64-84.

Conte, S.D. (1963). "The computation of satellite orbit trajectories." *Advances in Computers*, 3, pp. 1-76.

Davidson, J.M., C.L. Thornton, C.J. Vegos, L.E. Young and T.P. Yunck (1985), "The March 1985 demonstration of the fiducial network concept for GPS geodesy: A preliminary report." *First International Symposium on Precise Positioning with Global Positioning System - Positioning with GPS-1985,* U.S. Dept. of Commerce, NOAA, Rockville, Md., pp. 603 - 611.

Delikaraoglou, D., N. Beck, D. McArthur, And K. Lochhead (1985). "On the Establishment of 3-D Geodetic Control by Interferometry with the TI 4100 GPS Receiver", *First International Symposium on Precise Positioning with Global Positioning System - Positioning with GPS-1985,* U.S. Dept. of Commerce, NOAA, Rockville, Md., pp. 645-655.

Delikaraoglou, D., R.R. Steeves and N. Beck (1986). "Development of a Canadian Active Control System using GPS.", *Proceedings of the Fourth International Geodetic Symposium on Satellite Positioning*, Vol. 2, pp. 1189-1203.

Delikaraoglou D. (1987). "Determination of highly precise orbits for GPS satellites over continental areas", Paper presented at the IUGG XIX General Assembly, Vancouver, Canada, 9-22 August.

Escopal, P.R. (1976). *Methods of Orbit Determination*, John Wiley & Sons, Inc. New York, 479 pp.

Fliegel, H. F., W. A. Fees, W. C. Layton and N. W. Rhodus (1985). "The GPS radiation force model." *First International Symposium on Precise Positioning with Global Positioning System - Positioning with GPS-1985,* U.S. Dept. of Commerce, NOAA, Rockville, Md., pp. 113-120.

Goad, C.C. (1985), "Precise positioning with the Global Positioning System", *Paper presented at Third International Symposium on ISS*, Banff, September.

Gurtner, W., G. Beutler, I. Bauersima, T. Schildknecht (1985). " Evaluation of GPS carrier difference observations: The Bernese second generation software package." *First International Symposium on Precise Positioning with Global Positioning System - Positioning with GPS-1985,* U.S. Dept. of Commerce, NOAA, Rockville, Md., pp. 363 - 372.

Hamming R.W., (1962). *Numerical Methods for Scientists and Engineers.* McGraw-Hill Book Company Inc, New York, 411 pp.

Hogg, D.C., F.O. Guiraud, and M.T. Decker (1981). "Measurement of excess radio transmission length on earth-space paths." *Astron. Astrophys.*, 95, pp. 304-307.

Jones, A.C., D.R. Larden, and J.S. Allman (1987). "First order geodetic surveying using multi-station Global Positioning System techniques." Paper presented at the Institution of Surveyors, Australia, 29th Australian Survey Congress, Perth, Western Australia, 4-11 April.

Kaplan, G.H. (1981). "The IAU resolutions on astronomical constants, time scales, and the fundamental reference frame." Circular No. 163, U.S. Naval Observatory, Washington, D.C.

Kaula, W. M. (1966). *Introduction to Satellite Geodesy.* Blaisdell, Waltham, Mass., 124 pp.

King, R. W., E. G. Masters, C. Rizos, A. Stolz and J. Collins (1985). *Surveying with GPS,* Monograph No. 9, School of Surveying. The University of New South Wales, Kensington , N.S.W. Australia.

King, R.W, Y. Bock, M.H. Murray and D.-N. Dong (1987). "Optimal determination of GPS orbits", Paper presented at the IUGG XIX General Assembly, Vancouver, Canada, 9 - 22 August.

Klau, R.L. (1986), "GPS surveying in Australia using the TRIMBLE 4000 SX." *The Australian Surveyor*, Vol. 33, No. 4, pp. 284-291.

Kleusberg, A., R.B. Langley, R. Santerre, P. Vanicek, D.E. Wells and G. Beutler (1985). "Comparison of survey results from different types of GPS receivers." *Proceedings of the First International Symposium on Precise Positioning with the Global Positioning System - Positioning with GPS-1985,* U.S. Dept. of Commerce, NOAA, Rockville, Md., pp. 579-592.

Kleusberg, A. (1986). "Ionospheric propagation effects in geodetic relative GPS positioning." *Manuscripta geodaetica*, 11, pp. 256-261.

Kleusberg, A. and L. Wanninger (1987). "Analysis of the Juan de Fuca GPS Survey 1986." Final contract report, University of New Brunswick, Fredericton, Canada.

Krakiwsky, E.J., and D.E. Wells (1971). "Coordinate systems in geodesy." Department of Surveying Engineering Lecture Notes No. 16, University of New Brunswick, Fredericton, Canada.

Kroger, P.M. (1986). Jet Propulsion Laboratory, Interoffice Memorandum, 14 July.

Lachapelle, G. and E. Cannon (1986). "Single and dual frequency GPS results for baselines of 10 to 500 km." *Proceedings of the Fourth International Geodetic Symposium on Satellite Positioning*, Vol. 2, pp. 1119-1134.

Lachapelle, G., B. Wanless, H. Janes, R. Leeman, E.J. Krakiwsky, K.P. Schwartz, E. Cannon, K. Pointon, M. Craymer, A. Kleusberg, R. Langley, P. Vanicek and D.E. Wells (1988). "Design of a general software structure for the processing, statistical analysis, and quality control of GPS networks". Geodetic Survey of Canada, Contract Report 88-002.

Lambeck, K. and R. Coleman (1983). " The earth's shape and gravity field: a report of progress from 1958 to 1982." *Geophys. J. R. Astr. Soc.*, 74, pp. 25-54.

Landau H., and D. Hagmaier (1986). "Analysis of the required force-modelling for NAVSTAR / GPS satellites." GPS Research 1985 at the Institute of Astronomical and Physical Geodesy, Universität der Bundeswehr München, pp. 193-208.

Langley, R.B., G. Beutler, D. Delikaraoglou, B. Nickerson, R. Santerre, P. Vanicek, and D.E. Wells (1984). "Studies in the application of the Global Positioning System to differential positioning." Department of Surveying Engineering Technical Report No. 108, University of New Brunswick, Fredericton, Canada.

Langley, R.B., A. Kleusberg, R. Santerre, D.E.Wells and P. Vanicek (1986a). "DIPOP: An interative software package for precise positioning with GPS." Paper presented at the American Congress on Surveying and Mapping, Spring Convention, Washington, D.C., 16-21 March.

Langley, R. B., D. Parrot, R. Santerre, P. Vanicek and D. E. Wells (1986b). "The spring 1985 GPS high-precision baseline test: preliminary analyses with DIPOP." *Proceedings of the Fourth International Geodetic Symposium on Satellite Positioning*, Vol. 2, pp. 1073-1088.

Langley, R.B. and D. Parrot (1987). "The detection and removal of cycle slips in GPS phase data." Terra Cognita, Vol. 7, No. 2-3.

Langley, R.B. (1987). Department of Surveying Engineering, University of New Brunswick, Fredericton, Canada. Personal communication.

Leeman, R.W., H.D. MacAulay and L.B. Fletcher (1985). "GPS - A user's critique." *First International Symposium on Precise Positioning with Global Positioning System - Positioning with GPS-1985,* U.S. Dept. of Commerce, NOAA, Rockville, Md., pp. 613-624.

Martin T.V., W.F. Eddy, A. Brenner, B. Rosen and J. McCarthy (1980). *GEODYN, System description*, Goddard Space Flight Center, Greenbelt, Maryland.

Martin T.V., M.H. Torrence and C.W. Misner (1985). "Relativistic effects on an earth-orbiting satellite in the barycenter coordinate system." *JGR*, Vol.90, No.B11, pp. 9403-9410.

McArthur, D., N. Beck, K. Lochhead and D. Delikaraoglou (1985). "Precise relative positioning with the Macrometer V-1000 interferometric surveyor: experiences at the Geodetic Survey of Canada." *First International Symposium on Precise Positioning with Global Positioning System - Positioning with GPS-1985,* U.S. Dept. of Commerce, NOAA, Rockville, Md., pp.521 - 528.

McLellan, J.F. and J.B. Schleppe (1987). "Control survey project in the Beaufort sea area in support of the Inuvialuit final agreement." Unpublished Report of The McElhanney Group Ltd.

Melbourne, W., R. Anderle, M. Feissel, R. King, D. McCarthy, D. Smith, B. Tapley, R. Vicente (1983). "Project Merit Standard." Circular No. 167, U.S. Naval Observatory, Washington, D.C.

Merell, R.L. (1986a). " Application of GPS for transportation related engineering surveys." *Proceedings of the Fourth International Geodetic Symposium on Satellite Positioning*, Vol. 2, pp. 1165-1179.

Merell, R.L. (1986b). "Geodetic reference systems in GPS environment", *Journal of Surveying Engineering*, Vol. 112, No. 2, p. 83-89.

Mikhail, E.M. and F. Ackerman (1976). *Observations and Least Squares*. University Press of America, Harper & Row, Publishers, 497 pp.

Moreau, R., G. Beutler, J.G. Leclerc, B. Labrecque, R.B. Langley, and R. Santerre (1985). "Comparison of phase-difference processing and network solution methods." *First International Symposium on Precise Positioning with Global Positioning System - Positioning with GPS-1985,* U.S. Dept. of Commerce, NOAA, Rockville, Md., pp. 557-566.

Moursund, D.G. and C.S. Duris (1967). *Elementary Theory and Application of Numerical Analysis*. McGraw-Hill Book Compagny, New York, 297 p.

Mueller, I.I. (1964). *Introduction to Satellite Geodesy*. Frederick Ungar Publishing Co., New York, 415 pp.

Mueller. I.I. (1969). *Spherical and Practical Astronomy*. Frederick Ungar Publishing Co., New York, 615 pp.

Nakiboglu, M., B. Buffet, K. P. Schwarz, E. J. Krakiwsky and B. Wanless (1984). "A multi-pass, multi-station approach to GPS orbital improvement and precise positioning." *Proceedings of IEEE PLANS 1984*, pp. 153-162.

Nakiboglu, M., E. J. Krakiwsky, K. P. Schwarz, B. Buffet and B. Wanless (1985). "A multi-Station, multi-Pass approach to Global Positioning System orbital improvement and precise positioning." Geodetic Survey of Canada, Final Contract Report #OST83-00340.

Parrot, D. (1988), "Ambiguity and cycle slip software development". Geodetic Survey of Canada, Final Contract Report No. (DSS) 34SZ.23244-7-4251.

Remondi, B.W. (1984). "Using the Global Positioning System (GPS) phase observable for relative geodesy: modeling, processing, and results." Ph. D. Dissertation, Center for Space Research, The University of Texas at Austin, 360 pp.

Remondi, B.W. (1986). "Distribution of Global Position System ephemerides by the National Geodetic Survey." U.S. Department of Commerce, NOAA, National Ocean Service Charting and Geodetic Services.

Rizos C. and A. Stolz (1985). "Force modelling For GPS satellite orbits." *First International Symposium on Precese Positioning with Global Positioning System - Positioning with GPS-1985,* U.S. Dept. of Commerce, NOAA, Rockville, Md., pp. 87-96.

Santerre, R., A. Kleusberg, and G. Beutler (1985). "DIPOP: Software documentation." Department of Surveying Engineering Technical Memorandum TM-6, University of New Brunswick, Fredericton, Canada.

Santerre R., M.R. Craymer, A. Kleusberg, R.B. Langley, D. Parrot, S.H. Quek, P. Vanicek, D.E. Wells and F. Wilkins (1987), "Precise relative positioning with DIPOP 2.0." Paper presented at the IUGG XIX General Assembly, Vancouver, Canada, 9-22 August.

Santerre, R. (1987). Department of Surveying Engineering, University of New Brunswick, Fredericton, Canada. Personal communication.

Scott V.D., J.R. Clynch and J.G. Peters (1986). "A proposed standardized exchange format for NAVSTAR GPS geodetic data." Applied Research Laboratory, University of Texas, Austin, Texas.

Strange, W.E. (1985). " High-precision, three-dimensional differential positioning using GPS." *First International Symposium on Precise Positioning with Global Positioning System - Positioning with GPS-1985,* U.S. Dept. of Commerce, NOAA, Rockville, Md., pp. 543-548.

Tessier, P. (1987), "Expérimentation du récepteur GPS TRIMBLE 4000 SX." Rapport non publié du Service de la Géodésie, Direction des Relevés Techniques, Ministère de l'Énergie et des Ressources du Gouvernement du Québec.

Thomson, D.B. (1976). "Combination of geodetic networks." Department of Surveying Engineering Technical Report No. 30, University of New Brunswick, Fredericton, Canada.

Thornton, C., J.M. Davidson, B.C. Beckman, L.E. Young, J.B. Thomas, T.H. Dixon, and D.W. Trask (1983). "System study for global positioning satellite (GPS) geodesy in the Caribbeans." Jet Propulsion Laboratory Document D-941.

Torge, W. (1980). *Geodesy*. Walter de Gruyter, Berlin, 245 pp.

Van Dierendonck, A.J., S.S. Russell, E.R. Kopitze, M. Birnbaum (1980). "The GPS Navigation Message." *Navigation,* Journal of The Institute of Navigation (U.S.), Vol. 25, No. 2, pp. 147-165.

Vanicek, P. (1973). "Gravimetric Satellite Geodesy." Department of Surveying Engineering Lecture Notes No. 32, University of New Brunswick, Fredericton, Canada.

Vanicek, P. and J. Krakiwsky (1986). *Geodesy, The Concepts,* 2nd rev. ed., North-Holland, Amsterdam, The Netherlands, 697 pp.

Vanicek, P., G. Beutler, A. Kleusberg, R. B. Langley, R. Santerre. and D. E. Wells (1985). "DIPOP Differential positioning program package for the Global Positioning System." Department of Surveying Engineering Technical Report No. 115, University of New Brunswick, Fredericton, Canada.

Velez, C.E., and J.L. Maury (1970). "Derivation of Newtonian-type integration coefficients and some applications to orbit calculations." NASA Technical Note TN D-5958, Goddard Space Flight Center, Greenbelt, Md. 20771.

Ware, R.H., C. Rocken, and J.B. Snider (1985). "Experimental verification of improved GPS-measured baseline repeatability using water-vapor radiometer corrections." IEEE Transactions on Geoscience and Remote Sensing, Vol. GE-23, No. 4, pp. 467-473.

Ware, R.H., C. Rocken, K.J. Hurst and G.H. Rosborough (1986). "Determination of the OVRO-Mojave baseline during the spring 1985 GPS test." *Proceedings of the Fourth International Geodetic Symposium on Satellite Positioning*, Vol. 2, pp. 1089-1101.

Wahr, J.M. (1981). "The forced nutations of an elliptical, rotating, elastic and oceanless earth." *Geophys. J.R. astr. Soc.*, 64, pp. 705-727.

Wells, D.E. (1974). " Doppler satellite control." Department of Surveying Engineering Technical Report No. 29, University of New Brunswick, Fredericton, Canada.

Wells, D.E. (1985). "Recommended GPS terminology." *Proceedings of the First International Symposium on Precise Positioning with the Global Positioning System*, Rockville, MD, 15-19 April, pp. 903-931.

Wells, D.E., N. Beck, D. Delikaraoglou, A. Kleusberg, E.J. Krakiwsky, G. Lachapelle, R.B. Langley, M. Nakiboglu, K.P. Schwarz, J.M. Tranquilla and P. Vanicek (1986). *Guide to GPS positioning*. Canadian GPS Associates, Fredericton, N.B., Canada.

Williams B.G. (1986). "GPS satellite orbit determination results from the March 1985 field test." *Proceedings of the Fourth International Geodetic Symposium on Satellite Positioning*, Vol. 1, pp. 289-302.

Willis, P., C. Boucher, C. Le Coq (1986). "The I.G.N. geodetic software system for GPS data analysis." *Proceedings of the Fourth International Geodetic Symposium on Satellite Positioning*, Vol. 2, pp. 1181 -1188.

Wu, S.C., S.M. Lichten, W.I. Bertiger, J.T. Wu, J.S. Border, B.G. Williams, and T.P. Yunck (1986). "Precise orbit determination of GPS and Landsat-5." *Proceedings of the Fourth International Geodetic Symposium on Satellite Positioning*, Vol. 1, pp. 275-288.

APPENDIX 1

STARTER AND
PREDICTOR - CORRECTOR COEFFICIENTS

STARTER AND
PREDICTOR - CORRECTOR COEFFICIENTS

(from Velez and Maury, 1970)

The ordinate 11-point predictor formula is:

$$\mathbf{r}(t) = 2\,\mathbf{r}(t-h) - \mathbf{r}(t-2h) + h^2 \sum_{i=0}^{10} \xi_i\, \mathbf{r}''(t-(1+i)h)$$

where the coefficients ξ_i are the following:

$$\xi_0 = 263\,465\,639 \;/\; 159\,667\,200$$
$$\xi_1 = -296\,725\,183 \;/\; 79\,833\,600$$
$$\xi_2 = 1\,742\,930\,263 \;/\; 159\,667\,200$$
$$\xi_3 = -424\,402\,351 \;/\; 19\,958\,400$$
$$\xi_4 = 2\,337\,301\,223 \;/\; 79\,833\,600$$
$$\xi_5 = -1\,155\,556\,697 \;/\; 39\,916\,800$$
$$\xi_6 = 1\,637\,523\,683 \;/\; 79\,833\,600$$
$$\xi_7 = -29\,064\,973 \;/\; 2\,851\,200$$
$$\xi_8 = 539\,999\,083 \;/\; 159\,667\,200$$
$$\xi_9 = -53\,797\,223 \;/\; 79\,833\,600$$
$$\xi_{10} = 3\,250\,433 \;/\; 53\,222\,400$$

The 11-point corrector formula is:

$$\mathbf{r}(t) = 2\,\mathbf{r}(t-h) - \mathbf{r}(t-2h) + h^2 \sum_{i=0}^{10} \beta_i\, \mathbf{r}''(t - ih)$$

where the coefficients β_i are the following:

$$\begin{aligned}
\beta_0 &= 3\,250\,433 \;/\; 53\,222\,400 \\
\beta_1 &= 3\,124\,027 \;/\; 3\,193\,344 \\
\beta_2 &= -57\,128\,921 \;/\; 159\,667\,200 \\
\beta_3 &= 16\,745\,741 \;/\; 19\,958\,400 \\
\beta_4 &= -88\,645\,069 \;/\; 79\,833\,600 \\
\beta_5 &= 42\,375\,577 \;/\; 39\,916\,800 \\
\beta_6 &= -\,2\,342\,533 \;/\; 3\,193\,344 \\
\beta_7 &= 7\,139\,837 \;/\; 19\,958\,400 \\
\beta_8 &= -18\,674\,153 \;/\; 159\,667\,200 \\
\beta_9 &= 1\,838\,819 \;/\; 79\,833\,600 \\
\beta_{10} &= -330\,157 \;/\; 159\,667\,200
\end{aligned}$$

The starter formulas are in the following form:

$$\mathbf{r}(t_o + Kh) = \mathbf{r}(t_o) + K\,h\,\mathbf{r}'(t_o) + h^2 \sum_{i=0}^{10} \alpha_{Ji}\,\mathbf{r}''(t_o + Kh + (J-i)h)$$

where 10 equations can be written for $-5 \le K \le -1$ and $1 \le K \le 5$ and
$10 \le J \le 6$ and $4 \le J \le 0$, i e $J = 5 - K$

The coefficients α_{Ji} are the following for the different values of J and K:

J = 10 K = -5

$\alpha_{10,0}$ = -77 425 / 38 320 128
$\alpha_{10,1}$ = 62 875 / 2 737 152
$\alpha_{10,2}$ = -1 539 875 / 12 773 376
$\alpha_{10,3}$ = 208 625 / 532 224
$\alpha_{10,4}$ = -5 942 875 / 6 386 688
$\alpha_{10,5}$ = 10 314 625 / 3 193 344
$\alpha_{10,6}$ = 22 426 625 / 6 386 688
$\alpha_{10,7}$ = 5 650 375 / 1 596 672
$\alpha_{10,8}$ = 21 348 625 / 12 773 376
$\alpha_{10,9}$ = 21 621 125 / 19 160 064
$\alpha_{10,10}$ = 202 025 / 3 483 648

J = 9 K = -4

$\alpha_{9,0}$ = -52 / 467 775
$\alpha_{9,1}$ = 758 / 467 775
$\alpha_{9,2}$ = -356 / 31 185
$\alpha_{9,3}$ = 8 368 / 155 925
$\alpha_{9,4}$ = -6 584 / 31 185
$\alpha_{9,5}$ = 280 124 / 155 925
$\alpha_{9,6}$ = 532 184 / 155 925
$\alpha_{9,7}$ = 2 704 / 1 485
$\alpha_{9,8}$ = 23 756 / 22 275
$\alpha_{9,9}$ = 122 / 1 701
$\alpha_{9,10}$ = -124 / 93 555

J = 8 K = -3

$\alpha_{8,0}$ = -1 063 / 3 942 400
$\alpha_{8,1}$ = 6 511 / 1 971 200
$\alpha_{8,2}$ = -10 833 / 563 200
$\alpha_{8,3}$ = 1 029 / 14 080
$\alpha_{8,4}$ = -88 827 / 394 240
$\alpha_{8,5}$ = 280 821 / 197 120
$\alpha_{8,6}$ = 4 345 149 / 1 971 200
$\alpha_{8,7}$ = 464 187 / 492 800
$\alpha_{8,8}$ = 7 443 / 71 680
$\alpha_{8,9}$ = -529 / 78 848
$\alpha_{8,10}$ = 1 693 / 3 942 400

J = 7 K = -2

$\alpha_{7,0}$ = -263 / 1 871 100
$\alpha_{7,1}$ = 263 / 149 688
$\alpha_{7,2}$ = -131 / 12 474
$\alpha_{7,3}$ = 159 / 3 850
$\alpha_{7,4}$ = -41 543 / 311 850
$\alpha_{7,5}$ = 111 973 / 124 740
$\alpha_{7,6}$ = 35 932 / 31 185
$\alpha_{7,7}$ = 263 / 5 670
$\alpha_{7,8}$ = 3 587 / 623 700
$\alpha_{7,9}$ = -707 / 534 600
$\alpha_{7,10}$ = 109 / 935 550

J = 6 K = -1

$\alpha_{6,0}$ = -14 797 / 191 600 640
$\alpha_{6,1}$ = 90 817 / 95 800 320
$\alpha_{6,2}$ = -1 763 939 / 319 334 400
$\alpha_{6,3}$ = 166 919 / 7 983 360
$\alpha_{6,4}$ = -10 111 819 / 159 667 200
$\alpha_{6,5}$ = 31 494 553 / 79 833 600
$\alpha_{6,6}$ = 14 797 / 82 944
$\alpha_{6,7}$ = -60 917 / 1 900 800
$\alpha_{6,8}$ = 466 157 / 63 866 880
$\alpha_{6,9}$ = -79 829 / 68 428 800
$\alpha_{6,10}$ = 87 299 / 958 003 200

J = 4 K = 1

$\alpha_{4,0}$ = 87 299 / 958 003 200
$\alpha_{4,1}$ = -79 829 / 68 428 800
$\alpha_{4,2}$ = 466 157 / 63 866 880
$\alpha_{4,3}$ = -60 917 / 1 900 800
$\alpha_{4,4}$ = 14 797 / 82 944
$\alpha_{4,5}$ = 31 494 553 / 79 833 600
$\alpha_{4,6}$ = -10 111 819 / 159 667 200
$\alpha_{4,7}$ = 166 919 / 7 983 360
$\alpha_{4,8}$ = -1 763 939 / 319 334 400
$\alpha_{4,9}$ = 90 817 / 95 800 320
$\alpha_{4,10}$ = -14 797 / 191 600 640

J = 3 K = 2

$\alpha_{3,0}$ = 109 / 935 550
$\alpha_{3,1}$ = -707 / 534 600
$\alpha_{3,2}$ = 3 587 / 623 700
$\alpha_{3,3}$ = 263 / 5 670
$\alpha_{3,4}$ = 35 932 / 31 185
$\alpha_{3,5}$ = 111 973 / 124 740
$\alpha_{3,6}$ = -41 543 / 311 850
$\alpha_{3,7}$ = 159 / 3 850
$\alpha_{3,8}$ = -131 / 12 474
$\alpha_{3,9}$ = 263 / 149 688
$\alpha_{3,10}$ = -263 / 1 871 100

J = 2 K = 3

$\alpha_{2,0}$ = 1 693 / 3 942 400
$\alpha_{2,1}$ = -529 / 78 848
$\alpha_{2,2}$ = 7 443 / 71 680
$\alpha_{2,3}$ = 464 187 / 492 800
$\alpha_{2,4}$ = 4 345 149 / 1 971 200
$\alpha_{2,5}$ = 280 821 / 197 120
$\alpha_{2,6}$ = -88 827 / 394 240
$\alpha_{2,7}$ = 1 029 / 14 080
$\alpha_{2,8}$ = -10 833 / 563 200
$\alpha_{2,9}$ = 6 511 / 1 971 200
$\alpha_{2,10}$ = -1 063 / 3 942 400

J = 1 K = 4

$\alpha_{1,0}$ = -124 / 93 555
$\alpha_{1,1}$ = 122 / 1 701
$\alpha_{1,2}$ = 23 756 / 22 275
$\alpha_{1,3}$ = 2 704 / 1 485
$\alpha_{1,4}$ = 532 184 / 155 925
$\alpha_{1,5}$ = 280 124 / 155 925
$\alpha_{1,6}$ = -6 584 / 31 185
$\alpha_{1,7}$ = 8 368 / 155 925
$\alpha_{1,8}$ = -356 / 31 185
$\alpha_{1,9}$ = 758 / 467 775
$\alpha_{1,10}$ = -52 / 467 775

J = 0 K = 5

$\alpha_{0,0}$ = 202 025 / 3 483 648

$\alpha_{0,1}$ = 21 621 125 / 19 160 064

$\alpha_{0,2}$ = 21 348 625 / 12 773 376

$\alpha_{0,3}$ = 5 650 375 / 1 596 672

$\alpha_{0,4}$ = 22 426 625 / 6 386 688

$\alpha_{0,5}$ = 10 314 625 / 3 193 344

$\alpha_{0,6}$ = -5 942 875 / 6 386 688

$\alpha_{0,7}$ = 208 625 / 532 224

$\alpha_{0,8}$ = -1 539 875 / 12 773 376

$\alpha_{0,9}$ = 62 875 / 2 737 152

$\alpha_{0,10}$ = -77 425 / 38 320 128

APPENDIX 2

"ORDAP" PROGRAM SUBROUTINES LIST

"ORDAP" PROGRAM SUBROUTINES LIST

Subroutine	Description	From
ORDAP	Main program.	D. Parrot
ADJUS	Least-squares adjustment for preliminary inititial conditions improvement.	D. Parrot
ANMLY	Compute mean, eccentric and true anomaly from ephemerides.	UNBLIB
ANML2	Convert eccentricity and mean anomaly to eccentric and mean anomaly.	UNBLIB
ATAP2	Compute matrix A^TA and vector A^TW for coefficients computation (least-squares approximation).	D. Parrot
BROA3	Read broadcast message files.	D. Parrot
CGMST	Compute Greenwich mean sidereal time.	D. Parrot
CKCOR	Convert GPS times to GPS times from reference epoch t_o.	UNBLIB
CLKAN	Correct coefficients for improved clock model.	UNBLIB
COWEL	Numerical integration.	D. Parrot
DATUM	Initialize datum values.	UNBLIB
DENOR	Denormalized geopotential coefficients.	D. Parrot
DJUL1	Compute Modified Julian Day from y/m/d.	ASTLIB
ECLIP	Compute eclipse factor.	D. Parrot
EPHEM	Compute satatellite position and velocity from osculating elements.	ASTLIB
FFIEL	Compute acceleration acting on a satellite.	D. Parrot
GEOPT	Block data to initialize the geopotential coeffficients.	D. Parrot

GRAVI	Compute acceleration due to the earth gravity field.	D. Parrot
INTV	Manage the computation of the starting values require for the numerical integration.	D. Parrot
INTCD	Manage intial conditions computation from broadcast ephemerides.	D. Parrot
IRTV	Select position in the geopotential coefficients vector.	D. Parrot
IZERO	Zero integer arrays.	D. Parrot
KLORB	Compute satellite earth-fixed position and velocity from broad. ephemerides.	UNBLIB
LEGEN	Compute associated Legendre functions.	D. Parrot
MONSO	Compute perturbation of the moon.	ASTLIB
MOON	Compute moon position.	ASTLIB
MUL33	3 X 3 matrix multiplication.	D. Parrot
NORM	Compute the norm of a vector.	D. Parrot
NRINT	Manage numerical integration and orbital coefficients computation.	D. Parrot
NUTAT	Nutation matrix computation.	UNBLIB (mod.)
OPERV	Perform vectorial operations.	D. Parrot
RANGE	Compute range between two points.	UNBLIB
SATCP	Manage satellite pos. and vel. computation from broadcast ephemerides.	D. Parrot
RCTLF	Read control file.	D. Parrot
RESI	Radial, along-track and cross-track from x, y, z residuals.	D. Parrot
RDIN	Read input osculating elements file.	D. Parrot
RPART	Partial derivatives of satellite positions with respect to initial conditions (Keplerian approximation).	ASTLIB (mod.)

SIDER	GAST rotation matrix.	D. Parrot
SOLPR	Solar radiation pressure (acceleration).	D. Parrot
SPIN	Matrix inversion.	UNBLIB
START	Starter iterative procedure.	D. Parrot
SUN1	Compute sun positions.	ASTLIB (mod.)
THBOD	Compute acceleration due to a third-body.	D. Parrot
VALID	Validate control file information.	D. Parrot
XYZEE	Orbital elements computation from satellite position and velocity.	ASTLIB
ZERO	Zero real matrices.	D. Parrot

APPENDIX 3

"ORDAP" PROGRAM
INPUT AND OUTPUT FILES

"ORDAP" PROGRAM INPUT FILE

(example)

(integration of one satellite)

```
                ORBIT GENERATION CONTROL FILE
                =============================
FORCE FIELD PARAMETERS
RADIATION PRESSURE COEF. (CR)    :0.940000D-07
DEGREE AND ORDER (MAX 10X10)     :  8  8
COMPUTE SUN EFFECT  (1 YES,0 NO):  1
        MOON EFFECT              :  1
        SOLAR PRESSURE EFFECT    :  1
-----------------------------------------------------------------
NUMBER OF ITERATIONS             :  1
-----------------------------------------------------------------
SESSION INFORMATION
NUMBER OF ORBITAL SESSIONS       :  1
-----------------------------------------------------------------
SESSION NUMBER                   :  1
GPST-UTC (SECOND)                :  4
XP, YP   (ARC-SECOND)            :-0.1927 +0.2169
UT1-UTC  (SECOND)                :-0.30242
STEP SIZE (SECOND) FOR NUM. INT.:  720
SEGMENTATION LENGTH (HRS)        :  2.0
POLYNOMIAL DEGREE  (max. 9)      :  9
NUMBER OF SATELLITE              :  1
ISAT  YRS1  M1  D1  HRS1  YRS2  M2  D2  HRS2  (HRS MUST BE UT TIME)
   9  1985   3  30  05.3  1985   3  30   9.2
-----------------------------------------------------------------
COEFFICIENTS FILE NAME           : DEMO.COE
INITIAL CONDITION FILE NAME      : DEMO.INT
BRODCAST MESSAGE (=1),  OSCULATING ELEMENTS (=2)
 1  ZFA1:[017015.DATA.SPR85]BRD89A.EPH
```

"ORDAP" PROGRAM OUTPUT FILE

(output of the previous control file)

```
ORBITAL DATA PREPROCESSING (summary)
====================================

Input file
Control file name .............:  TEST.COR

Output files
Initial conditions file name ..:  DEMO.INT

Coefficients file name ........:  DEMO.COE



Force field parameters

- Earth gravity field ................: GEM-L2
  (degree  8 order  8)
  Geocentric gravitational constant...: 0.398600800000D+15
  Equatorial radius (Ae) .............: 0.637814411000D+07

- Gravitational attraction of the sun
  Heliocentric gravitational constant : 0.132712440000D+21

- Gravitational attraction of the moon
  Lunar gravitational constant........: 0.490279930000D+13

- Solar radiation pressure (flat-plate model)
  Solar pressure constant.............: 0.940000000000D-07



ORBITAL SESSION INFORMATION
===========================

SESSION  :  1


- Earth rotation parameters:
  UT1-UTC (sec.)......................: -0.30242D+00
  X pole (arc-sec.)...................: -0.19270D+00
  Y pole (arc-sec.)...................:  0.21690D+00
```

- Time frame :
  GPST-UTC (sec.).....: 4

- Integration parameters:
  Integration step (sec.) .....: 720
  Segmentation length (hrs).....: 2.0
  Algebraic polynomial degree.....: 9

- Constellation to be integrated:

Sat. PRN	Time start (mjd)	int. period (hrs)
9	46154.2208333333	3.90

- Broadcast file used to compute
  initial conditions.....:ZFA1:[017015.DATA.SPR85]BRD89A.EPH

- Difference between initial condition epoch and referecence
  time of the braodcast message used in the computation

Sat. PRN	Time difference (hrs)
9	-0.699

- SV accuracy table

Sat. PRN	Accuracy (m) for each message												
9	4	4	4	4	4	4	4	0	0	0	0	0	0
	0	0	0	0	0	0	0	0	0	0	0	0	0
	0	0	0	0	0	0	0	0	0	0	0	0	0

- SV health table

Sat. PRN	Health for each message												
9	0	0	0	0	0	0	0	0	0	0	0	0	0
	0	0	0	0	0	0	0	0	0	0	0	0	0
	0	0	0	0	0	0	0	0	0	0	0	0	0

- GPS week table

Sat. PRN	Week number of each message												
9	272	272	272	272	272	272	272	0	0	0	0	0	0
	0	0	0	0	0	0	0	0	0	0	0	0	0
	0	0	0	0	0	0	0	0	0	0	0	0	0

- Satellite PRN number 9

  Iteration : 0

Epoch (mjd)	radial(m)	along tr.(m)	cross tr.(m)
46154.2208333333	0.00	0.00	0.00
46154.2312500000	-0.01	0.05	-0.05
46154.2416666667	-0.03	0.05	-0.06
46154.2520833333	-0.05	0.01	-0.04
46154.2625000000	-0.04	-0.08	0.02
46154.2729166667	0.01	-0.17	0.14
46154.2833333333	0.12	-0.26	0.31
46154.2937500000	0.38	-6.76	-6.05
46154.3041666667	0.44	-6.81	-7.17
46154.3145833333	0.55	-6.84	-8.12
46154.3250000000	0.69	-6.88	-8.86
46154.3354166667	0.86	-6.97	-9.50
46154.3458333333	1.02	-7.12	-9.82
46154.3562500000	1.19	-7.32	-9.91
46154.3666666667	1.35	-7.58	-9.80
46154.3770833333	1.52	-7.82	-9.70

INITIAL CONDITIONS

SEMI-MAJOR AXIS (m)	26558781.226
ECCENTRICITY	0.010706511
INCLINATION (deg)	63.85218
ASCENDING NODE (deg)	26.13577
PERIGEE (deg)	70.34261
TIME OF PERIGE PASSAGE (hr).	0.20786

CORRECTIVE TERMS

SEMI-MAJOR AXIS (m)	4.038
ECCENTRICITY	0.000000127
INCLINATION (")	0.00769
ASCENDING NODE (")	0.08240
PERIGEE (")	3.50856
TIME OF PERIGE PASSAGE (sec):	0.11522

  Iteration : 1

Epoch (mjd)	radial(m)	along tr.(m)	cross tr.(m)
46154.2208333333	1.16	0.36	-3.26
46154.2312500000	0.50	0.46	-2.09
46154.2416666667	-0.12	0.66	-0.85
46154.2520833333	-0.67	0.98	0.45

46154.2625000000	-1.11	1.38	1.77
46154.2729166667	-1.41	1.88	3.12
46154.2833333333	-1.56	2.47	4.46
46154.2937500000	-1.45	-3.29	-0.79
46154.3041666667	-1.45	-2.58	-0.91
46154.3145833333	-1.30	-1.85	-0.95
46154.3250000000	-1.01	-1.15	-0.92
46154.3354166667	-0.59	-0.55	-0.92
46154.3458333333	-0.09	-0.09	-0.75
46154.3562500000	0.51	0.22	-0.51
46154.3666666667	1.19	0.35	-0.23
46154.3770833333	1.93	0.35	-0.12

"ORDAP" PROGRAM INPUT FILE

(example)

(Integration of 7 satellites over 4 orbital arcs each)

```
                    ORBIT GENERATION CONTROL FILE
                    =============================
FORCE FIELD PARAMETERS
RADIATION PRESSURE COEF. (CR)    :0.940000D-07
DEGREE AND ORDER (MAX 10X10)     :  8  8
COMPUTE SUN EFFECT  (1 YES,0 NO):  1
        MOON EFFECT              :  1
        SOLAR PRESSURE EFFECT    :  1
-----------------------------------------------------------------
NUMBER OF ITERATIONS             :  1
-----------------------------------------------------------------
SESSION INFORMATION
NUMBER OF ORBITAL SESSIONS       :  4
-----------------------------------------------------------------
SESSION NUMBER                   :  1
GPST-UTC (SECOND)                :  4
XP, YP   (ARC-SECOND)            :-0.1927 +0.2169
UT1-UTC  (SECOND)                :-0.30242
STEP SIZE (SECOND) FOR NUM. INT.:  720
SEGMENTATION LENGTH (HRS)        :  2.0
POLYNOMIAL DEGREE  (max. 9)      :  9
NUMBER OF SATELLITE              :  7
ISAT  YRS1  M1  D1  HRS1  YRS2  M2  D2  HRS2  (HRS MUST BE UT TIME)
   6  1985   3  30  03.0  1985   3  30  07.0
   8  1985   3  30  03.0  1985   3  30  07.0
  11  1985   3  30  03.8  1985   3  30  10.9
   9  1985   3  30  05.3  1985   3  30   9.2
  13  1985   3  30  06.8  1985   3  30  11.0
  12  1985   3  30  07.2  1985   3  30  10.3
   4  1985   3  30  09.1  1985   3  30  11.6
-----------------------------------------------------------------
SESSION NUMBER                   :  2
GPST-UTC (SECOND)                :  4
XP, YP   (ARC-SECOND)            :-0.1927 +0.2169
UT1-UTC  (SECOND)                :-0.30242
STEP SIZE (SECOND) FOR NUM. INT.:  720
SEGMENTATION LENGTH (HRS)        :  2.0
POLYNOMIAL DEGREE  (max. 9)      :  9
NUMBER OF SATELLITE              :  7
ISAT  YRS1  M1  D1  HRS1  YRS2  M2  D2  HRS2  (HRS MUST BE UT TIME)
   6  1985   3  31  03.0  1985   3  31  07.0
   8  1985   3  31  03.0  1985   3  31  07.0
  11  1985   3  31  03.8  1985   3  31  10.9
```

```
   9  1985    3  31   04.4  1985    3  31    9.2
  13  1985    3  31   06.8  1985    3  31   11.0
  12  1985    3  31   06.9  1985    3  31   10.3
   4  1985    3  31   09.1  1985    3  31   11.6
-----------------------------------------------------------------
SESSION NUMBER                    :  3
GPST-UTC (SECOND)                 :  4
XP, YP    (ARC-SECOND)            :-0.1927 +0.2169
UT1-UTC   (SECOND)                :-0.30242
STEP SIZE (SECOND) FOR NUM. INT.:  720
SEGMENTATION LENGTH (HRS)         :  2.0
POLYNOMIAL DEGREE  (max. 9)       :  9
NUMBER OF SATELLITE               :  7
ISAT  YRS1  M1  D1  HRS1  YRS2  M2  D2  HRS2  (HRS MUST BE UT TIME)
   6  1985   4  01  02.9  1985   4  01  06.9
   8  1985   4  01  02.9  1985   4  01  06.9
  11  1985   4  01  03.7  1985   4  01  10.8
   9  1985   4  01  05.2  1985   4  01   9.1
  13  1985   4  01  06.7  1985   4  01  10.9
  12  1985   4  01  07.1  1985   4  01  10.2
   4  1985   4  01  09.0  1985   4  01  12.0
-----------------------------------------------------------------
SESSION NUMBER                    :  4
GPST-UTC (SECOND)                 :  4
XP, YP    (ARC-SECOND)            :-0.1963 +0.23459
UT1-UTC   (SECOND)                :-0.31181
STEP SIZE (SECOND) FOR NUM. INT.:  720
SEGMENTATION LENGTH (HRS)         :  2.0
POLYNOMIAL DEGREE  (max. 9)       :  9
NUMBER OF SATELLITE               :  7
ISAT  YRS1  M1  D1  HRS1  YRS2  M2  D2  HRS2  (HRS MUST BE UT TIME)
   6  1985   4  04  02.6  1985   4  04  06.9
   8  1985   4  04  02.6  1985   4  04  06.9
  11  1985   4  04  03.4  1985   4  04  10.7
   9  1985   4  04  04.1  1985   4  04   9.1
  13  1985   4  04  06.6  1985   4  04  10.9
  12  1985   4  04  06.5  1985   4  04  10.2
   4  1985   4  04  08.7  1985   4  04  12.0
-----------------------------------------------------------------
COEFFICIENTS FILE NAME            : NETBR.COE
INITIAL CONDITION FILE NAME       : NETBR.INT
BRODCAST MESSAGE (=1),  OSCULATING ELEMENTS (=2)
 1  ZFA0:[017004.SPR85]BRD89A.EPH
 1  ZFA0:[017004.SPR85]BRD90A.EPH
 1  ZFA0:[017004.SPR85]BRD91A.EPH
 1  ZFA0:[017004.SPR85]BRD94A.EPH
```

APPENDIX 4

SINGLE, DOUBLE AND CSLIP PROGRAM SUBROUTINES LIST

"SINGLE" PROGRAM SUBROUTINES LIST

Subroutine	Description	From
SINGLE	Main program.	D. Parrot
ANMLY	Compute mean, eccentric and true anomaly from ephemerides.	UNBLIB
ANML2	Convert eccentricity and mean anomaly to eccentric and mean anomaly.	UNBLIB
BROA2	Read broadcast messages.	D. Parrot
CGMST	Compute Greenwich mean sidereal time.	D. Parrot
CKCOR	Convert GPS times to GPS times from reference epoch t_o.	UNBLIB
CONT1	Read single-difference control file.	D. Parrot
DATUM	Initialize datum values.	UNBLIB
IZERO	Zero integer arrays.	D. Parrot
IMPCK	Modification of CLKAN subroutine.	D. Parrot
KLORB	Compute satellite earth-fixed position and velocity from broadcast ephemerides.	UNBLIB
MUL33	3 X 3 matrix multiplication.	D. Parrot
RANGE	Compute range between two points.	UNBLIB
RDCOE	Read orbital coefficients.	D. Parrot
REA11	Read observations from the first observation files.	D. Parrot
REA22	Read observations from all subsequent observation file.	D. Parrot
REFS2	Get reference satellite from scenario file.	D. Parrot
REFS4	Get reference satellite from observation file.	D. Parrot

SATRD	Manage satellite coordinates computation.	D. Parrot
SATR2	Satellite coordinates computation from polynomial coefficients.	D. Parrot
SIDER	GAST rotation matrix.	D. Parrot
TIMET	Find time tag aligned with the GESAR software synchronization.	D. Parrot
ZERO	Zero real arrays.	D. Parrot

"DOUBLE" PROGRAM SUBROUTINES LIST

Subroutine	Description	From
DOUBLE	Main program.	D. Parrot
AMBCR	Compute double-difference a priori ambiguities.	D. Parrot
AMBGT	Apply double-difference a priori ambiguities.	D. Parrot
IZERO	Zero integer arrays.	D. Parrot
RSTAC	Read a priori station coordinates.	D.Parrot
RANGE	Compute range between two points.	UNBLIB
ZERO	Zero real arrays.	D. Parrot

"CSLIP" PROGRAM SUBROUTINES LIST

Subroutine	Description	From
CSLIP	Main program.	D. Parrot
DIST1	Compute theoritical single-difference.	D. Parrot
DIST2	Compute theoritical double-difference.	D. Parrot
IZERO	Zero integer arrays.	D. Parrot
LSQR	Estimation of cycle-slip.	D. Parrot
RCON2	Read CSLIP control file.	D. Parrot
RECRD	Record clean observation file.	D. Parrot
RSTAC	Read a priori station coordinates.	D.Parrot
RANGE	Compute range between two points.	UNBLIB
SPIN	Matrix inversion.	D. Parrot
ZERO	Zero real arrays.	D. Parrot

APPENDIX 5

CONTROL FILE FOR NEW VERSION OF DIPOP

CONTROL FILE FOR NEW VERSION OF DIPOP
(example from our fiducial network solution)

```
                    CONTROL FILE
                    ============

|                                                                              |
| GENERAL FILE INFORMATION                                                     |
|   1) MAIN PROCESSOR                          (OUTPUT)                        |
|   2) INTERMEDIATE SOLUTION                   (OUTPUT)                        |
|   3) FINAL SOLUTION (MPROC)                  (OUTPUT)                        |
|   4) NUISANCE PARAMETERS                     (OUTPUT)                        |
|   5) RESIDUALS                               (OUTPUT)                        |
|   6) POST PROCESSOR                          (OUTPUT)                        |
|   7) DISCREPANCIES                           (OUTPUT)                        |
|   8) FINAL SOLUTION & COV. (PPROC)           (OUTPUT)                        |
|   9) ORBITAL COEFFICIENTS FILE               (INPUT )                        |
|  10) INITIAL CONDITIONS FILE NAME            (INPUT )                        |
|  11) A-PRIORI STATION COORD. FILE            (INPUT )                        |
|  12) UPDATED INITIAL CONDITIONS FILE NAME    (OUTPUT)                        |
|  13) SEVEN-PARAMETER TRANSFORMATION FILE     (OUTPUT)                        |
|                                                                              |
|   1) MPNETFD.OUT                                                             |
|   2) INTSOL.OUT                                                              |
|   3) FIN.OUT                                                                 |
|   4) NUIS.OUT                                                                |
|   5) DUMMY.OUT                                                               |
|   6) PRNETFD.OUT                                                             |
|   7) DI.OUT                                                                  |
|   8) FINS.OUT                                                                |
|   9) ZFA0:[017004.SOURCE.ORBIT]NETBR.COE                                     |
|  10) ZFA0:[017004.SOURCE.ORBIT]NETBR.INT                                     |
|  11) SPR85.AP3                                                               |
|  12) ZFA0:[017004.SOURCE.ORBIT]NETFD.INT                                     |
|  13) NETFD.CRD                                                               |
|------------------------------------------------------------------------------|
|                                                                              |
| OPTION INFORMATION          Y(1), N(0)                                       |
| RESIDUAL COMPUTATION,                      : 0                               |
| TAKE INTO ACCOUNT DBL.-DIFF. CORRELATION   : 0                               |
|------------------------------------------------------------------------------|
|                                                                              |
| INITIAL CONDITIONS                                                           |
| COMPUTED FROM COEFFICIENTS          (0)                                      |
| READ FROM INITIAL CONDITIONS FILE (1)      : 1                               |
|------------------------------------------------------------------------------|
|                                                                              |
| NUIS. PAR. SEQ. SOLUTION EACH N EPOCH      : 500                             |
| STA. COORD. SEQ. SOLUTION EACH M EPOCH     : 500                             |
|------------------------------------------------------------------------------|
|                                                                              |
| CROSS-CORRELATION VALUE COMPARISON         : 0.9                             |
|------------------------------------------------------------------------------|
```

```
|                                                                              |
| OBSERVATION FILES, BINARY(0) OR ASCII(1) : 1                                 |
|------------------------------------------------------------------------------|
|                                                                              |
| CUT OFF ANGLE (degree)                   : 20                                |
|------------------------------------------------------------------------------|
|                                                                              |
| WAVELENGTH SC. FAC. (TI4100=1, V-1000=2) : 1                                 |
|------------------------------------------------------------------------------|
|                                                                              |
| DEFAULT MSL METEOROLOGICAL VALUES                                            |
|                                 -------.------                               |
| PRESSURE (mbar)              :    1013.25                                    |
| TEMPERATURE (Celsius)        :      17.85                                    |
| RELATIVE HUMIDITY (%)        :      48.34                                    |
|------------------------------------------------------------------------------|
|                                                                              |
| ORBITAL A-PRIORI INFORMATION   (0 IF NOT ESTIMATED)                          |
| (SIGMA)                         -------.-------                              |
| SEMIMAJOR AXIS       (M)     :      50.0000000                               |
| ECCENTRICITY                 :       0.0000200                               |
| INCLINATION          (")     :       1.0000000                               |
| ASCENDING NODE       (")     :       1.0000000                               |
| PERIGEE              (")     :       0.0000000                               |
| PERIGEE PASSING TIME (SEC)   :       0.2500000                               |
|                                                                              |
| SOLAR RADIATION PRESSURE COEFFICIENTS                                        |
| A-PRIORI INFORMATION           (0 IF NOT ESTIMATED)                          |
|                                      -.-----D+--                             |
| DIRECT RPR PARAMETERS        :       0.00000D+08                             |
| (RESERVED FOR A SECOND PARAMETER)                                            |
| (RESERVED FOR A THIRD PARAMETER )                                            |
|-----------------+------------------------------------------------------------|
|                                                                              |
|                                      -.-------D+-- (m**3 /sec**2)            |
| GM VALUE (WGS72)                     3.9860080D+14                           |
|------------------------------------------------------------------------------|
|                                                                              |
| OBSERVATION INFORMATION                                                      |
|------------------------------------------------------------------------------|
|                                                                              |
| ORBITAL SESSION                          : 1                                 |
| AMBIGUITY EVALUATION,      Y(1), N(0)    : 1                                 |
| ROUND OFF NEAREST INTEGER, Y(1), N(0)    : 0                                 |
| TROPOSPHERIC SCALE FACTOR  Y(1), N(0)    : 1                                 |
| SIGMA FOR TROPOSPHERIC SCALE FACTOR      : 1.0D-00                           |
| NUMBER OF CLOCK PARAMETERS TO BE ESTIMATE: 1                                 |
| RESPECTIVE SIGMA FOR EACH PARAMETER      : 1.0D-01   1.0D-04                 |
|                                                                  |A-PRIORI   |
| OBSERVATION FILE + TYPE OF SOLUTION + 2 METEO FILES              |SIGMA mm   |
|                                                                              |
| HYRC89A.DB5                                                            10    |
| SOLUTION  L1:1, L2:2, L1&L2:3            : 3                                 |
| HY89A.MET                                                                    |
```

```
| RC89A.MET                                                                  |
|                                                                            |
| HYFD89A.DB5                                                          10    |
| SOLUTION  L1:1, L2:2, L1&L2:3            : 3                               |
| HY89A.MET                                                                  |
| FD89A.MET                                                                  |
|                                                                            |
| HYHT89A.DB5                                                          10    |
| SOLUTION  L1:1, L2:2, L1&L2:3            : 3                               |
| HY89A.MET                                                                  |
| HT89A.MET                                                                  |
|                                                                            |
| HYBP89A.DB5                                                          10    |
| SOLUTION  L1:1, L2:2, L1&L2:3            : 3                               |
| HY89A.MET                                                                  |
| BP89A.MET                                                                  |
|                                                                            |
| HYMJ89A.DB5                                                          10    |
| SOLUTION  L1:1, L2:2, L1&L2:3            : 3                               |
| HY89A.MET                                                                  |
| MJ89A.MET                                                                  |
|                                                                            |
| HYAR89A.DB5                                                          10    |
| SOLUTION  L1:1, L2:2, L1&L2:3            : 3                               |
| HY89A.MET                                                                  |
| AR89A.MET                                                                  |
|                                                                            |
| HYNS89A.DB5                                                          10    |
| SOLUTION  L1:1, L2:2, L1&L2:3            : 3                               |
| HY89A.MET                                                                  |
| NS89A.MET                                                                  |
|                                                                            |
| HYMM89A.DB5                                                          10    |
| SOLUTION  L1:1, L2:2, L1&L2:3            : 3                               |
| HY89A.MET                                                                  |
| MM89A.MET                                                                  |
------------------------------------------------------------------------------
|                                                                            |
| ORBITAL SESSION                          : 2                               |
| AMBIGUITY EVALUATION,      Y(1), N(0)    : 1                               |
| ROUND OFF NEAREST INTEGER, Y(1), N(0)    : 0                               |
| TROPOSPHERIC SCALE FACTOR  Y(1), N(0)    : 1                               |
| SIGMA FOR TROPOSPHERIC SCALE FACTOR      : 1.0D-00                         |
| NUMBER OF CLOCK PARAMETERS TO BE ESTIMATE: 1                               |
| RESPECTIVE SIGMA FOR EACH PARAMETER      : 1.0D-01   1.0D-04               |
|                                                                 |A-PRIORI  |
| OBSERVATION FILE + TYPE OF SOLUTION + 2 METEO FILES             |SIGMA mm  |
|                                                                            |
| HTRC90A.DB5                                                          10    |
| SOLUTION  L1:1, L2:2, L1&L2:3            : 3                               |
| HT90A.MET                                                                  |
| RC90A.MET                                                                  |
|                                                                            |
| HTFD90A.DB5                                                          10    |
```

```
| SOLUTION  L1:1, L2:2, L1&L2:3           : 3                                |
| HT90A.MET                                                                  |
| FD90A.MET                                                                  |
|                                                                            |
| HTBP90A.DB5                                                          10    |
| SOLUTION  L1:1, L2:2, L1&L2:3           : 3                                |
| HT90A.MET                                                                  |
| BP90A.MET                                                                  |
|                                                                            |
| HTMJ90A.DB5                                                          10    |
| SOLUTION  L1:1, L2:2, L1&L2:3           : 3                                |
| HT90A.MET                                                                  |
| MJ90A.MET                                                                  |
|                                                                            |
| HTAR90A.DB5                                                          10    |
| SOLUTION  L1:1, L2:2, L1&L2:3           : 3                                |
| HT90A.MET                                                                  |
| AR90A.MET                                                                  |
|                                                                            |
| HTNS90A.DB5                                                          10    |
| SOLUTION  L1:1, L2:2, L1&L2:3           : 3                                |
| HT90A.MET                                                                  |
| NS90A.MET                                                                  |
|                                                                            |
| HTMM90A.DB5                                                          10    |
| SOLUTION  L1:1, L2:2, L1&L2:3           : 3                                |
| HT90A.MET                                                                  |
| MM90A.MET                                                                  |
------------------------------------------------------------------------------
|                                                                            |
| ORBITAL SESSION                         : 3                                |
| AMBIGUITY EVALUATION,      Y(1), N(0)   : 1                                |
| ROUND OFF NEAREST INTEGER, Y(1), N(0)   : 0                                |
| TROPOSPHERIC SCALE FACTOR  Y(1), N(0)   : 1                                |
| SIGMA FOR TROPOSPHERIC SCALE FACTOR     : 1.0D-00                          |
| NUMBER OF CLOCK PARAMETERS TO BE ESTIMATE: 1                               |
| RESPECTIVE SIGMA FOR EACH PARAMETER     : 1.0D-01   1.0D-04                |
|                                                                 |A-PRIORI  |
| OBSERVATION FILE + TYPE OF SOLUTION + 2 METEO FILES             |SIGMA mm  |
|                                                                            |
| HYRC91A.DB5                                                          10    |
| SOLUTION  L1:1, L2:2, L1&L2:3           : 3                                |
| HY91A.MET                                                                  |
| RC91A.MET                                                                  |
|                                                                            |
| HYFD91A.DB5                                                          10    |
| SOLUTION  L1:1, L2:2, L1&L2:3           : 3                                |
| HY91A.MET                                                                  |
| FD91A.MET                                                                  |
| -.000000D-01                                                               |
|                                                                            |
| HYHT91A.DB5                                                          10    |
| SOLUTION  L1:1, L2:2, L1&L2:3           : 3                                |
| HY91A.MET                                                                  |
```

```
| HT91A.MET                                                                  |
|                                                                            |
| HYBP91A.DB5                                                          10    |
| SOLUTION  L1:1, L2:2, L1&L2:3          : 3                                 |
| HY91A.MET                                                                  |
| BP91A.MET                                                                  |
|                                                                            |
| HYMJ91A.DB5                                                          10    |
| SOLUTION  L1:1, L2:2, L1&L2:3          : 3                                 |
| HY91A.MET                                                                  |
| MJ91A.MET                                                                  |
|                                                                            |
| HYAR91A.DB5                                                          10    |
| SOLUTION  L1:1, L2:2, L1&L2:3          : 3                                 |
| HY91A.MET                                                                  |
| AR91A.MET                                                                  |
|                                                                            |
| HYNS91A.DB5                                                          10    |
| SOLUTION  L1:1, L2:2, L1&L2:3          : 3                                 |
| HY91A.MET                                                                  |
| NS91A.MET                                                                  |
|                                                                            |
| HYMM91A.DB5                                                          10    |
| SOLUTION  L1:1, L2:2, L1&L2:3          : 3                                 |
| HY91A.MET                                                                  |
| MM91A.MET                                                                  |
| -.000000D-01                                                               |
------------------------------------------------------------------------------
|                                                                            |
| ORBITAL SESSION                        : 4                                 |
| AMBIGUITY EVALUATION,      Y(1), N(0)  : 1                                 |
| ROUND OFF NEAREST INTEGER, Y(1), N(0)  : 0                                 |
| TROPOSPHERIC SCALE FACTOR  Y(1), N(0)  : 1                                 |
| SIGMA FOR TROPOSPHERIC SCALE FACTOR    : 1.0D-00                           |
| NUMBER OF CLOCK PARAMETERS TO BE ESTIMATE: 1                               |
| RESPECTIVE SIGMA FOR EACH PARAMETER    : 1.0D-01   1.0D-04                 |
|                                                              |A-PRIORI     |
| OBSERVATION FILE + TYPE OF SOLUTION + 2 METEO FILES          |SIGMA mm     |
|                                                                            |
| HYRC94A.DB5                                                          10    |
| SOLUTION  L1:1, L2:2, L1&L2:3          : 3                                 |
| HY94A.MET                                                                  |
| RC94A.MET                                                                  |
|                                                                            |
| HYFD94A.DB5                                                          10    |
| SOLUTION  L1:1, L2:2, L1&L2:3          : 3                                 |
| HY94A.MET                                                                  |
| FD94A.MET                                                                  |
|                                                                            |
| HYHT94A.DB5                                                          10    |
| SOLUTION  L1:1, L2:2, L1&L2:3          : 3                                 |
| HY94A.MET                                                                  |
| HT94A.MET                                                                  |
|                                                                            |
```

```
| HYBP94A.DB5                                                          10 |
| SOLUTION  L1:1, L2:2, L1&L2:3          : 3                             |
| HY94A.MET                                                              |
| BP94A.MET                                                              |
|                                                                        |
| HYMJ94A.DB5                                                          10 |
| SOLUTION  L1:1, L2:2, L1&L2:3          : 3                             |
| HY94A.MET                                                              |
| MJ94A.MET                                                              |
|                                                                        |
| HYAR94A.DB5                                                          10 |
| SOLUTION  L1:1, L2:2, L1&L2:3          : 3                             |
| HY94A.MET                                                              |
| AR94A.MET                                                              |
|                                                                        |
| HYNS94A.DB5                                                          10 |
| SOLUTION  L1:1, L2:2, L1&L2:3          : 3                             |
| HY94A.MET                                                              |
| NS94A.MET                                                              |
|                                                                        |
| HYMM94A.DB5                                                          10 |
| SOLUTION  L1:1, L2:2, L1&L2:3          : 3                             |
| HY94A.MET                                                              |
| MM94A.MET                                                              |
--------------------------------------------------------------------------
```

APPENDIX 6

SEVEN-PARAMETER TRANSFORMATION

SEVEN-PARAMETER TRANSFORMATION

The seven-parameter transformation model (used in chapter 6) expresses the relationship between two coordinate systems by three translations (X_o, Y_o, Z_o), three rotations (ε_x, ε_y, ε_z) and one scale factor (κ).

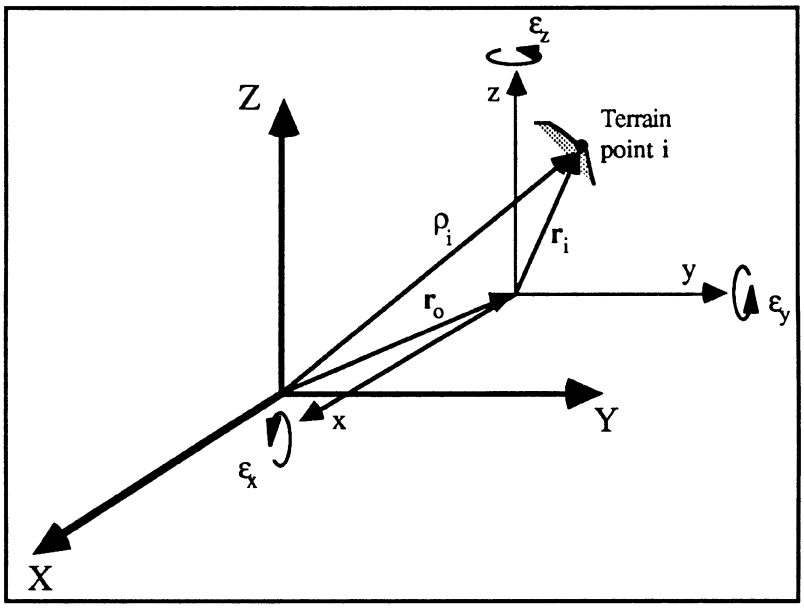

Seven-parameter transformation model
FIGURE A6.1

According to Fig.A6.1, the two sets of network coordinates for any terrain point i are related as follows:

$$\rho_i = r_o + (1+\kappa)\, \mathbf{R}_\varepsilon\, r_i \qquad \text{(A6.1)}$$

the rotation angles being small values, the rotation matrix $\mathbf{R}_\varepsilon$ is given by:

$$\mathbf{R}_{\varepsilon} = \begin{bmatrix} 1 & \varepsilon_z & -\varepsilon_y \\ -\varepsilon_z & 1 & \varepsilon_x \\ \varepsilon_y & -\varepsilon_x & 1 \end{bmatrix}$$

The vectors $\mathbf{r}_i$ (and ρ_i) are used as observables. Thus, the observation equation can be derived directly from equation (A6.1):

$$\mathbf{F}_i = \mathbf{r}_o + (1+\kappa)\,\mathbf{R}_{\varepsilon}\,\mathbf{r}_i - \rho_i = 0 \qquad \text{(A6.2)}$$

Let us define the parameter vector as $\mathbf{X} = \{X_o, Y_o, Z_o, \varepsilon_x, \varepsilon_y, \varepsilon_z, \kappa\}$. The equation (A6.2) being linear, the a priori values $\mathbf{X}^o$ required to evaluate the partial derivatives of function $\mathbf{F}$ with respect to $\mathbf{X}$ can be chosen as follows:

$$\mathbf{X}^o = \left\{X_o^o, Y_o^o, Z_o^o, \varepsilon_x^o, \varepsilon_y^o, \varepsilon_z^o, \kappa^o\right\} = 0 \qquad \text{(A6.3)}$$

Thus, according to (A6.2) and (A6.3), the elements of the design matrix $\mathbf{A}_i$ can be evaluated following the simple form:

$$\mathbf{A}_i = \frac{\partial \mathbf{F}_i}{\partial \mathbf{X}}\Big|_{\mathbf{X}^o} = \begin{bmatrix} 1 & 0 & 0 & 0 & -z_i & y_i & x_i \\ 0 & 1 & 0 & z_i & 0 & -x_i & y_i \\ 0 & 0 & 1 & -y_i & x_i & 0 & z_i \end{bmatrix} \qquad \text{(A6.4)}$$

One sub-matrix $\mathbf{A}_i$ is generated for each point i known in both coordinate systems. The design matrix $\mathbf{A}$ is the concatenation of all sub-matrices $\mathbf{A}_i$. The misclosure vector $\mathbf{W}_i$ is also obtained using (A6.2) and (A6.3):

$$\mathbf{W}_i = \begin{bmatrix} x_i - X_i \\ y_i - Y_i \\ z_i - Z_i \end{bmatrix} \qquad \text{(A6.5)}$$

The least-squares solution is finally obtained as follows:

$$\mathbf{X} = -\left(\mathbf{A}^T\mathbf{A}\right)^{-1}\mathbf{A}^T\mathbf{W} \qquad \text{(A6.6)}$$

APPENDIX 7

FIDUCIAL NETWORK SOLUTION

RE-EVALUATION OF NUISANCE PARAMETERS
==========

ORBITAL SESSION: 1

ORBITAL PARAMETERS (improvement in kepl. elements)

SATELLITE ID.:	6				
A	(m)	:	-3.541	+/-	2.207
E		:	-0.00000033	+/-	0.00000006
I	(")	:	0.0458	+/-	0.0089
KN	(")	:	-0.0624	+/-	0.0119
PER	(")	:	-1.3879	+/-	1.1399
T0	(sec)	:	-0.04551	+/-	0.03751
SATELLITE ID.:	8				
A	(m)	:	3.235	+/-	1.378
E		:	-0.00000011	+/-	0.00000002
I	(")	:	-0.0454	+/-	0.0158
KN	(")	:	0.1393	+/-	0.0093
PER	(")	:	-4.5118	+/-	1.5553
T0	(sec)	:	-0.14843	+/-	0.05112
SATELLITE ID.:	11				
A	(m)	:	-0.073	+/-	1.027
E		:	-0.00000002	+/-	0.00000002
I	(")	:	0.0125	+/-	0.0129
KN	(")	:	0.1016	+/-	0.0118
PER	(")	:	2.9149	+/-	0.4456
T0	(sec)	:	0.09932	+/-	0.01607
SATELLITE ID.:	9				
A	(m)	:	7.018	+/-	2.350
E		:	0.00000001	+/-	0.00000002
I	(")	:	0.0074	+/-	0.0132
KN	(")	:	-0.0535	+/-	0.0071
PER	(")	:	6.5420	+/-	1.0581
T0	(sec)	:	0.21422	+/-	0.03387
SATELLITE ID.:	13				
A	(m)	:	2.683	+/-	1.909
E		:	0.00000008	+/-	0.00000002
I	(")	:	0.0251	+/-	0.0123
KN	(")	:	0.1158	+/-	0.0161
PER	(")	:	-0.8218	+/-	1.5784
T0	(sec)	:	-0.02506	+/-	0.05153
SATELLITE ID.:	12				
A	(m)	:	-15.793	+/-	6.118

```
   E           :              0.00000054   +/-  0.00000017
   I   (")     :                  0.0163   +/-      0.0142
   KN  (")     :                  0.0182   +/-      0.0131
   PER (")     :                 -2.7551   +/-      1.3910
   T0  (sec)   :                -0.07257   +/-     0.05159

SATELLITE ID.:   4
   A   (m)     :                  24.096   +/-      12.839
   E           :             -0.00000166   +/-  0.00000060
   I   (")     :                  0.5733   +/-      0.1793
   KN  (")     :                 -0.5179   +/-      0.1586
   PER (")     :                  0.0690   +/-      1.8992
   T0  (sec)   :                 0.02214   +/-     0.06256


TROPOSPHERIC SCALE FACTOR (1+k)
-------------------------------

 HY  -0.0028  +/-  0.0038
 RC   0.0127  +/-  0.0057
 FD   0.0078  +/-  0.0051
 NS   0.0331  +/-  0.0040
 HT   0.0063  +/-  0.0067
 AR   0.0329  +/-  0.0042
 BP  -0.0246  +/-  0.0058
 MM  -0.0034  +/-  0.0068
 MJ  -0.0088  +/-  0.0053


CLOCK AND AMBIGUITY PARAMETERS
------------------------------

FILE: HYRC89A.DB5
STATIONS:  HY RC

CLOCK PARAMETERS (RECEIVER 2 WRT RECEIVER 1)

OFFSET : -.545713D-02   +/-0.137771D-03
 DRIFT : 0.827427D-08   +/-0.893280D-08

AMBIGUITY WRT REFERENCE SATELLITE :   11
AMBIGUITY   6 :                  -3306.42   +/-   6.79
AMBIGUITY   8 :                   -728.48   +/-  10.61
AMBIGUITY  31 :                     10.42   +/-   2.41
AMBIGUITY   9 :                  -3335.33   +/-  12.68
AMBIGUITY  13 :                  -1982.18   +/-  16.56
AMBIGUITY  12 :                  -3767.69   +/-  29.72
AMBIGUITY   4 :                  -3788.82   +/- 292.65
AMBIGUITY  51 :                  -1358.81   +/-   1.90

FILE: HYFD89A.DB5
STATIONS:  HY FD

CLOCK PARAMETERS (RECEIVER 2 WRT RECEIVER 1)

OFFSET : 0.126247D-02   +/-0.168059D-03
```

```
 DRIFT : 0.219179D-08   +/-0.135722D-07

AMBIGUITY WRT REFERENCE SATELLITE :   11
AMBIGUITY   6 :                  -2337.29   +/-  22.84
AMBIGUITY   8 :                  -2012.61   +/-  22.53
AMBIGUITY  31 :                      3.62   +/-   1.18
AMBIGUITY   9 :                  -1876.28   +/-  17.03
AMBIGUITY  13 :                     68.88   +/-  27.00
AMBIGUITY  12 :                  -1291.39   +/-  21.01
AMBIGUITY   4 :                  -1149.81   +/- 184.38

FILE: HYHT89A.DB5
STATIONS:  HY HT

CLOCK PARAMETERS (RECEIVER 2 WRT RECEIVER 1)

OFFSET : -.557052D-02   +/-0.219590D-03
 DRIFT : 0.265542D-07   +/-0.195469D-07

AMBIGUITY WRT REFERENCE SATELLITE :   11
AMBIGUITY   6 :                  -1264.36   +/-  33.51
AMBIGUITY   8 :                  -1896.81   +/-  28.29
AMBIGUITY  31 :                     -2.92   +/-   1.53
AMBIGUITY   9 :                  -1240.26   +/-  29.77
AMBIGUITY  13 :                    632.60   +/-  38.45
AMBIGUITY  12 :                   -842.35   +/-  29.82
AMBIGUITY   4 :                    573.83   +/- 235.99

FILE: HYBP89A.DB5
STATIONS:  HY BP

CLOCK PARAMETERS (RECEIVER 2 WRT RECEIVER 1)

OFFSET : -.535425D-02   +/-0.209964D-03
 DRIFT : 0.131240D-07   +/-0.180034D-07

AMBIGUITY WRT REFERENCE SATELLITE :   11
AMBIGUITY   6 :                  -1471.04   +/-  32.66
AMBIGUITY   8 :                  -1800.43   +/-  28.57
AMBIGUITY  31 :                     -2.21   +/-   1.13
AMBIGUITY   9 :                  -1640.54   +/-  27.72
AMBIGUITY  13 :                    252.65   +/-  36.38
AMBIGUITY  12 :                  -1289.81   +/-  25.56
AMBIGUITY   4 :                   -299.56   +/- 167.88

FILE: HYMJ89A.DB5
STATIONS:  HY MJ

CLOCK PARAMETERS (RECEIVER 2 WRT RECEIVER 1)

OFFSET : -.585651D-02   +/-0.205572D-03
 DRIFT : 0.956297D-08   +/-0.174597D-07

AMBIGUITY WRT REFERENCE SATELLITE :   11
AMBIGUITY   6 :                  -1688.24   +/-  32.25
AMBIGUITY   8 :                  -1628.02   +/-  28.83
```

```
AMBIGUITY  31 :                    -1.11   +/-   1.14
AMBIGUITY   9 :                 -2004.20   +/-  26.79
AMBIGUITY  13 :                  -116.53   +/-  35.76
AMBIGUITY  12 :                 -1720.39   +/-  24.25
AMBIGUITY   4 :                 -1059.34   +/- 147.87

FILE: HYAR89A.DB5
STATIONS:  HY AR

CLOCK PARAMETERS (RECEIVER 2 WRT RECEIVER 1)

OFFSET : 0.118275D-02   +/-0.152248D-03
 DRIFT : 0.226351D-08   +/-0.119284D-07

AMBIGUITY WRT REFERENCE SATELLITE :   11
AMBIGUITY   6 :                 -3312.03   +/-  17.52
AMBIGUITY   8 :                  -807.93   +/-  18.58
AMBIGUITY  31 :                    -1.67   +/-   1.26
AMBIGUITY   9 :                 -3058.08   +/-  13.16
AMBIGUITY  13 :                 -2204.54   +/-  22.69
AMBIGUITY  12 :                 -3244.38   +/-  21.40
AMBIGUITY   4 :                -12963.70   +/- 210.45

FILE: HYNS89A.DB5
STATIONS:  HY NS

CLOCK PARAMETERS (RECEIVER 2 WRT RECEIVER 1)

OFFSET : -.577807D-02   +/-0.570053D-04
 DRIFT : -.167572D-07   +/-0.407786D-08

AMBIGUITY WRT REFERENCE SATELLITE :   11
AMBIGUITY   6 :                 -1284.30   +/-   3.29
AMBIGUITY   8 :                   207.12   +/-   4.08
AMBIGUITY  29 :                 12277.24   +/-   3.94
AMBIGUITY  31 :                 26695.84   +/-   1.13
AMBIGUITY  13 :                 12118.84   +/-   5.93
AMBIGUITY  12 :                 12126.47   +/-   9.22
AMBIGUITY   4 :                 10708.95   +/-  92.12
AMBIGUITY  51 :                 14907.28   +/-   1.45

FILE: HYMM89A.DB5
STATIONS:  HY MM

CLOCK PARAMETERS (RECEIVER 2 WRT RECEIVER 1)

OFFSET : -.529526D-02   +/-0.212437D-03
 DRIFT : 0.157995D-07   +/-0.182587D-07

AMBIGUITY WRT REFERENCE SATELLITE :   11
AMBIGUITY   6 :                  1211.03   +/-  32.95
AMBIGUITY   8 :                 -3413.78   +/-  28.70
AMBIGUITY  31 :                     0.84   +/-   1.16
AMBIGUITY   9 :                    47.24   +/-  28.15
AMBIGUITY  13 :                  2496.42   +/-  36.82
AMBIGUITY  12 :                  3668.27   +/-  26.19
```

AMBIGUITY 4 : 2809.75 +/- 176.65

ORBITAL SESSION: 2

ORBITAL PARAMETERS (improvement in kepl. elements)

SATELLITE ID.: 6				
A (m)	:	11.873	+/-	2.469
E	:	0.00000011	+/-	0.00000006
I (")	:	0.1175	+/-	0.0101
KN (")	:	0.1018	+/-	0.0174
PER (")	:	-4.6515	+/-	1.2555
T0 (sec)	:	-0.14520	+/-	0.04144
SATELLITE ID.: 8				
A (m)	:	6.995	+/-	1.709
E	:	0.00000023	+/-	0.00000005
I (")	:	-0.0357	+/-	0.0177
KN (")	:	0.3464	+/-	0.0119
PER (")	:	0.5329	+/-	1.8233
T0 (sec)	:	0.02558	+/-	0.05993
SATELLITE ID.: 9				
A (m)	:	5.889	+/-	1.287
E	:	-0.00000005	+/-	0.00000002
I (")	:	0.0582	+/-	0.0124
KN (")	:	-0.0006	+/-	0.0098
PER (")	:	2.3649	+/-	0.6014
T0 (sec)	:	0.08157	+/-	0.01929
SATELLITE ID.: 11				
A (m)	:	4.106	+/-	1.521
E	:	-0.00000007	+/-	0.00000004
I (")	:	0.0048	+/-	0.0142
KN (")	:	0.2602	+/-	0.0081
PER (")	:	1.7120	+/-	0.4393
T0 (sec)	:	0.05721	+/-	0.01664
SATELLITE ID.: 13				
A (m)	:	8.322	+/-	1.375
E	:	0.00000018	+/-	0.00000002
I (")	:	0.0805	+/-	0.0095
KN (")	:	0.1703	+/-	0.0116
PER (")	:	3.1563	+/-	1.2011
T0 (sec)	:	0.11184	+/-	0.03917
SATELLITE ID.: 12				
A (m)	:	4.843	+/-	2.015
E	:	-0.00000010	+/-	0.00000004
I (")	:	0.0871	+/-	0.0140
KN (")	:	0.0586	+/-	0.0141
PER (")	:	-1.3509	+/-	0.8665
T0 (sec)	:	-0.04221	+/-	0.03187

```
SATELLITE ID.:   4
   A    (m)      :                  19.372   +/-       1.681
   E             :              -0.00000197   +/-  0.00000002
   I    (")      :                  -0.0274   +/-      0.0119
   KN   (")      :                   0.1947   +/-      0.0172
   PER  (")      :                   6.3720   +/-      1.4192
   T0   (sec)    :                  0.23158   +/-     0.04629


TROPOSPHERIC SCALE FACTOR (1+k)
-------------------------------

 HY   0.0000  +/-  0.0192
 RC  -0.0025  +/-  0.0057
 FD  -0.0026  +/-  0.0053
 NS   0.0242  +/-  0.0052
 HT   0.0128  +/-  0.0049
 AR  -0.0080  +/-  0.0045
 BP  -0.0120  +/-  0.0046
 MM  -0.0041  +/-  0.0055
 MJ   0.0090  +/-  0.0048


CLOCK AND AMBIGUITY PARAMETERS
------------------------------

FILE: HTRC90A.DB5
STATIONS:  HT RC

CLOCK PARAMETERS (RECEIVER 2 WRT RECEIVER 1)

OFFSET : -.245313D-04   +/-0.202898D-03
 DRIFT : -.115345D-06   +/-0.179196D-07

AMBIGUITY WRT REFERENCE SATELLITE :   11
AMBIGUITY   6 :                  -3877.63   +/-  61.72
AMBIGUITY   8 :                   1051.85   +/-  33.69
AMBIGUITY   9 :                  -1638.32   +/-  36.72
AMBIGUITY  13 :                  -2242.37   +/-  27.55
AMBIGUITY  12 :                  -2638.95   +/-  39.29

FILE: HTFD90A.DB5
STATIONS:  HT FD

CLOCK PARAMETERS (RECEIVER 2 WRT RECEIVER 1)

OFFSET : 0.587296D-03   +/-0.144065D-03
 DRIFT : -.653972D-07   +/-0.857559D-08

AMBIGUITY WRT REFERENCE SATELLITE :   11
AMBIGUITY   6 :                   -841.52   +/-  21.95
AMBIGUITY   8 :                    800.44   +/-  11.21
AMBIGUITY  31 :                    765.95   +/-   4.47
AMBIGUITY   9 :                  -1208.13   +/-  13.94
AMBIGUITY  13 :                  -1216.50   +/-  12.21
AMBIGUITY  12 :                  -1638.43   +/-  18.39
```

```
AMBIGUITY   4 :                  -1042.03   +/-  22.92
AMBIGUITY  33 :                  -5513.88   +/-  12.12
AMBIGUITY  24 :                  -2247.46   +/-  22.94

FILE: HTBP90A.DB5
STATIONS:  HT BP

CLOCK PARAMETERS (RECEIVER 2 WRT RECEIVER 1)

OFFSET : 0.219040D-03   +/-0.427214D-04
 DRIFT : -.205202D-07   +/-0.285988D-08

AMBIGUITY WRT REFERENCE SATELLITE :   11
AMBIGUITY   6 :                   -385.18   +/-   3.69
AMBIGUITY   8 :                    155.48   +/-   3.29
AMBIGUITY  31 :                    308.47   +/-   1.60
AMBIGUITY   9 :                   -627.68   +/-   2.41
AMBIGUITY  13 :                   -612.75   +/-   4.16
AMBIGUITY  12 :                   -740.05   +/-   5.09
AMBIGUITY   4 :                   -725.90   +/-   7.27

FILE: HTMJ90A.DB5
STATIONS:  HT MJ

CLOCK PARAMETERS (RECEIVER 2 WRT RECEIVER 1)

OFFSET : 0.306489D-03   +/-0.615076D-04
 DRIFT : -.215673D-07   +/-0.399047D-08

AMBIGUITY WRT REFERENCE SATELLITE :   11
AMBIGUITY   6 :                   -747.48   +/-   5.35
AMBIGUITY   8 :                    351.59   +/-   4.59
AMBIGUITY  31 :                    346.60   +/-   2.22
AMBIGUITY   9 :                  -1189.15   +/-   3.48
AMBIGUITY  29 :                  -7865.17   +/-   4.60
AMBIGUITY  28 :                   7605.39   +/-   4.73
AMBIGUITY  49 :                  13307.73   +/-   3.70
AMBIGUITY  13 :                  -7958.56   +/-   5.65
AMBIGUITY  12 :                  -8502.89   +/-   7.16
AMBIGUITY   4 :                  -8278.27   +/-   9.96

FILE: HTAR90A.DB5
STATIONS:  HT AR

CLOCK PARAMETERS (RECEIVER 2 WRT RECEIVER 1)

OFFSET : 0.726372D-02   +/-0.183571D-03
 DRIFT : -.917890D-07   +/-0.102102D-07

AMBIGUITY WRT REFERENCE SATELLITE :   11
AMBIGUITY   6 :                  -2999.52   +/-  31.55
AMBIGUITY   8 :                   1413.16   +/-  15.85
AMBIGUITY  31 :                    717.98   +/-   5.78
AMBIGUITY   9 :                  -1486.22   +/-  19.59
AMBIGUITY  13 :                  -2655.50   +/-  15.50
AMBIGUITY  12 :                  -2035.61   +/-  23.30
```

```
AMBIGUITY   4 :                  -2984.99   +/-  28.50

FILE: HTNS90A.DB5
STATIONS:  HT NS

CLOCK PARAMETERS (RECEIVER 2 WRT RECEIVER 1)

OFFSET : 0.930851D-03   +/-0.259706D-03
 DRIFT : -.179247D-06   +/-0.159991D-07

AMBIGUITY WRT REFERENCE SATELLITE :    9
AMBIGUITY   6 :                    1222.27   +/-  52.19
AMBIGUITY   8 :                    2560.48   +/-  47.75
AMBIGUITY  11 :                     -99.09   +/-  33.13
AMBIGUITY  13 :                   -2170.86   +/-  31.73
AMBIGUITY  33 :                   -2176.92   +/-  31.68
AMBIGUITY  12 :                  -14934.22   +/-  34.67
AMBIGUITY   4 :                   -1512.47   +/-  49.03

FILE: HTMM90A.DB5
STATIONS:  HT MM

CLOCK PARAMETERS (RECEIVER 2 WRT RECEIVER 1)

OFFSET : 0.179417D-03   +/-0.371073D-04
 DRIFT : -.108745D-07   +/-0.241740D-08

AMBIGUITY WRT REFERENCE SATELLITE :   11
AMBIGUITY   6 :                    3281.17   +/-   3.14
AMBIGUITY   8 :                    -668.33   +/-   3.01
AMBIGUITY  31 :                    1561.57   +/-   1.51
AMBIGUITY   9 :                    4651.39   +/-   2.08
AMBIGUITY  13 :                    5270.16   +/-   3.74
AMBIGUITY  12 :                    8455.02   +/-   4.45
AMBIGUITY   4 :                    5964.93   +/-   6.39
AMBIGUITY  33 :                   11170.32   +/-   3.75
AMBIGUITY  24 :                   11866.53   +/-   6.39

ORBITAL SESSION:   3


ORBITAL PARAMETERS (improvement in kepl. elements)
--------------------------------------------------

SATELLITE ID.:   6
   A   (m)      :                    18.404   +/-       2.063
   E            :                0.00000016   +/-  0.00000005
   I   (")      :                    0.0715   +/-       0.0076
   KN  (")      :                   -0.0568   +/-       0.0118
   PER (")      :                    3.6325   +/-       1.0161
   T0  (sec)    :                   0.12066   +/-     0.03346

SATELLITE ID.:   8
   A   (m)      :                     9.267   +/-       1.439
   E            :                0.00000001   +/-  0.00000002
   I   (")      :                    0.0565   +/-       0.0155
```

```
   KN  (")       :                  0.3224   +/-      0.0092
   PER (")       :                 -0.6939   +/-      1.5492
   T0  (sec)     :                -0.02494   +/-     0.05090

SATELLITE ID.:  11
   A   (m)       :                  7.834   +/-       0.967
   E             :             0.00000000   +/-  0.00000002
   I   (")       :                 0.0755   +/-      0.0129
   KN  (")       :                 0.1347   +/-      0.0101
   PER (")       :                 1.3308   +/-      0.4083
   T0  (sec)     :                0.03294   +/-     0.01475

SATELLITE ID.:   9
   A   (m)       :                  3.482   +/-       2.051
   E             :            -0.00000014   +/-  0.00000002
   I   (")       :                -0.0152   +/-      0.0110
   KN  (")       :                -0.0877   +/-      0.0071
   PER (")       :                 0.8531   +/-      0.9919
   T0  (sec)     :                0.02919   +/-     0.03178

SATELLITE ID.:  13
   A   (m)       :                 -2.693   +/-       1.485
   E             :             0.00000002   +/-  0.00000001
   I   (")       :                 0.0938   +/-      0.0106
   KN  (")       :                 0.0933   +/-      0.0125
   PER (")       :                -7.3117   +/-      1.2583
   T0  (sec)     :                -0.23901   +/-     0.04099

SATELLITE ID.:   4
   A   (m)       :                 11.047   +/-       1.591
   E             :            -0.00000200   +/-  0.00000002
   I   (")       :                -0.0212   +/-      0.0143
   KN  (")       :                 0.0458   +/-      0.0151
   PER (")       :                11.8381   +/-      1.2209
   T0  (sec)     :                0.40249   +/-     0.03981

SATELLITE ID.:  12
   A   (m)       :                -16.585   +/-       4.847
   E             :             0.00000074   +/-  0.00000013
   I   (")       :                 0.0603   +/-      0.0120
   KN  (")       :                 0.0621   +/-      0.0119
   PER (")       :               -10.6326   +/-      1.3378
   T0  (sec)     :                -0.33840   +/-     0.04921


TROPOSPHERIC SCALE FACTOR (1+k)
-------------------------------

 HY  -0.0256  +/-  0.0035
 RC  -0.0194  +/-  0.0050
 FD   0.0088  +/-  0.0045
 NS  -0.0671  +/-  0.0038
 HT   0.0027  +/-  0.0065
 AR  -0.0082  +/-  0.0036
 BP   0.0130  +/-  0.0056
 MM   0.0261  +/-  0.0066
```

```
 MJ   0.0173  +/-  0.0051


CLOCK AND AMBIGUITY PARAMETERS
------------------------------

FILE: HYRC91A.DB5
STATIONS:  HY RC

CLOCK PARAMETERS (RECEIVER 2 WRT RECEIVER 1)

OFFSET : -.635029D-02   +/-0.134786D-03
 DRIFT : 0.633423D-07   +/-0.809313D-08

AMBIGUITY WRT REFERENCE SATELLITE :   11
AMBIGUITY   6 :                  -3108.08   +/-   5.77
AMBIGUITY   8 :                   -611.40   +/-  10.21
AMBIGUITY  31 :                     15.95   +/-   2.42
AMBIGUITY   9 :                  -3348.25   +/-  12.07
AMBIGUITY  13 :                  -1891.85   +/-  12.95
AMBIGUITY   4 :                  -2635.39   +/-  19.18
AMBIGUITY  51 :                  -1264.79   +/-   3.77

FILE: HYFD91A.DB5
STATIONS:  HY FD

CLOCK PARAMETERS (RECEIVER 2 WRT RECEIVER 1)

OFFSET : -.631926D-02   +/-0.161667D-03
 DRIFT : 0.115286D-06   +/-0.123238D-07

AMBIGUITY WRT REFERENCE SATELLITE :   11
AMBIGUITY   6 :                  -1475.50   +/-  21.30
AMBIGUITY   8 :                  -1322.16   +/-  19.44
AMBIGUITY  31 :                      5.28   +/-   1.16
AMBIGUITY   9 :                  -2572.40   +/-  17.45
AMBIGUITY  13 :                   -722.79   +/-  23.68
AMBIGUITY  12 :                  -2503.00   +/-  20.40
AMBIGUITY   4 :                  -2043.08   +/-  38.20

FILE: HYHT91A.DB5
STATIONS:  HY HT

CLOCK PARAMETERS (RECEIVER 2 WRT RECEIVER 1)

OFFSET : -.590685D-02   +/-0.211857D-03
 DRIFT : 0.145677D-06   +/-0.168146D-07

AMBIGUITY WRT REFERENCE SATELLITE :   11
AMBIGUITY   6 :                   -532.46   +/-  31.45
AMBIGUITY   8 :                  -1870.46   +/-  24.62
AMBIGUITY  31 :                     -4.54   +/-   1.48
AMBIGUITY   9 :                  -1310.97   +/-  32.32
AMBIGUITY  13 :                    458.81   +/-  41.60
AMBIGUITY  12 :                  -1179.78   +/-  30.27
AMBIGUITY   4 :                   -858.65   +/-  53.68
```

```
AMBIGUITY  33 :                    5977.72   +/-  41.75
AMBIGUITY  24 :                    4659.87   +/-  54.06

FILE: HYBP91A.DB5
STATIONS:  HY BP

CLOCK PARAMETERS (RECEIVER 2 WRT RECEIVER 1)

OFFSET : -.582993D-02   +/-0.198389D-03
 DRIFT : 0.128240D-06   +/-0.157882D-07

AMBIGUITY WRT REFERENCE SATELLITE :   11
AMBIGUITY   6 :                     343.81   +/-  30.64
AMBIGUITY   8 :                    -464.93   +/-  24.76
AMBIGUITY  31 :                    1335.15   +/-   1.12
AMBIGUITY   9 :                    -402.86   +/-  29.68
AMBIGUITY  13 :                    1362.00   +/-  37.74
AMBIGUITY  12 :                    -208.90   +/-  26.50
AMBIGUITY   4 :                    -136.23   +/-  51.45

FILE: HYMJ91A.DB5
STATIONS:  HY MJ

CLOCK PARAMETERS (RECEIVER 2 WRT RECEIVER 1)

OFFSET : -.602011D-02   +/-0.194666D-03
 DRIFT : 0.137167D-06   +/-0.154224D-07

AMBIGUITY WRT REFERENCE SATELLITE :   11
AMBIGUITY   6 :                   -1225.60   +/-  30.23
AMBIGUITY   8 :                   -1592.25   +/-  24.93
AMBIGUITY  31 :                       3.62   +/-   1.14
AMBIGUITY   9 :                   -2099.71   +/-  28.44
AMBIGUITY  13 :                    -314.17   +/-  36.12
AMBIGUITY  12 :                   -1987.84   +/-  25.21
AMBIGUITY   4 :                   -1981.20   +/-  50.79

FILE: HYAR91A.DB5
STATIONS:  HY AR

CLOCK PARAMETERS (RECEIVER 2 WRT RECEIVER 1)

OFFSET : 0.161716D-04   +/-0.148510D-03
 DRIFT : 0.101099D-06   +/-0.109349D-07

AMBIGUITY WRT REFERENCE SATELLITE :   11
AMBIGUITY   6 :                   -2965.29   +/-  16.38
AMBIGUITY   8 :                    -743.96   +/-  16.12
AMBIGUITY  31 :                       3.39   +/-   1.24
AMBIGUITY   9 :                   -3151.67   +/-  13.19
AMBIGUITY  13 :                   -2360.22   +/-  18.51
AMBIGUITY  12 :                   -3356.72   +/-  19.78
AMBIGUITY   4 :                   -4282.16   +/-  31.34

FILE: HYNS91A.DB5
STATIONS:  HY NS
```

```
CLOCK PARAMETERS (RECEIVER 2 WRT RECEIVER 1)

OFFSET : -.580452D-02   +/-0.568023D-04
 DRIFT : 0.582842D-08   +/-0.365354D-08

AMBIGUITY WRT REFERENCE SATELLITE :   11
AMBIGUITY   6 :                  -1051.53   +/-   3.00
AMBIGUITY   8 :                    285.71   +/-   3.58
AMBIGUITY  29 :                  12165.15   +/-   3.60
AMBIGUITY  31 :                  29596.88   +/-   1.18
AMBIGUITY  13 :                  12008.06   +/-   4.06
AMBIGUITY  12 :                  12363.09   +/-   7.87
AMBIGUITY   4 :                  10877.45   +/-   7.00
AMBIGUITY  51 :                  14818.60   +/-   1.38

FILE: HYMM91A.DB5
STATIONS:  HY MM

CLOCK PARAMETERS (RECEIVER 2 WRT RECEIVER 1)

OFFSET : -.589867D-02   +/-0.200758D-03
 DRIFT : 0.142109D-06   +/-0.159876D-07

AMBIGUITY WRT REFERENCE SATELLITE :   11
AMBIGUITY   6 :                   1794.48   +/-  30.92
AMBIGUITY   8 :                  -3316.70   +/-  24.88
AMBIGUITY  31 :                     -2.39   +/-   1.15
AMBIGUITY   9 :                     37.16   +/-  30.20
AMBIGUITY  13 :                   2327.89   +/-  38.42
AMBIGUITY  12 :                   3450.27   +/-  27.07
AMBIGUITY   4 :                   1645.11   +/-  52.01

ORBITAL SESSION:   4


ORBITAL PARAMETERS (improvement in kepl. elements)
--------------------------------------------------

SATELLITE ID.:   6
   A    (m)      :                    1.135   +/-       1.926
   E             :               -0.00000025   +/-  0.00000005
   I    (")      :                    0.0562   +/-       0.0069
   KN   (")      :                   -0.0320   +/-       0.0100
   PER  (")      :                   -1.6192   +/-       0.9948
   T0   (sec)    :                  -0.05292   +/-      0.03276

SATELLITE ID.:   8
   A    (m)      :                    1.119   +/-       1.263
   E             :               -0.00000021   +/-  0.00000002
   I    (")      :                   -0.0837   +/-       0.0137
   KN   (")      :                    0.2268   +/-       0.0088
   PER  (")      :                   -6.6546   +/-       1.4741
   T0   (sec)    :                  -0.22087   +/-      0.04845

SATELLITE ID.:  11
```

A	(m)	:	-3.137	+/-	0.802
E		:	0.00000010	+/-	0.00000002
I	(")	:	-0.0273	+/-	0.0116
KN	(")	:	0.0996	+/-	0.0088
PER	(")	:	4.6492	+/-	0.3686
T0	(sec)	:	0.16043	+/-	0.01329

SATELLITE ID.: 9

A	(m)	:	7.897	+/-	1.881
E		:	-0.00000008	+/-	0.00000002
I	(")	:	-0.0033	+/-	0.0097
KN	(")	:	-0.0651	+/-	0.0069
PER	(")	:	4.6605	+/-	0.8909
T0	(sec)	:	0.15307	+/-	0.02853

SATELLITE ID.: 13

A	(m)	:	-2.332	+/-	1.404
E		:	0.00000003	+/-	0.00000001
I	(")	:	-0.0079	+/-	0.0100
KN	(")	:	0.0725	+/-	0.0113
PER	(")	:	-6.2048	+/-	1.2026
T0	(sec)	:	-0.20291	+/-	0.03915

SATELLITE ID.: 12

A	(m)	:	0.434	+/-	4.392
E		:	0.00000005	+/-	0.00000012
I	(")	:	0.0430	+/-	0.0101
KN	(")	:	0.0210	+/-	0.0105
PER	(")	:	-4.9851	+/-	1.1709
T0	(sec)	:	-0.16466	+/-	0.04348

SATELLITE ID.: 4

A	(m)	:	5.675	+/-	1.473
E		:	-0.00000199	+/-	0.00000002
I	(")	:	-0.1010	+/-	0.0136
KN	(")	:	0.0023	+/-	0.0129
PER	(")	:	7.0664	+/-	1.1257
T0	(sec)	:	0.23540	+/-	0.03664

TROPOSPHERIC SCALE FACTOR (1+k)

HY	-0.0275	+/-	0.0032
RC	-0.0053	+/-	0.0045
FD	0.0116	+/-	0.0042
NS	-0.0557	+/-	0.0034
HT	0.0077	+/-	0.0062
AR	-0.0011	+/-	0.0034
BP	-0.0176	+/-	0.0053
MM	0.0026	+/-	0.0063
MJ	0.0081	+/-	0.0048

CLOCK AND AMBIGUITY PARAMETERS

```
FILE: HYRC94A.DB5
STATIONS:  HY RC

CLOCK PARAMETERS (RECEIVER 2 WRT RECEIVER 1)

OFFSET : 0.637027D-03   +/-0.125880D-03
 DRIFT : 0.975318D-08   +/-0.731200D-08

AMBIGUITY WRT REFERENCE SATELLITE :   11
AMBIGUITY   6 :                -1783.24   +/-   5.16
AMBIGUITY   8 :                  -40.93   +/-   9.36
AMBIGUITY  31 :                 1123.64   +/-   2.27
AMBIGUITY   9 :                -1547.42   +/-  10.26
AMBIGUITY  13 :                 -349.57   +/-  11.36
AMBIGUITY  12 :                -1734.96   +/-  22.10
AMBIGUITY   4 :                -1190.27   +/-  17.93
AMBIGUITY  51 :                  -54.12   +/-   1.25

FILE: HYFD94A.DB5
STATIONS:  HY FD

CLOCK PARAMETERS (RECEIVER 2 WRT RECEIVER 1)

OFFSET : -.581904D-02   +/-0.148425D-03
 DRIFT : 0.282533D-07   +/-0.109725D-07

AMBIGUITY WRT REFERENCE SATELLITE :   11
AMBIGUITY   6 :                 -429.72   +/-  20.61
AMBIGUITY   8 :                 -121.95   +/-  18.15
AMBIGUITY  31 :                 1355.63   +/-   1.12
AMBIGUITY   9 :                -1181.15   +/-  14.78
AMBIGUITY  13 :                  696.24   +/-  17.70
AMBIGUITY  12 :                -1300.84   +/-  16.48
AMBIGUITY   4 :                 -897.43   +/-  30.72

FILE: HYHT94A.DB5
STATIONS:  HY HT

CLOCK PARAMETERS (RECEIVER 2 WRT RECEIVER 1)

OFFSET : -.794201D-02   +/-0.185324D-03
 DRIFT : 0.681953D-07   +/-0.143205D-07

AMBIGUITY WRT REFERENCE SATELLITE :   11
AMBIGUITY   6 :                   21.74   +/-  30.08
AMBIGUITY   8 :                -1000.16   +/-  22.86
AMBIGUITY  31 :                 1016.31   +/-   1.44
AMBIGUITY   9 :                 -330.55   +/-  24.91
AMBIGUITY  13 :                 1413.45   +/-  29.02
AMBIGUITY  12 :                 -266.29   +/-  25.07
AMBIGUITY   4 :                   39.53   +/-  39.69

FILE: HYBP94A.DB5
STATIONS:  HY BP
```

```
CLOCK PARAMETERS (RECEIVER 2 WRT RECEIVER 1)

OFFSET : -.444740D-02   +/-0.176722D-03
 DRIFT : 0.420327D-07   +/-0.135610D-07

AMBIGUITY WRT REFERENCE SATELLITE :   11
AMBIGUITY   6 :                    -125.85   +/-  29.43
AMBIGUITY   8 :                    -733.17   +/-  23.02
AMBIGUITY  31 :                    1248.10   +/-   1.10
AMBIGUITY   9 :                    -555.88   +/-  23.34
AMBIGUITY  13 :                    1222.29   +/-  26.31
AMBIGUITY  12 :                    -463.64   +/-  21.34
AMBIGUITY   4 :                    -449.77   +/-  38.37

FILE: HYMJ94A.DB5
STATIONS:  HY MJ

CLOCK PARAMETERS (RECEIVER 2 WRT RECEIVER 1)

OFFSET : -.674451D-02   +/-0.173981D-03
 DRIFT : 0.475028D-07   +/-0.133088D-07

AMBIGUITY WRT REFERENCE SATELLITE :   11
AMBIGUITY   6 :                    -263.77   +/-  29.09
AMBIGUITY   8 :                    -407.52   +/-  23.17
AMBIGUITY  31 :                    1379.73   +/-   1.11
AMBIGUITY   9 :                    -789.32   +/-  22.66
AMBIGUITY  13 :                     904.71   +/-  25.32
AMBIGUITY  12 :                    -902.87   +/-  20.07
AMBIGUITY   4 :                    -853.40   +/-  38.25

FILE: HYAR94A.DB5
STATIONS:  HY AR

CLOCK PARAMETERS (RECEIVER 2 WRT RECEIVER 1)

OFFSET : -.575594D-02   +/-0.137081D-03
 DRIFT : 0.216711D-07   +/-0.981766D-08

AMBIGUITY WRT REFERENCE SATELLITE :   11
AMBIGUITY   6 :                   -1233.62   +/-  15.85
AMBIGUITY   8 :                    1364.90   +/-  15.10
AMBIGUITY  31 :                    1639.27   +/-   1.19
AMBIGUITY   9 :                   -2066.45   +/-  11.64
AMBIGUITY  13 :                   -1200.68   +/-  14.60
AMBIGUITY  12 :                   -2900.43   +/-  16.62
AMBIGUITY   4 :                   -3448.62   +/-  26.08

FILE: HYNS94A.DB5
STATIONS:  HY NS

CLOCK PARAMETERS (RECEIVER 2 WRT RECEIVER 1)

OFFSET : -.628516D-02   +/-0.525339D-04
 DRIFT : 0.525159D-08   +/-0.337025D-08
```

```
AMBIGUITY WRT REFERENCE SATELLITE :   11
AMBIGUITY   6 :                    774.02   +/-   3.19
AMBIGUITY   8 :                   2111.39   +/-   3.83
AMBIGUITY  31 :                   1834.36   +/-   1.09
AMBIGUITY   9 :                   -361.99   +/-   3.44
AMBIGUITY  13 :                   -565.21   +/-   3.84
AMBIGUITY  12 :                   -479.60   +/-   6.83
AMBIGUITY   4 :                  -1673.56   +/-   6.60
AMBIGUITY  51 :                   2214.86   +/-   0.89

FILE: HYMM94A.DB5
STATIONS:  HY MM

CLOCK PARAMETERS (RECEIVER 2 WRT RECEIVER 1)

OFFSET : -.617353D-02   +/-0.178544D-03
 DRIFT : 0.552196D-07   +/-0.137103D-07

AMBIGUITY WRT REFERENCE SATELLITE :   11
AMBIGUITY   6 :                   4966.67   +/-  29.68
AMBIGUITY   8 :                     72.83   +/-  23.13
AMBIGUITY  31 :                   3569.66   +/-   1.13
AMBIGUITY   9 :                   3519.00   +/-  23.68
AMBIGUITY  13 :                   5853.90   +/-  26.77
AMBIGUITY  12 :                   6806.72   +/-  21.89
AMBIGUITY   4 :                   5074.54   +/-  38.70



REFERENCE ELLIPSOID
AE =  6378135.0, F-1 =   298.2600, XE =     0.000, YE =     0.000, ZE =     0.000

A POSTERIORI VARIANCE FACTOR :     3.6692

CROSS-CORRELATION BETWEEN STATIONS
ALL |CROSS-CORRELATION VALUES| SMALLER THAN  0.90



BASELINE:      STATION : HY AND STATION : RC
==============================================

STATION NAME : HY
-----------------

A-PRIORI ELLIPSOIDAL COORDINATES
LATITUDE  :    42 37 21.84550
LONGITUDE :  - 71 29 18.02122
HEIGHT    :    93.8914

A POSTERIORI ELLIPSOIDAL COORDINATES
LATITUDE  :    42 37 21.84550        +/-         0 MM
LONGITUDE :  - 71 29 18.02122        +/-         0 MM
HEIGHT    :    93.8914               +/-         0 MM

CROSS-CORRELATION BETWEEN COORDINATES
```

```
ALL |CROSS-CORRELATION VALUES| SMALLER THAN  0.90

A POSTERIORI CARTESIAN   COORDINATES
X :      1492398.4454 M   +/-         0 MM
Y :     -4457293.8953 M   +/-         0 MM
Z :      4296819.2655 M   +/-         0 MM

CROSS-CORRELATION BETWEEN COORDINATES
ALL |CROSS-CORRELATION VALUES| SMALLER THAN  0.90

STATION NAME : RC
-----------------

A-PRIORI ELLIPSOIDAL COORDINATES
LATITUDE  :    25 36 50.75301
LONGITUDE :  - 80 23  3.17181
HEIGHT    :   -21.1879

A POSTERIORI ELLIPSOIDAL COORDINATES
LATITUDE  :    25 36 50.75301        +/-         0 MM
LONGITUDE :  - 80 23  3.17181        +/-         0 MM
HEIGHT    :   -21.1879               +/-         0 MM

CROSS-CORRELATION BETWEEN COORDINATES
ALL |CROSS-CORRELATION VALUES| SMALLER THAN  0.90

A POSTERIORI CARTESIAN   COORDINATES
X :       961302.9852 M   +/-         0 MM
Y :     -5674057.1094 M   +/-         0 MM
Z :      2740563.8693 M   +/-         0 MM

CROSS-CORRELATION BETWEEN COORDINATES
ALL |CROSS-CORRELATION VALUES| SMALLER THAN  0.90


BASELINE :   HY  RC
-------------------

A-PRIORI     ELLIPSOID BASELINE COMPONENTS
DELTA  LATITUDE :  - 17  0 31.09250
DELTA LONGITUDE :  -  8 53 45.15059
DELTA    HEIGHT :  -115.0793

A POSTERIORI ELLIPSOID BASELINE COMPONENTS
DELTA  LATITUDE :  - 17  0 31.09250        +/-         0 MM
DELTA LONGITUDE :  -  8 53 45.15059        +/-         0 MM
DELTA    HEIGHT :  -115.0793               +/-         0 MM

CROSS-CORRELATION BETWEEN BASELINE COMPONENTS
ALL |CROSS-CORRELATION VALUES| SMALLER THAN  0.90

A POSTERIORI CARTESIAN BASELINE COMPONENTS
DELTA X :      -531095.4602 M  +/-         0 MM
DELTA Y :     -1216763.2141 M  +/-         0 MM
DELTA Z :     -1556255.3962 M  +/-         0 MM
```

```
CROSS-CORRELATION BETWEEN BASELINE COMPONENTS
ALL |CROSS-CORRELATION VALUES| SMALLER THAN  0.90

BASELINE LENGTH  : 2045606.5030 M +/-         0 MM

AZIMUTH HY TO RC : -153 50 46.214 +/-     0.000 SEC
AZIMUTH RC TO HY :   21  6  6.230 +/-     0.000 SEC


BASELINE:      STATION : HY AND STATION : FD
==========================================

STATION NAME : HY
-----------------

A-PRIORI ELLIPSOIDAL COORDINATES
LATITUDE  :    42 37 21.84550
LONGITUDE :  - 71 29 18.02122
HEIGHT    :    93.8914

A POSTERIORI ELLIPSOIDAL COORDINATES
LATITUDE  :    42 37 21.84550        +/-         0 MM
LONGITUDE :  - 71 29 18.02122        +/-         0 MM
HEIGHT    :    93.8914               +/-         0 MM

CROSS-CORRELATION BETWEEN COORDINATES
ALL |CROSS-CORRELATION VALUES| SMALLER THAN  0.90

A POSTERIORI CARTESIAN   COORDINATES
X :      1492398.4454 M   +/-         0 MM
Y :     -4457293.8953 M   +/-         0 MM
Z :      4296819.2655 M   +/-         0 MM

CROSS-CORRELATION BETWEEN COORDINATES
ALL |CROSS-CORRELATION VALUES| SMALLER THAN  0.90

STATION NAME : FD
-----------------

A-PRIORI ELLIPSOIDAL COORDINATES
LATITUDE  :    30 38  9.60561
LONGITUDE :  -103 56 49.65601
HEIGHT    :  1585.3693

A POSTERIORI ELLIPSOIDAL COORDINATES
LATITUDE  :    30 38  9.60561        +/-         0 MM
LONGITUDE :  -103 56 49.65601        +/-         0 MM
HEIGHT    :  1585.3693               +/-         0 MM

CROSS-CORRELATION BETWEEN COORDINATES
ALL |CROSS-CORRELATION VALUES| SMALLER THAN  0.90

A POSTERIORI CARTESIAN   COORDINATES
X :     -1324205.7179 M   +/-         0 MM
Y :     -5332056.0713 M   +/-         0 MM
```

```
Z :      3232043.6300 M   +/-         0 MM

CROSS-CORRELATION BETWEEN COORDINATES
ALL |CROSS-CORRELATION VALUES| SMALLER THAN  0.90


BASELINE :   HY  FD
-------------------

A-PRIORI     ELLIPSOID BASELINE COMPONENTS
DELTA  LATITUDE :  - 11 59 12.23990
DELTA LONGITUDE :  - 32 27 31.63479
DELTA    HEIGHT :  1491.4779

A POSTERIORI ELLIPSOID BASELINE COMPONENTS
DELTA  LATITUDE :  - 11 59 12.23990        +/-         0 MM
DELTA LONGITUDE :  - 32 27 31.63479        +/-         0 MM
DELTA    HEIGHT :  1491.4779               +/-         0 MM

CROSS-CORRELATION BETWEEN BASELINE COMPONENTS
ALL |CROSS-CORRELATION VALUES| SMALLER THAN  0.90

A POSTERIORI CARTESIAN BASELINE COMPONENTS
DELTA X :     -2816604.1633 M  +/-         0 MM
DELTA Y :      -874762.1760 M  +/-         0 MM
DELTA Z :     -1064775.6355 M  +/-         0 MM

CROSS-CORRELATION BETWEEN BASELINE COMPONENTS
ALL |CROSS-CORRELATION VALUES| SMALLER THAN  0.90

BASELINE LENGTH  : 3135636.3040 M +/-         0 MM

AZIMUTH HY TO FD : -104  4 54.034 +/-     0.000 SEC
AZIMUTH FD TO HY :   56  6 27.069 +/-     0.000 SEC



BASELINE:      STATION : HY AND STATION : NS
============================================

STATION NAME : HY
-----------------

A-PRIORI ELLIPSOIDAL COORDINATES
LATITUDE  :    42 37 21.84550
LONGITUDE :  - 71 29 18.02122
HEIGHT    :    93.8914

A POSTERIORI ELLIPSOIDAL COORDINATES
LATITUDE  :    42 37 21.84550        +/-         0 MM
LONGITUDE :  - 71 29 18.02122        +/-         0 MM
HEIGHT    :    93.8914               +/-         0 MM

CROSS-CORRELATION BETWEEN COORDINATES
ALL |CROSS-CORRELATION VALUES| SMALLER THAN  0.90
```

```
A POSTERIORI CARTESIAN   COORDINATES
X :      1492398.4454 M   +/-         0 MM
Y :     -4457293.8953 M   +/-         0 MM
Z :      4296819.2655 M   +/-         0 MM

CROSS-CORRELATION BETWEEN COORDINATES
ALL |CROSS-CORRELATION VALUES| SMALLER THAN  0.90

STATION NAME : NS
-----------------

A-PRIORI ELLIPSOIDAL COORDINATES
LATITUDE  :    38 19 55.47490
LONGITUDE :  - 77  2 32.50317
HEIGHT    :   -18.4557

A POSTERIORI ELLIPSOIDAL COORDINATES
LATITUDE  :    38 19 55.47388        +/-         5 MM
LONGITUDE :  - 77  2 32.49886        +/-         9 MM
HEIGHT    :   -18.2342               +/-        17 MM

CROSS-CORRELATION BETWEEN COORDINATES
ALL |CROSS-CORRELATION VALUES| SMALLER THAN  0.90

A POSTERIORI CARTESIAN   COORDINATES
X :      1123313.6887 M   +/-        10 MM
Y :     -4882071.0587 M   +/-        12 MM
Z :      3934412.0257 M   +/-        13 MM

CROSS-CORRELATION BETWEEN COORDINATES
ALL |CROSS-CORRELATION VALUES| SMALLER THAN  0.90


BASELINE :   HY  NS
-------------------

A-PRIORI     ELLIPSOID BASELINE COMPONENTS
DELTA  LATITUDE :  -  4 17 26.37060
DELTA LONGITUDE :  -  5 33 14.48194
DELTA    HEIGHT :  -112.3471

A POSTERIORI ELLIPSOID BASELINE COMPONENTS
DELTA  LATITUDE :  -  4 17 26.37163        +/-         5 MM
DELTA LONGITUDE :  -  5 33 14.47763        +/-         9 MM
DELTA    HEIGHT :  -112.1256               +/-        17 MM

CROSS-CORRELATION BETWEEN BASELINE COMPONENTS
ALL |CROSS-CORRELATION VALUES| SMALLER THAN  0.90

A POSTERIORI CARTESIAN BASELINE COMPONENTS
DELTA X :      -369084.7567 M  +/-        10 MM
DELTA Y :      -424777.1634 M  +/-        12 MM
DELTA Z :      -362407.2398 M  +/-        13 MM

CROSS-CORRELATION BETWEEN BASELINE COMPONENTS
ALL |CROSS-CORRELATION VALUES| SMALLER THAN  0.90
```

```
BASELINE LENGTH  :  669326.6793 M +/-         5 MM

AZIMUTH HY TO NS : -133 29 53.300 +/-     0.003 SEC
AZIMUTH NS TO HY :   42 53 32.331 +/-     0.003 SEC


BASELINE:      STATION : HY AND STATION : HT
==========================================

STATION NAME : HY
-----------------

A-PRIORI ELLIPSOIDAL COORDINATES
LATITUDE  :    42 37 21.84550
LONGITUDE :  - 71 29 18.02122
HEIGHT    :    93.8914

A POSTERIORI ELLIPSOIDAL COORDINATES
LATITUDE  :    42 37 21.84550        +/-         0 MM
LONGITUDE :  - 71 29 18.02122        +/-         0 MM
HEIGHT    :    93.8914               +/-         0 MM

CROSS-CORRELATION BETWEEN COORDINATES
ALL |CROSS-CORRELATION VALUES| SMALLER THAN  0.90

A POSTERIORI CARTESIAN   COORDINATES
X :      1492398.4454 M   +/-         0 MM
Y :     -4457293.8953 M   +/-         0 MM
Z :      4296819.2655 M   +/-         0 MM

CROSS-CORRELATION BETWEEN COORDINATES
ALL |CROSS-CORRELATION VALUES| SMALLER THAN  0.90

STATION NAME : HT
-----------------

A-PRIORI ELLIPSOIDAL COORDINATES
LATITUDE  :    40 49  1.36259
LONGITUDE :  -121 28  9.18879
HEIGHT    :   997.9798

A POSTERIORI ELLIPSOIDAL COORDINATES
LATITUDE  :    40 49  1.36259        +/-         0 MM
LONGITUDE :  -121 28  9.18879        +/-         0 MM
HEIGHT    :   997.9798               +/-         0 MM

CROSS-CORRELATION BETWEEN COORDINATES
ALL |CROSS-CORRELATION VALUES| SMALLER THAN  0.90

A POSTERIORI CARTESIAN   COORDINATES
X :     -2523882.5946 M   +/-         0 MM
Y :     -4123573.0094 M   +/-         0 MM
Z :      4147719.3431 M   +/-         0 MM
```

```
CROSS-CORRELATION BETWEEN COORDINATES
ALL |CROSS-CORRELATION VALUES| SMALLER THAN  0.90


BASELINE :   HY  HT
-------------------

A-PRIORI     ELLIPSOID BASELINE COMPONENTS
DELTA  LATITUDE :  -  1 48 20.48291
DELTA LONGITUDE :  - 49 58 51.16756
DELTA    HEIGHT :   904.0884

A POSTERIORI ELLIPSOID BASELINE COMPONENTS
DELTA  LATITUDE :  -  1 48 20.48291        +/-         0 MM
DELTA LONGITUDE :  - 49 58 51.16756        +/-         0 MM
DELTA    HEIGHT :   904.0884               +/-         0 MM

CROSS-CORRELATION BETWEEN BASELINE COMPONENTS
ALL |CROSS-CORRELATION VALUES| SMALLER THAN  0.90

A POSTERIORI CARTESIAN BASELINE COMPONENTS
DELTA X :     -4016281.0400 M  +/-         0 MM
DELTA Y :       333720.8859 M  +/-         0 MM
DELTA Z :      -149099.9224 M  +/-         0 MM

CROSS-CORRELATION BETWEEN BASELINE COMPONENTS
ALL |CROSS-CORRELATION VALUES| SMALLER THAN  0.90

BASELINE LENGTH  : 4032879.0967 M +/-         0 MM

AZIMUTH HY TO HT : - 75 20 49.948 +/-     0.000 SEC
AZIMUTH HT TO HY :   70 10 56.192 +/-     0.000 SEC



BASELINE:      STATION : HY AND STATION : AR
============================================

STATION NAME : HY
-----------------

A-PRIORI ELLIPSOIDAL COORDINATES
LATITUDE  :    42 37 21.84550
LONGITUDE :  - 71 29 18.02122
HEIGHT    :    93.8914

A POSTERIORI ELLIPSOIDAL COORDINATES
LATITUDE  :    42 37 21.84550        +/-         0 MM
LONGITUDE :  - 71 29 18.02122        +/-         0 MM
HEIGHT    :    93.8914               +/-         0 MM

CROSS-CORRELATION BETWEEN COORDINATES
ALL |CROSS-CORRELATION VALUES| SMALLER THAN  0.90

A POSTERIORI CARTESIAN   COORDINATES
X :      1492398.4454 M   +/-         0 MM
```

```
Y :     -4457293.8953 M   +/-         0 MM
Z :      4296819.2655 M   +/-         0 MM

CROSS-CORRELATION BETWEEN COORDINATES
ALL |CROSS-CORRELATION VALUES| SMALLER THAN  0.90

STATION NAME : AR
-----------------

A-PRIORI ELLIPSOIDAL COORDINATES
LATITUDE  :    30 23  1.00124
LONGITUDE :  - 97 43 32.93395
HEIGHT    :   217.5207

A POSTERIORI ELLIPSOIDAL COORDINATES
LATITUDE  :    30 23  1.00160        +/-         3 MM
LONGITUDE :  - 97 43 32.93692        +/-         8 MM
HEIGHT    :   217.6016               +/-         9 MM

CROSS-CORRELATION BETWEEN COORDINATES
ALL |CROSS-CORRELATION VALUES| SMALLER THAN  0.90

A POSTERIORI CARTESIAN   COORDINATES
X :      -740328.3905 M   +/-         8 MM
Y :     -5457067.6475 M   +/-         8 MM
Z :      3207239.6910 M   +/-         6 MM

CROSS-CORRELATION BETWEEN COORDINATES
ALL |CROSS-CORRELATION VALUES| SMALLER THAN  0.90


BASELINE :   HY  AR
-------------------

A-PRIORI     ELLIPSOID BASELINE COMPONENTS
DELTA  LATITUDE :  - 12 14 20.84426
DELTA LONGITUDE :  - 26 14 14.91273
DELTA    HEIGHT :   123.6293

A POSTERIORI ELLIPSOID BASELINE COMPONENTS
DELTA  LATITUDE :  - 12 14 20.84391        +/-         3 MM
DELTA LONGITUDE :  - 26 14 14.91570        +/-         8 MM
DELTA    HEIGHT :   123.7102               +/-         9 MM

CROSS-CORRELATION BETWEEN BASELINE COMPONENTS
ALL |CROSS-CORRELATION VALUES| SMALLER THAN  0.90

A POSTERIORI CARTESIAN BASELINE COMPONENTS
DELTA X :     -2232726.8359 M  +/-         8 MM
DELTA Y :      -999773.7522 M  +/-         8 MM
DELTA Z :     -1089579.5745 M  +/-         6 MM

CROSS-CORRELATION BETWEEN BASELINE COMPONENTS
ALL |CROSS-CORRELATION VALUES| SMALLER THAN  0.90

BASELINE LENGTH  : 2678021.7192 M +/-         6 MM
```

```
AZIMUTH HY TO AR : -111 35 42.169 +/-     0.000 SEC
AZIMUTH AR TO HY :   52 31 47.465 +/-     0.000 SEC


BASELINE:      STATION : HY AND STATION : BP
===========================================

STATION NAME : HY
-----------------

A-PRIORI ELLIPSOIDAL COORDINATES
LATITUDE  :    42 37 21.84550
LONGITUDE :  - 71 29 18.02122
HEIGHT    :    93.8914

A POSTERIORI ELLIPSOIDAL COORDINATES
LATITUDE  :    42 37 21.84550        +/-         0 MM
LONGITUDE :  - 71 29 18.02122        +/-         0 MM
HEIGHT    :    93.8914               +/-         0 MM

CROSS-CORRELATION BETWEEN COORDINATES
ALL |CROSS-CORRELATION VALUES| SMALLER THAN  0.90

A POSTERIORI CARTESIAN   COORDINATES
X :      1492398.4454 M   +/-         0 MM
Y :     -4457293.8953 M   +/-         0 MM
Z :      4296819.2655 M   +/-         0 MM

CROSS-CORRELATION BETWEEN COORDINATES
ALL |CROSS-CORRELATION VALUES| SMALLER THAN  0.90

STATION NAME : BP
-----------------

A-PRIORI ELLIPSOIDAL COORDINATES
LATITUDE  :    37 13 55.17406
LONGITUDE :  -118 17  1.40030
HEIGHT    :  1183.2557

A POSTERIORI ELLIPSOIDAL COORDINATES
LATITUDE  :    37 13 55.17452        +/-         2 MM
LONGITUDE :  -118 17  1.40343        +/-         7 MM
HEIGHT    :  1183.3112               +/-         8 MM

CROSS-CORRELATION BETWEEN COORDINATES
ALL |CROSS-CORRELATION VALUES| SMALLER THAN  0.90

A POSTERIORI CARTESIAN   COORDINATES
X :     -2409654.8262 M   +/-         7 MM
Y :     -4478261.9452 M   +/-         6 MM
Z :      3838638.7780 M   +/-         6 MM

CROSS-CORRELATION BETWEEN COORDINATES
ALL |CROSS-CORRELATION VALUES| SMALLER THAN  0.90
```

```
BASELINE :   HY  BP
-------------------

A-PRIORI     ELLIPSOID BASELINE COMPONENTS
DELTA  LATITUDE :  -  5 23 26.67145
DELTA LONGITUDE :  - 46 47 43.37908
DELTA    HEIGHT :  1089.3643

A POSTERIORI ELLIPSOID BASELINE COMPONENTS
DELTA  LATITUDE :  -  5 23 26.67098        +/-         2 MM
DELTA LONGITUDE :  - 46 47 43.38220        +/-         7 MM
DELTA    HEIGHT :  1089.4198               +/-         8 MM

CROSS-CORRELATION BETWEEN BASELINE COMPONENTS
ALL |CROSS-CORRELATION VALUES| SMALLER THAN  0.90

A POSTERIORI CARTESIAN BASELINE COMPONENTS
DELTA X :     -3902053.2716 M  +/-         7 MM
DELTA Y :       -20968.0499 M  +/-         6 MM
DELTA Z :      -458180.4875 M  +/-         6 MM

CROSS-CORRELATION BETWEEN BASELINE COMPONENTS
ALL |CROSS-CORRELATION VALUES| SMALLER THAN  0.90

BASÈLINE LENGTH  : 3928916.9948 M +/-         6 MM

AZIMUTH HY TO BP : - 82 29 42.462 +/-     0.000 SEC
AZIMUTH BP TO HY :   66 25 52.950 +/-     0.000 SEC



BASELINE:      STATION : HY AND STATION : MM
============================================

STATION NAME : HY
-----------------

A-PRIORI ELLIPSOIDAL COORDINATES
LATITUDE  :    42 37 21.84550
LONGITUDE :  - 71 29 18.02122
HEIGHT    :    93.8914

A POSTERIORI ELLIPSOIDAL COORDINATES
LATITUDE  :    42 37 21.84550        +/-         0 MM
LONGITUDE :  - 71 29 18.02122        +/-         0 MM
HEIGHT    :    93.8914               +/-         0 MM

CROSS-CORRELATION BETWEEN COORDINATES
ALL |CROSS-CORRELATION VALUES| SMALLER THAN  0.90

A POSTERIORI CARTESIAN   COORDINATES
X :      1492398.4454 M   +/-         0 MM
Y :     -4457293.8953 M   +/-         0 MM
Z :      4296819.2655 M   +/-         0 MM
```

```
CROSS-CORRELATION BETWEEN COORDINATES
ALL |CROSS-CORRELATION VALUES| SMALLER THAN  0.90

STATION NAME : MM
-----------------

A-PRIORI ELLIPSOIDAL COORDINATES
LATITUDE  :    37 38 39.88027
LONGITUDE :  -118 53 48.28696
HEIGHT    :  2390.9932

A POSTERIORI ELLIPSOIDAL COORDINATES
LATITUDE  :    37 38 39.88019        +/-         2 MM
LONGITUDE :  -118 53 48.28684        +/-         7 MM
HEIGHT    :  2390.9409               +/-         7 MM

CROSS-CORRELATION BETWEEN COORDINATES
ALL |CROSS-CORRELATION VALUES| SMALLER THAN  0.90

A POSTERIORI CARTESIAN   COORDINATES
X :     -2444443.5976 M   +/-         7 MM
Y :     -4428696.3285 M   +/-         6 MM
Z :      3875726.8993 M   +/-         5 MM

CROSS-CORRELATION BETWEEN COORDINATES
ALL |CROSS-CORRELATION VALUES| SMALLER THAN  0.90


BASELINE :   HY  MM
-------------------

A-PRIORI     ELLIPSOID BASELINE COMPONENTS
DELTA  LATITUDE :  -  4 58 41.96524
DELTA LONGITUDE :  - 47 24 30.26574
DELTA    HEIGHT :  2297.1018

A POSTERIORI ELLIPSOID BASELINE COMPONENTS
DELTA  LATITUDE :  -  4 58 41.96531        +/-         2 MM
DELTA LONGITUDE :  - 47 24 30.26561        +/-         7 MM
DELTA    HEIGHT :  2297.0494               +/-         7 MM

CROSS-CORRELATION BETWEEN BASELINE COMPONENTS
ALL |CROSS-CORRELATION VALUES| SMALLER THAN  0.90

A POSTERIORI CARTESIAN BASELINE COMPONENTS
DELTA X :     -3936842.0430 M  +/-         7 MM
DELTA Y :        28597.5668 M  +/-         6 MM
DELTA Z :      -421092.3662 M  +/-         5 MM

CROSS-CORRELATION BETWEEN BASELINE COMPONENTS
ALL |CROSS-CORRELATION VALUES| SMALLER THAN  0.90

BASELINE LENGTH  : 3959401.7065 M +/-         6 MM

AZIMUTH HY TO MM : - 81 31 28.625 +/-     0.000 SEC
```

```
AZIMUTH MM TO HY :   66 50 37.068 +/-     0.000 SEC


BASELINE:      STATION : HY AND STATION : MJ
==========================================

STATION NAME : HY
-----------------

A-PRIORI ELLIPSOIDAL COORDINATES
LATITUDE  :    42 37 21.84550
LONGITUDE :  - 71 29 18.02122
HEIGHT    :    93.8914

A POSTERIORI ELLIPSOIDAL COORDINATES
LATITUDE  :    42 37 21.84550        +/-         0 MM
LONGITUDE :  - 71 29 18.02122        +/-         0 MM
HEIGHT    :    93.8914               +/-         0 MM

CROSS-CORRELATION BETWEEN COORDINATES
ALL |CROSS-CORRELATION VALUES| SMALLER THAN  0.90

A POSTERIORI CARTESIAN   COORDINATES
X :      1492398.4454 M   +/-         0 MM
Y :     -4457293.8953 M   +/-         0 MM
Z :      4296819.2655 M   +/-         0 MM

CROSS-CORRELATION BETWEEN COORDINATES
ALL |CROSS-CORRELATION VALUES| SMALLER THAN  0.90

STATION NAME : MJ
-----------------

A-PRIORI ELLIPSOIDAL COORDINATES
LATITUDE  :    35 19 52.48371
LONGITUDE :  -116 53 33.13647
HEIGHT    :   898.0025

A POSTERIORI ELLIPSOIDAL COORDINATES
LATITUDE  :    35 19 52.48588        +/-         3 MM
LONGITUDE :  -116 53 33.13694        +/-         9 MM
HEIGHT    :   897.9119               +/-         8 MM

CROSS-CORRELATION BETWEEN COORDINATES
ALL |CROSS-CORRELATION VALUES| SMALLER THAN  0.90

A POSTERIORI CARTESIAN   COORDINATES
X :     -2356576.1146 M   +/-         8 MM
Y :     -4646564.9994 M   +/-         8 MM
Z :      3668427.6554 M   +/-         6 MM

CROSS-CORRELATION BETWEEN COORDINATES
ALL |CROSS-CORRELATION VALUES| SMALLER THAN  0.90
```

```
BASELINE :   HY  MJ
-------------------

A-PRIORI     ELLIPSOID BASELINE COMPONENTS
DELTA  LATITUDE :  -  7 17 29.36179
DELTA LONGITUDE :  - 45 24 15.11525
DELTA    HEIGHT :   804.1111

A POSTERIORI ELLIPSOID BASELINE COMPONENTS
DELTA  LATITUDE :  -  7 17 29.35963        +/-         3 MM
DELTA LONGITUDE :  - 45 24 15.11571        +/-         9 MM
DELTA    HEIGHT :   804.0205               +/-         8 MM

CROSS-CORRELATION BETWEEN BASELINE COMPONENTS
ALL |CROSS-CORRELATION VALUES| SMALLER THAN  0.90

A POSTERIORI CARTESIAN BASELINE COMPONENTS
DELTA X :     -3848974.5600 M  +/-         8 MM
DELTA Y :      -189271.1041 M  +/-         8 MM
DELTA Z :      -628391.6101 M  +/-         6 MM

CROSS-CORRELATION BETWEEN BASELINE COMPONENTS
ALL |CROSS-CORRELATION VALUES| SMALLER THAN  0.90

BASELINE LENGTH  : 3904523.6240 M +/-         8 MM

AZIMUTH HY TO MJ : - 86 14 35.611 +/-     0.000 SEC
AZIMUTH MJ TO HY :   64 12 49.147 +/-     0.000 SEC



BASELINE:      STATION : RC AND STATION : HT
============================================

STATION NAME : RC
-----------------

A-PRIORI ELLIPSOIDAL COORDINATES
LATITUDE  :    25 36 50.75301
LONGITUDE :  - 80 23  3.17181
HEIGHT    :   -21.1879

A POSTERIORI ELLIPSOIDAL COORDINATES
LATITUDE  :    25 36 50.75301        +/-         0 MM
LONGITUDE :  - 80 23  3.17181        +/-         0 MM
HEIGHT    :   -21.1879               +/-         0 MM

CROSS-CORRELATION BETWEEN COORDINATES
ALL |CROSS-CORRELATION VALUES| SMALLER THAN  0.90

A POSTERIORI CARTESIAN   COORDINATES
X :       961302.9852 M   +/-         0 MM
Y :     -5674057.1094 M   +/-         0 MM
Z :      2740563.8693 M   +/-         0 MM

CROSS-CORRELATION BETWEEN COORDINATES
```

```
ALL |CROSS-CORRELATION VALUES| SMALLER THAN  0.90

STATION NAME : HT
-----------------

A-PRIORI ELLIPSOIDAL COORDINATES
LATITUDE  :    40 49  1.36259
LONGITUDE :  -121 28  9.18879
HEIGHT    :   997.9798

A POSTERIORI ELLIPSOIDAL COORDINATES
LATITUDE  :    40 49  1.36259        +/-         0 MM
LONGITUDE :  -121 28  9.18879        +/-         0 MM
HEIGHT    :   997.9798               +/-         0 MM

CROSS-CORRELATION BETWEEN COORDINATES
ALL |CROSS-CORRELATION VALUES| SMALLER THAN  0.90

A POSTERIORI CARTESIAN   COORDINATES
X :     -2523882.5946 M   +/-         0 MM
Y :     -4123573.0094 M   +/-         0 MM
Z :      4147719.3431 M   +/-         0 MM

CROSS-CORRELATION BETWEEN COORDINATES
ALL |CROSS-CORRELATION VALUES| SMALLER THAN  0.90


BASELINE :   RC  HT
-------------------

A-PRIORI     ELLIPSOID BASELINE COMPONENTS
DELTA  LATITUDE :    15 12 10.60959
DELTA LONGITUDE :  - 41  5  6.01698
DELTA    HEIGHT :  1019.1677

A POSTERIORI ELLIPSOID BASELINE COMPONENTS
DELTA  LATITUDE :    15 12 10.60959        +/-         0 MM
DELTA LONGITUDE :  - 41  5  6.01698        +/-         0 MM
DELTA    HEIGHT :  1019.1677               +/-         0 MM

CROSS-CORRELATION BETWEEN BASELINE COMPONENTS
ALL |CROSS-CORRELATION VALUES| SMALLER THAN  0.90

A POSTERIORI CARTESIAN BASELINE COMPONENTS
DELTA X :     -3485185.5798 M  +/-         0 MM
DELTA Y :      1550484.1000 M  +/-         0 MM
DELTA Z :      1407155.4738 M  +/-         0 MM

CROSS-CORRELATION BETWEEN BASELINE COMPONENTS
ALL |CROSS-CORRELATION VALUES| SMALLER THAN  0.90

BASELINE LENGTH  : 4065784.7948 M +/-         0 MM

AZIMUTH RC TO HT : - 55 31 38.528 +/-     0.000 SEC
AZIMUTH HT TO RC :  101  4 19.994 +/-     0.000 SEC
```

```
BASELINE:      STATION : FD AND STATION : HT
==========================================

STATION NAME : FD
-----------------

A-PRIORI ELLIPSOIDAL COORDINATES
LATITUDE  :    30 38  9.60561
LONGITUDE :  -103 56 49.65601
HEIGHT    :  1585.3693

A POSTERIORI ELLIPSOIDAL COORDINATES
LATITUDE  :    30 38  9.60561        +/-         0 MM
LONGITUDE :  -103 56 49.65601        +/-         0 MM
HEIGHT    :  1585.3693               +/-         0 MM

CROSS-CORRELATION BETWEEN COORDINATES
ALL |CROSS-CORRELATION VALUES| SMALLER THAN  0.90

A POSTERIORI CARTESIAN   COORDINATES
X :     -1324205.7179 M   +/-         0 MM
Y :     -5332056.0713 M   +/-         0 MM
Z :      3232043.6300 M   +/-         0 MM

CROSS-CORRELATION BETWEEN COORDINATES
ALL |CROSS-CORRELATION VALUES| SMALLER THAN  0.90

STATION NAME : HT
-----------------

A-PRIORI ELLIPSOIDAL COORDINATES
LATITUDE  :    40 49  1.36259
LONGITUDE :  -121 28  9.18879
HEIGHT    :   997.9798

A POSTERIORI ELLIPSOIDAL COORDINATES
LATITUDE  :    40 49  1.36259        +/-         0 MM
LONGITUDE :  -121 28  9.18879        +/-         0 MM
HEIGHT    :   997.9798               +/-         0 MM

CROSS-CORRELATION BETWEEN COORDINATES
ALL |CROSS-CORRELATION VALUES| SMALLER THAN  0.90

A POSTERIORI CARTESIAN   COORDINATES
X :     -2523882.5946 M   +/-         0 MM
Y :     -4123573.0094 M   +/-         0 MM
Z :      4147719.3431 M   +/-         0 MM

CROSS-CORRELATION BETWEEN COORDINATES
ALL |CROSS-CORRELATION VALUES| SMALLER THAN  0.90


BASELINE :   FD  HT
-------------------
```

```
A-PRIORI     ELLIPSOID BASELINE COMPONENTS
DELTA  LATITUDE :    10 10 51.75699
DELTA LONGITUDE :  - 17 31 19.53277
DELTA    HEIGHT :  -587.3895

A POSTERIORI ELLIPSOID BASELINE COMPONENTS
DELTA  LATITUDE :    10 10 51.75699        +/-          0 MM
DELTA LONGITUDE :  - 17 31 19.53277        +/-          0 MM
DELTA    HEIGHT :  -587.3895               +/-          0 MM

CROSS-CORRELATION BETWEEN BASELINE COMPONENTS
ALL |CROSS-CORRELATION VALUES| SMALLER THAN  0.90

A POSTERIORI CARTESIAN BASELINE COMPONENTS
DELTA X :     -1199676.8767 M  +/-          0 MM
DELTA Y :      1208483.0619 M  +/-          0 MM
DELTA Z :       915675.7131 M  +/-          0 MM

CROSS-CORRELATION BETWEEN BASELINE COMPONENTS
ALL |CROSS-CORRELATION VALUES| SMALLER THAN  0.90

BASELINE LENGTH  : 1933421.3020 M +/-          0 MM

AZIMUTH FD TO HT : - 49 36 50.461 +/-      0.000 SEC
AZIMUTH HT TO FD :  120  3 40.496 +/-      0.000 SEC



BASELINE:      STATION : NS AND STATION : HT
==============================================

STATION NAME : NS
-----------------

A-PRIORI ELLIPSOIDAL COORDINATES
LATITUDE  :    38 19 55.47490
LONGITUDE :  - 77  2 32.50317
HEIGHT    :   -18.4557

A POSTERIORI ELLIPSOIDAL COORDINATES
LATITUDE  :    38 19 55.47388        +/-          5 MM
LONGITUDE :  - 77  2 32.49886        +/-          9 MM
HEIGHT    :   -18.2342               +/-         17 MM

CROSS-CORRELATION BETWEEN COORDINATES
ALL |CROSS-CORRELATION VALUES| SMALLER THAN  0.90

A POSTERIORI CARTESIAN   COORDINATES
X :       1123313.6887 M   +/-        10 MM
Y :      -4882071.0587 M   +/-        12 MM
Z :       3934412.0257 M   +/-        13 MM

CROSS-CORRELATION BETWEEN COORDINATES
ALL |CROSS-CORRELATION VALUES| SMALLER THAN  0.90
```

```
STATION NAME : HT
-----------------

A-PRIORI ELLIPSOIDAL COORDINATES
LATITUDE  :    40 49  1.36259
LONGITUDE :  -121 28  9.18879
HEIGHT    :   997.9798

A POSTERIORI ELLIPSOIDAL COORDINATES
LATITUDE  :    40 49  1.36259        +/-         0 MM
LONGITUDE :  -121 28  9.18879        +/-         0 MM
HEIGHT    :   997.9798               +/-         0 MM

CROSS-CORRELATION BETWEEN COORDINATES
ALL |CROSS-CORRELATION VALUES| SMALLER THAN  0.90

A POSTERIORI CARTESIAN   COORDINATES
X :     -2523882.5946 M   +/-         0 MM
Y :     -4123573.0094 M   +/-         0 MM
Z :      4147719.3431 M   +/-         0 MM

CROSS-CORRELATION BETWEEN COORDINATES
ALL |CROSS-CORRELATION VALUES| SMALLER THAN  0.90


BASELINE :   NS  HT
-------------------

A-PRIORI     ELLIPSOID BASELINE COMPONENTS
DELTA  LATITUDE :     2 29  5.88769
DELTA LONGITUDE :  - 44 25 36.68562
DELTA    HEIGHT :  1016.4355

A POSTERIORI ELLIPSOID BASELINE COMPONENTS
DELTA  LATITUDE :     2 29  5.88872        +/-         5 MM
DELTA LONGITUDE :  - 44 25 36.68993        +/-         9 MM
DELTA    HEIGHT :  1016.2141               +/-        17 MM

CROSS-CORRELATION BETWEEN BASELINE COMPONENTS
ALL |CROSS-CORRELATION VALUES| SMALLER THAN  0.90

A POSTERIORI CARTESIAN BASELINE COMPONENTS
DELTA X :     -3647196.2833 M  +/-        10 MM
DELTA Y :       758498.0493 M  +/-        12 MM
DELTA Z :       213307.3174 M  +/-        13 MM

CROSS-CORRELATION BETWEEN BASELINE COMPONENTS
ALL |CROSS-CORRELATION VALUES| SMALLER THAN  0.90

BASELINE LENGTH  : 3731334.8860 M +/-        11 MM

AZIMUTH NS TO HT : - 71 29 24.402 +/-     0.000 SEC
AZIMUTH HT TO NS :   79 20 14.811 +/-     0.000 SEC
```

```
BASELINE:      STATION : HT AND STATION : AR
===========================================

STATION NAME : HT
-----------------

A-PRIORI ELLIPSOIDAL COORDINATES
LATITUDE  :    40 49  1.36259
LONGITUDE :  -121 28  9.18879
HEIGHT    :   997.9798

A POSTERIORI ELLIPSOIDAL COORDINATES
LATITUDE  :    40 49  1.36259        +/-         0 MM
LONGITUDE :  -121 28  9.18879        +/-         0 MM
HEIGHT    :   997.9798               +/-         0 MM

CROSS-CORRELATION BETWEEN COORDINATES
ALL |CROSS-CORRELATION VALUES| SMALLER THAN  0.90

A POSTERIORI CARTESIAN   COORDINATES
X :     -2523882.5946 M   +/-         0 MM
Y :     -4123573.0094 M   +/-         0 MM
Z :      4147719.3431 M   +/-         0 MM

CROSS-CORRELATION BETWEEN COORDINATES
ALL |CROSS-CORRELATION VALUES| SMALLER THAN  0.90

STATION NAME : AR
-----------------

A-PRIORI ELLIPSOIDAL COORDINATES
LATITUDE  :    30 23  1.00124
LONGITUDE :  - 97 43 32.93395
HEIGHT    :   217.5207

A POSTERIORI ELLIPSOIDAL COORDINATES
LATITUDE  :    30 23  1.00160        +/-         3 MM
LONGITUDE :  - 97 43 32.93692        +/-         8 MM
HEIGHT    :   217.6016               +/-         9 MM

CROSS-CORRELATION BETWEEN COORDINATES
ALL |CROSS-CORRELATION VALUES| SMALLER THAN  0.90

A POSTERIORI CARTESIAN   COORDINATES
X :      -740328.3905 M   +/-         8 MM
Y :     -5457067.6475 M   +/-         8 MM
Z :      3207239.6910 M   +/-         6 MM

CROSS-CORRELATION BETWEEN COORDINATES
ALL |CROSS-CORRELATION VALUES| SMALLER THAN  0.90


BASELINE :   HT  AR
-------------------

A-PRIORI     ELLIPSOID BASELINE COMPONENTS
```

```
DELTA  LATITUDE :  - 10 26  0.36135
DELTA LONGITUDE :    23 44 36.25484
DELTA    HEIGHT :  -780.4591

A POSTERIORI ELLIPSOID BASELINE COMPONENTS
DELTA  LATITUDE :  - 10 26  0.36099        +/-         3 MM
DELTA LONGITUDE :    23 44 36.25186        +/-         8 MM
DELTA    HEIGHT :  -780.3783               +/-         9 MM

CROSS-CORRELATION BETWEEN BASELINE COMPONENTS
ALL |CROSS-CORRELATION VALUES| SMALLER THAN  0.90

A POSTERIORI CARTESIAN BASELINE COMPONENTS
DELTA X :      1783554.2041 M  +/-         8 MM
DELTA Y :     -1333494.6381 M  +/-         8 MM
DELTA Z :      -940479.6521 M  +/-         6 MM

CROSS-CORRELATION BETWEEN BASELINE COMPONENTS
ALL |CROSS-CORRELATION VALUES| SMALLER THAN  0.90

BASELINE LENGTH  : 2417390.2302 M +/-         7 MM

AZIMUTH HT TO AR :  110 53 48.435 +/-     0.000 SEC
AZIMUTH AR TO HT : - 55  5 31.816 +/-     0.000 SEC



BASELINE:      STATION : HT AND STATION : BP
==========================================

STATION NAME : HT
-----------------

A-PRIORI ELLIPSOIDAL COORDINATES
LATITUDE  :    40 49  1.36259
LONGITUDE :  -121 28  9.18879
HEIGHT    :   997.9798

A POSTERIORI ELLIPSOIDAL COORDINATES
LATITUDE  :    40 49  1.36259        +/-         0 MM
LONGITUDE :  -121 28  9.18879        +/-         0 MM
HEIGHT    :   997.9798               +/-         0 MM

CROSS-CORRELATION BETWEEN COORDINATES
ALL |CROSS-CORRELATION VALUES| SMALLER THAN  0.90

A POSTERIORI CARTESIAN   COORDINATES
X :     -2523882.5946 M   +/-         0 MM
Y :     -4123573.0094 M   +/-         0 MM
Z :      4147719.3431 M   +/-         0 MM

CROSS-CORRELATION BETWEEN COORDINATES
ALL |CROSS-CORRELATION VALUES| SMALLER THAN  0.90

STATION NAME : BP
-----------------
```

```
A-PRIORI ELLIPSOIDAL COORDINATES
LATITUDE  :    37 13 55.17406
LONGITUDE :  -118 17  1.40030
HEIGHT    :  1183.2557

A POSTERIORI ELLIPSOIDAL COORDINATES
LATITUDE  :    37 13 55.17452        +/-         2 MM
LONGITUDE :  -118 17  1.40343        +/-         7 MM
HEIGHT    :  1183.3112               +/-         8 MM

CROSS-CORRELATION BETWEEN COORDINATES
ALL |CROSS-CORRELATION VALUES| SMALLER THAN  0.90

A POSTERIORI CARTESIAN   COORDINATES
X :     -2409654.8262 M   +/-         7 MM
Y :     -4478261.9452 M   +/-         6 MM
Z :      3838638.7780 M   +/-         6 MM

CROSS-CORRELATION BETWEEN COORDINATES
ALL |CROSS-CORRELATION VALUES| SMALLER THAN  0.90


BASELINE :   HT  BP
-------------------

A-PRIORI     ELLIPSOID BASELINE COMPONENTS
DELTA  LATITUDE :  -  3 35  6.18854
DELTA LONGITUDE :     3 11  7.78849
DELTA    HEIGHT :   185.2758

A POSTERIORI ELLIPSOID BASELINE COMPONENTS
DELTA  LATITUDE :  -  3 35  6.18807        +/-         2 MM
DELTA LONGITUDE :     3 11  7.78536        +/-         7 MM
DELTA    HEIGHT :   185.3314               +/-         8 MM

CROSS-CORRELATION BETWEEN BASELINE COMPONENTS
ALL |CROSS-CORRELATION VALUES| SMALLER THAN  0.90

A POSTERIORI CARTESIAN BASELINE COMPONENTS
DELTA X :       114227.7684 M  +/-         7 MM
DELTA Y :      -354688.9358 M  +/-         6 MM
DELTA Z :      -309080.5651 M  +/-         6 MM

CROSS-CORRELATION BETWEEN BASELINE COMPONENTS
ALL |CROSS-CORRELATION VALUES| SMALLER THAN  0.90

BASELINE LENGTH  :  484131.2012 M +/-         4 MM

AZIMUTH HT TO BP :  144 15 33.692 +/-     0.002 SEC
AZIMUTH BP TO HT : - 33 44  0.937 +/-     0.002 SEC


BASELINE:      STATION : HT AND STATION : MM
============================================
```

```
STATION NAME : HT
-----------------

A-PRIORI ELLIPSOIDAL COORDINATES
LATITUDE  :    40 49  1.36259
LONGITUDE : -121 28  9.18879
HEIGHT    :   997.9798

A POSTERIORI ELLIPSOIDAL COORDINATES
LATITUDE  :    40 49  1.36259        +/-         0 MM
LONGITUDE : -121 28  9.18879        +/-         0 MM
HEIGHT    :   997.9798              +/-         0 MM

CROSS-CORRELATION BETWEEN COORDINATES
ALL |CROSS-CORRELATION VALUES| SMALLER THAN  0.90

A POSTERIORI CARTESIAN   COORDINATES
X :     -2523882.5946 M   +/-         0 MM
Y :     -4123573.0094 M   +/-         0 MM
Z :      4147719.3431 M   +/-         0 MM

CROSS-CORRELATION BETWEEN COORDINATES
ALL |CROSS-CORRELATION VALUES| SMALLER THAN  0.90

STATION NAME : MM
-----------------

A-PRIORI ELLIPSOIDAL COORDINATES
LATITUDE  :    37 38 39.88027
LONGITUDE : -118 53 48.28696
HEIGHT    :  2390.9932

A POSTERIORI ELLIPSOIDAL COORDINATES
LATITUDE  :    37 38 39.88019        +/-         2 MM
LONGITUDE : -118 53 48.28684        +/-         7 MM
HEIGHT    :  2390.9409              +/-         7 MM

CROSS-CORRELATION BETWEEN COORDINATES
ALL |CROSS-CORRELATION VALUES| SMALLER THAN  0.90

A POSTERIORI CARTESIAN   COORDINATES
X :     -2444443.5976 M   +/-         7 MM
Y :     -4428696.3285 M   +/-         6 MM
Z :      3875726.8993 M   +/-         5 MM

CROSS-CORRELATION BETWEEN COORDINATES
ALL |CROSS-CORRELATION VALUES| SMALLER THAN  0.90


BASELINE :   HT  MM
-------------------

A-PRIORI     ELLIPSOID BASELINE COMPONENTS
DELTA  LATITUDE :  -  3 10 21.48233
DELTA LONGITUDE :     2 34 20.90183
```

```
DELTA    HEIGHT :  1393.0134

A POSTERIORI ELLIPSOID BASELINE COMPONENTS
DELTA  LATITUDE :  -  3 10 21.48240        +/-         2 MM
DELTA LONGITUDE :     2 34 20.90195        +/-         7 MM
DELTA    HEIGHT :  1392.9610               +/-         7 MM

CROSS-CORRELATION BETWEEN BASELINE COMPONENTS
ALL |CROSS-CORRELATION VALUES| SMALLER THAN  0.90

A POSTERIORI CARTESIAN BASELINE COMPONENTS
DELTA X :        79438.9970 M  +/-         7 MM
DELTA Y :      -305123.3191 M  +/-         6 MM
DELTA Z :      -271992.4438 M  +/-         5 MM

CROSS-CORRELATION BETWEEN BASELINE COMPONENTS
ALL |CROSS-CORRELATION VALUES| SMALLER THAN  0.90

BASELINE LENGTH  :  416402.0697 M +/-         4 MM

AZIMUTH HT TO MM :  146 56 32.713 +/-     0.003 SEC
AZIMUTH MM TO HT : - 31 25 47.523 +/-     0.003 SEC



BASELINE:      STATION : HT AND STATION : MJ
===========================================
STATION NAME : HT
-----------------

A-PRIORI ELLIPSOIDAL COORDINATES
LATITUDE  :    40 49  1.36259
LONGITUDE :  -121 28  9.18879
HEIGHT    :   997.9798

A POSTERIORI ELLIPSOIDAL COORDINATES
LATITUDE  :    40 49  1.36259        +/-         2 MM
LONGITUDE :  -121 28  9.18879        +/-         7 MM
HEIGHT    :   997.9798               +/-         7 MM

CROSS-CORRELATION BETWEEN COORDINATES
ALL |CROSS-CORRELATION VALUES| SMALLER THAN  0.90

A POSTERIORI CARTESIAN   COORDINATES
X :     -2523882.5946 M   +/-         0 MM
Y :     -4123573.0094 M   +/-         0 MM
Z :      4147719.3431 M   +/-         0 MM

CROSS-CORRELATION BETWEEN COORDINATES
ALL |CROSS-CORRELATION VALUES| SMALLER THAN  0.90

STATION NAME : MJ
-----------------
```

```
A-PRIORI ELLIPSOIDAL COORDINATES
LATITUDE  :    35 19 52.48371
LONGITUDE :  -116 53 33.13647
HEIGHT    :   898.0025

A POSTERIORI ELLIPSOIDAL COORDINATES
LATITUDE  :    35 19 52.48588        +/-         3 MM
LONGITUDE :  -116 53 33.13694        +/-         9 MM
HEIGHT    :   897.9119               +/-         8 MM

CROSS-CORRELATION BETWEEN COORDINATES
ALL |CROSS-CORRELATION VALUES| SMALLER THAN  0.90

A POSTERIORI CARTESIAN   COORDINATES
X :     -2356576.1146 M   +/-         8 MM
Y :     -4646564.9994 M   +/-         8 MM
Z :      3668427.6554 M   +/-         6 MM

CROSS-CORRELATION BETWEEN COORDINATES
ALL |CROSS-CORRELATION VALUES| SMALLER THAN  0.90


BASELINE :   HT  MJ
-------------------

A-PRIORI     ELLIPSOID BASELINE COMPONENTS
DELTA  LATITUDE :  -  5 29  8.87888
DELTA LONGITUDE :     4 34 36.05232
DELTA    HEIGHT :   -99.9773

A POSTERIORI ELLIPSOID BASELINE COMPONENTS
DELTA  LATITUDE :  -  5 29  8.87672        +/-         3 MM
DELTA LONGITUDE :     4 34 36.05185        +/-         9 MM
DELTA    HEIGHT :  -100.0680               +/-         8 MM

CROSS-CORRELATION BETWEEN BASELINE COMPONENTS
ALL |CROSS-CORRELATION VALUES| SMALLER THAN  0.90

A POSTERIORI CARTESIAN BASELINE COMPONENTS
DELTA X :       167306.4800 M  +/-         8 MM
DELTA Y :      -522991.9900 M  +/-         8 MM
DELTA Z :      -479291.6877 M  +/-         6 MM

CROSS-CORRELATION BETWEEN BASELINE COMPONENTS
ALL |CROSS-CORRELATION VALUES| SMALLER THAN  0.90

BASELINE LENGTH  :  728857.0517 M +/-         5 MM

AZIMUTH HT TO MM :  145  9 28.711 +/-     0.002 SEC
AZIMUTH MM TO HT : - 32  0 55.818 +/-     0.002 SEC
```

APPENDIX 8

COMPARISON BETWEEN A PRIORI ORBITS AND IMPROVED ORBITS FROM FIDUCIAL NETWORK SOLUTION (MARCH 30)

COMPARISON BETWEEN A PRIORI ORBITS AND IMPROVED ORBITS FROM FIDUCIAL NETWORK SOLUTION (MARCH 30)

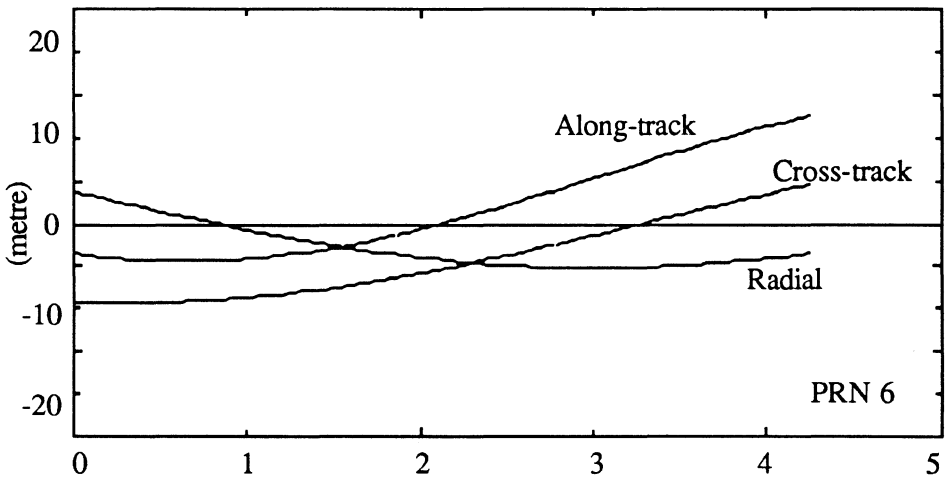

TIME PAST 30-MARCH-1985 03:00:00 UT (hour)
FIGURE A8.1

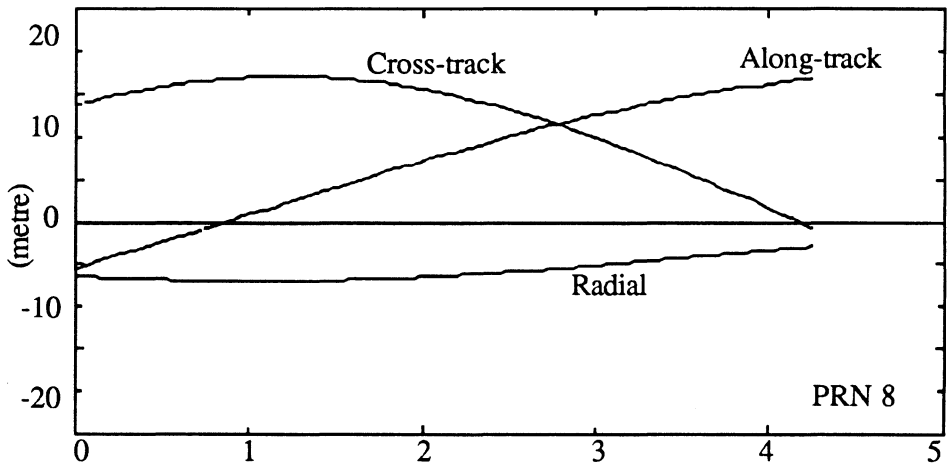

TIME PAST 30-MARCH-1985 03:00:00 UT (hour)
FIGURE A8.2

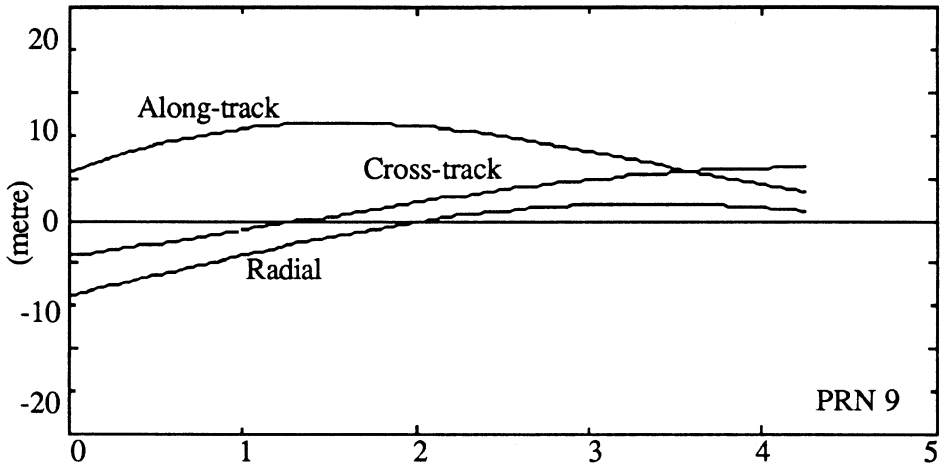

TIME PAST 30-MARCH-1985 05:18:00 UT (hour)
FIGURE A8.3

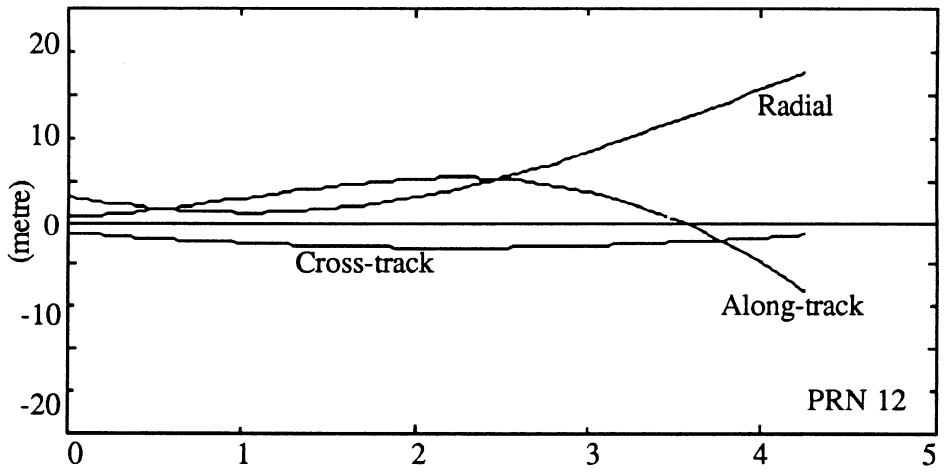

TIME PAST 30-MARCH-1985 07:12:00 UT (hour)
FIGURE A8.4

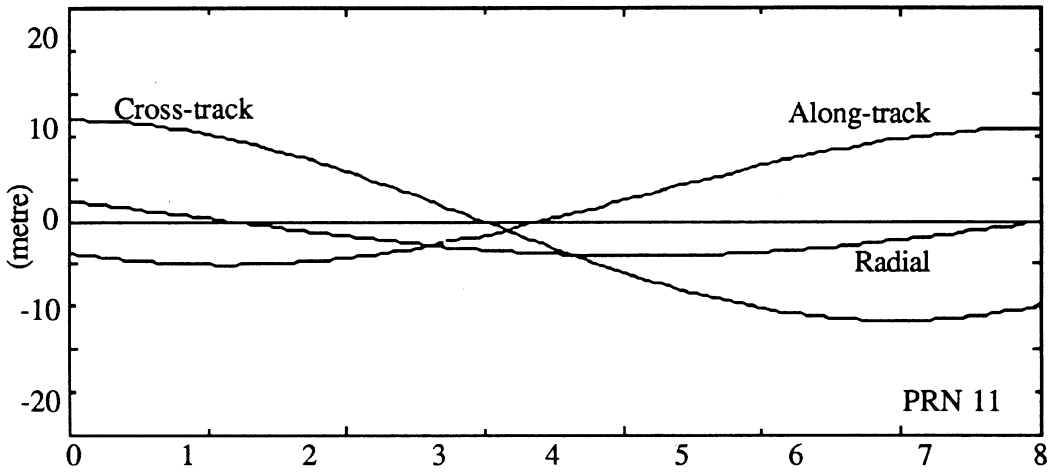

TIME PAST 30-MARCH-1985 03:48:00 UT (hour)
FIGURE A8.5

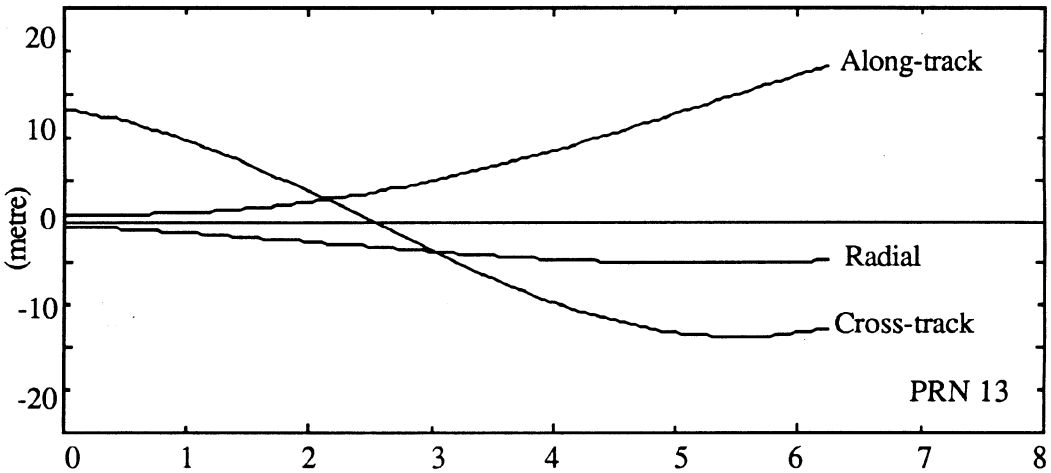

TIME PAST 30-MARCH-1985 06:48:00 UT (hour)
FIGURE A8.6

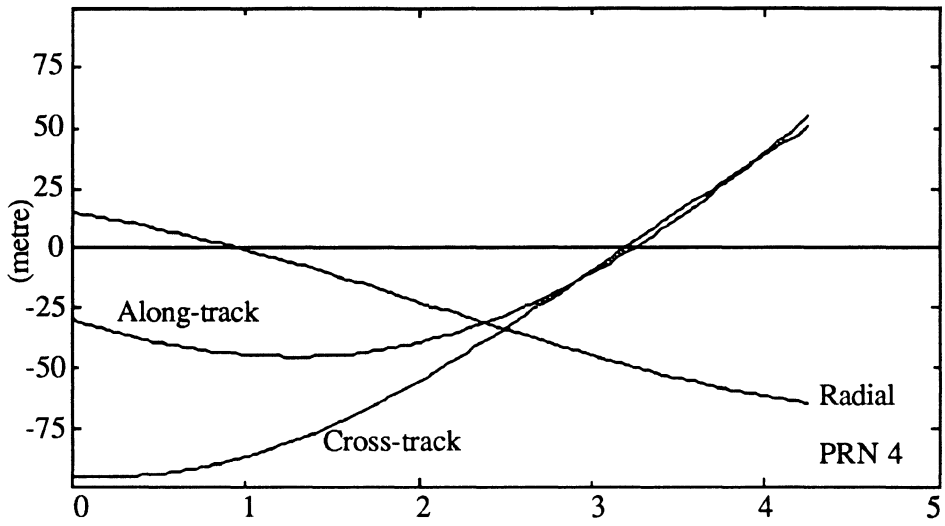

TIME PAST 30-MARCH-1985 09:12:00 UT (hour)
FIGURE A8.7